INVESTIGATION OF NICKEL RECOVERY BY BIOGRANULES TAILORED FOR METAL RECOVERY THROUGH BIOMINERALIZATION

BİYOMİNERALİZASYON YOLUYLA METAL GERİ KAZANIMINA YÖNELİK ÜRETİLEN BİYOGRANÜLLERLE NİKEL GERİ KAZANIMININ İNCELENMESİ

KADİR ŞEKERCİOĞLU

ASST. PROF. DR. YUSUF ÇAĞATAY ERŞAN

Supervisor

Submitted to

Graduate School of Science and Engineering of Hacettepe University

as a Partial Fulfillment to the Requirements for the Award of the Degree of Master of Science in Environmental Engineering

2022

To Better Future of The Planet…

ABSTRACT

INVESTIGATION OF NICKEL RECOVERY BY BIOGRANULES TAILORED FOR METAL RECOVERY THROUGH BIOMINERALIZATION

Kadir ŞEKERCİOĞLU

Master of Science, Department of Environmental Engineering

Supervisor: Assist. Prof. Dr. Yusuf Çağatay ERŞAN

January 2022, 120 pages

Electronic waste production in the world is increasing day by day. Nowadays, PCBs, which are one of the most important components of electronic waste, are considered as more valuable metal resources than ores due to their high value- and base-metal contents. Commercial metal recovery applications from WPCBs are mostly carried out using chemical techniques. However, due to the high chemical and energy consumption of these chemical techniques, development of alternative biological recovery techniques is essential to minimize the environmental impact of recovery processes.

In this thesis study, it is aimed to use biogranules that are capable of denitrification and urea hydrolysis for selective metal recovery from bioleachate solutions obtained via bioleaching of WPCBs. Selective nickel recovery performance of mature biogranules which were produced from seed sludge and exposed to incrementing nickel concentrations was investigated. Upon reaching steady conditions very compact and small granules with 0.2-0.6 mm size were obtained and the SVI_{30} values were recorded in the range of 7-9 mL/g. Produced biogranules could consume 55% and 100% of the urea and nitrate fed under anoxic conditions, respectively. Although the microbial

performance of the granules increased by 39.8% as a result of nickel acclimation, deterioration in the granule structure and increase in flocs were observed.

Upon acclimation, metal recovery performance of biogranules were investigated in bioleachate solutions prepared with 1:20, 1:10, 1:5 and 1:2.5 dilution ratios. As a result of the process, the biomineralization process performed in 1:10 dilution ratio was determined as the most efficient concentration in terms of both microbial activity and recovered nickel purity (24.82%). In addition to nickel, zinc and copper could be effectively separated from the liquid and thus nickel purity decreased.

Keywords: Bioleaching, Biomineralization, Metal Recovery, E-Waste, Waste Printed Circuit Board, Biogranule, Microbial Induced Calcite Precipitation

ÖZET

BİYOMİNERALİZASYON YOLUYLA METAL GERİ KAZANIMINA YÖNELİK ÜRETİLEN BİYOGRANÜLLERLE NİKEL GERİ KAZANIM PERFORMANSI

Kadir ŞEKERCİOĞLU

Yüksek Lisans, Çevre Mühendisliği Bölümü

Tez Danışmanı: Dr. Öğr. Ü. Yusuf Çağatay Erşan

Ocak 2022, 120 sayfa

Dünyada elektronik atık üretimi her geçen gün hızlanarak artış göstermektedir. Elektronik atıkların en önemli bileşenlerinden olan baskılı devre kartları (BDK) yüksek değerli- ve baz-metal içeriklerinden dolayı günümüzde maden cevherlerinden daha değerli metal kaynakları olarak görülmektedir. Atık baskılı devre kartlarından (ABDK) ticari boyutta metal geri kazanımı uygulamaları çoğunlukla kimyasal teknikler kullanılarak gerçekleştirilmektedir. Ancak yüksek kimyasal ve enerji tüketimleri nedeniyle bu kimyasal tekniklere alternatif olabilecek biyolojik geri kazanım tekniklerinin geliştirilmesi, geri kazanım süreçlerinde çevreye verilen zararın azaltılması anlamında önemlidir.

Tez çalışmasında ABDK'ların biyoliç işlemine maruz bırakılması sonucu elde edilen biyoliç çözeltisinden, seçici olarak metal geri kazanımı için üre hidrolizi ve denitrifikasyon yapabilen biyogranüllerin kullanılması amaçlanmıştır. Aşı çamurundan üretilerek olgunlaştırılan ve kademeli bir şekilde farklı nikel derişimlerine maruz bırakılan biyogranüllerin seçici nikel geri kazanımı performansı incelenmiştir.

Granülasyon periyodunda reaktör kararlılığı sağlandığında 0.2-0.6 mm boyuta sahip ve SVI_{30} değeri 7-9 ml/g aralığında olan oldukça yoğun ve küçük granüller elde edilmiştir. Üretilen biyogranüller anoksik şartlarda reaktöre beslenen üre ve nitratı sırasıyla %47.8±8.4 ve %100 oranında tüketmiştir. Nikel aklimasyonu sonucunda granüllerin mikrobiyal performanslarında %39.8 oranında bir artış elde edilmesine rağmen granül yapısında bozulmalar ve flok miktarında artış gözlemlenmiştir.

Nikel aklimasyonu sonrasında biyogranüllerin 1:20, 1:10, 1:5 ve 1:2.5 oranlarında seyreltilmiş biyoliç solüsyonlarında metal geri kazanımı performansları incelenmiştir. İşlem sonucunda 1:10 oranında seyreltilmiş çözeltide gerçekleştirilen biyomineralizasyon işlemi hem mikrobiyal aktivite hem de geri kazanılan nikel saflığı (%24.82) açısından en verimli derişim olarak belirlenmiştir. Nikel ile birlikte çinko ve bakırın da biyoliç solüsyonundan efektif bir şekilde ayrıştırılabildiği bu nedenle de saflığın düşük olduğu belirlenmiştir.

Anahtar Kelimeler: Biyoliç, Biyomineralizasyon, Metal Geri Kazanımı, E-atık, Atık Baskılı Devre Kartları, Biyogranül, Mikrobiyal Kaynaklı Kalsit Çökelmesi

ACKNOWLEDGMENT

Foremost, I would like to Express my sincere gratitude to my advisor Asst. Prof. Dr. Yusuf Çağatay Erşan for the continuous support of my thesis for his patience, motivation, enthusiasm, and immense knowledge. His guidance helped me in all the time of research and writing of this thesis.

I would also like to give special thanks to my father Halil Şekercioğlu, my mother Canan Şekercioğlu and my little sister Işıl Şekercioğlu for their great support. I would like to present the most important thank you to my life partner N. Pelin Eser, who was with me throughout the whole process.

Moreover, I would like to thank my laboratory partner Beyza Kardoğan for her help and support while I was conducting my thesis studies.

Furthermore, the funding by The Scientific and Technological Research Council of Turkey (TUBITAK) for Project No 120Y291 and titled “Production of Biogranules with Increased Biomineralization Capacity to Increase the Efficiency of Biomineralization Applications" is acknowledged.

TABLE OF CONTENTS

LIST OF FIGURES

LIST OF TABLES

ABBREVIATIONS

COD	Chemical Oxygen Demand
CRT	Cathode-Ray Tube
DO	Dissolved Oxygen
EC	European Commission
EEE	Electrical and Electronic Equipment
EPS	Extracellular Polymeric Substances
EU	European Union
HRT	Hydraulic Retention Time
HSF	Hydrodynamic shear force
ICP-MS	Inductively Coupled Plasma Mass Spectrometry
IT	Information Technology
MICP	Microbially-Induced Calcium Carbonate Precipitation
MLSS	Mixed Liquor Suspended Solids
MSP	Metal Sulfide Precipitation
NLR	Nitrogen Loading Rate
OLR	Organic Loading Rate
PCB	Printed Circuit Boards
REE	Rare Earth Elements
SBR	Sequencing Batch Reactor
SEM	Scanning Electron Microscope
SRT	Solid Retention Time
SVI	Sludge Volume Index
UASB	Upstream Anaerobic Sludge Blanket

WCC	Waste Collection Centers
WEEE	Waste Electrical and Electronic Equipment
WPCB	Waste Printed Circuit Boards

1. INTRODUCTION

Nowadays, Electrical and Electronic Equipment (EEE) are becoming more important day-by-day for society to satisfy their modern life needs [1]. The increase in the need for electronic equipment and consequently the consumption of these products cause massive amounts of electronic waste production as a result of the end-of-life of these items.

Waste Electrical and Electronic Equipment (WEEE), which is generally called e-waste, consists of several different waste electrical and electronic devices such as refrigerators, computers, mobile phones, TVs, LED bulbs, monitors, small home appliances [1]. WEEE is also defined as "*all components, sub-assemblies, and consumables, which are part of the product at the time of discarding"* by European Union (EU) in 2003 [2].

In addition to containing valuable materials, e-wastes contain materials that are highly harmful to the environment and extremely toxic to living things. The systematic collection of electronic wastes and recovery of valuable materials, in addition to reducing the increasing amount of electronic waste, reduces the negative environmental impact of these wastes by providing raw materials as a secondary source.

Constituents of electrical and electronic devices such as printed circuit boards (PCBs), lead capacitors, batteries, cathode-ray tubes (CRTs) are also defined as e-waste [3]. Among these devices, PCBs, which is a main part of nearly all EEE, appear as very valuable electronic wastes due to their precious metal content**.** In addition to being economically valuable, the metals contained in PCBs cause fatal toxic effects on living beings as a result of their uncontrolled disposal to the environment. For example, the legal limit value of the mercury content of WPCBs reaching groundwater is 2 ppb. Mercury poisoning and even deaths for humans are seen because of the consumption of water contaminated with mercury above this concentration [4]. Moreover, PCBs contain brominated flame retardants (BFR) and PVC plastics which are quite detrimental for environment as well as heavy metals. If these wastes are disposed of in unsanitary landfill areas, it may be possible for toxic substances to reach into underground waters together with the leachate that will occur. In addition, uncontrolled incineration of PCBs generates environmental emissions such as furans, polybrominated organic pollutants, polycyclic

aromatic hydrocarbons and dioxins, due to the presence of BFR, epoxy resins and plastics substances [5].

Typically, waste PCB has a content of 70% nonmetallic material and 30% metal consisting of copper, nickel, iron, aluminum, lead, zinc, even silver and gold [6]. The purity of these metals is 10 times higher than their natural metal ores, and therefore PCBs are described as "urban mineral resources" in the literature [7]. During metal exploitation from metal ores, important environmental burdens are created in terms of soil, water and air pollution, and the energy required for processing the ores is quite high. For example, according to a study conducted in China, 20 tons of wastewater and 3 tons of hazardous solid wastes are generated as a result of the process performed to obtain 1 ton of copper [8]. Therefore, recovering metal content of PCBs which constitutes over 80 % of their economic value, does not only create an important economic resource, but also a significant part of the environmental burden related to raw material extraction can be avoided [9].

Acid washing and open incineration processes are conventionally used for metal recovery from waste printed circuit boards (WPCB). However, heavy metal and organic pollutant emissions resulting from these processes are damaging people health who works at the recycling area [8]. In recent years, methods such as pneumatic separation, high temperature metallurgy, mechanical treatment, hydrometallurgy, supercritical process and bio-hydrometallurgy have been developed to both reduce the amount of emissions and increase the percentage of metal obtained [10,11,12,13,14]. However, it has been observed that using these processes separately could not be successful in increasing process efficiency. Therefore, it seems more beneficial to combine different processes in a single process chain and use them in an integrated way for metal recovery from WPCBs [8].

Among the aforementioned methods, number of research on development and improvement of bio-hydrometallurgical processes which exploits microbiological organisms has increased. This extra interest on bio-hydrometallurgical processes was due to the environmental impact and operational costs of hydrometallurgical methods. Ozkan evaluated pyrometallurgy, hydrometallurgy and biohydrometallurgy techniques on the basis of benefit, cost and risk clusters, using multi-criteria-decision-making methods. As

a result of the study, biohydrometallurgical methods emerged as the most efficient method with 72%, hydrometallurgical and pyrometallurgical methods remained at the rate of 26% and 2%, respectively [15].

Bio-hydrometallurgical processes were first used for mineral ores in the 1950s [16], and they are now considered as an environmentally friendly processes for metal recovery from electronic waste. The mechanism of bio-hydrometallurgical processes is actually quite similar with hydrometallurgical processes that use chemicals for extraction of metals from e-waste, but the former uses microorganisms to produce reagents such as H_2SO_4, HCN, $C_6H_8O_7$ which are used for extraction of metals from e-waste [17, 18, 19, 20].

Bio-hydrometallurgical processes generally classified under three main processes: (i) biosorption, (ii) bioleaching, (iii) biomineralization. Cost-effectiveness, environment friendliness and specificity are the major advantages of these biological metal recovery processes [21]. According to the studies in the literature, Cu and Zn recovery was achieved with approximately %100 recovery efficiency from wastes such as fly ash, slags, filter dust, galvanic sludge by using bio-hydrometallurgical methods [22]. Due to their high metal content PCBs appeared as a suitable WEEE for efficient metal recovery by means of bioleaching process.

Bioleaching is carried out with bacteria or fungus which can produce inorganic and organic acids or cyanide that stimulate enzymatic oxidation-reduction or ligand and complex formation [17]. Although many different types of microorganisms such as bacteria, fungi and yeast are used for the bioleaching processes [18, 19,20], iron-oxidizing bacteria and acidophilic sulfur-oxidizing bacteria are most commonly used. Previous studies revealed that bioleaching process is more suitable for metal extraction from low grade ore [23]. Nonetheless significant amount of bioleaching studies were also conducted for metal recovery from electronic waste and WPCBs. It was realized that the performance limiting parameter in bioleaching is the toxic effects of heavy metals on microorganisms [24]. In addition, some studies have also reported that organic content of PCBs such as brominated flame retardants (BFRs), might have toxic effects on microorganisms [25, 26]. Işıldar achieved 99% Cu and 92% Au recovery from PCBs by using acidophilic bacteria, despite the toxic effects of heavy metals formed during the process [27].

Biomineralization process is another technique used for metal recovery from contaminated soil, wastewater and metal ores. The biomineralization process generally takes place in two different ways as biologically induced mineralization (BIM) and biologically controlled mineralization (BCM) [28]. In the BIM mechanism, organisms provide a suitable physicochemical environment to precipitate metals. Calcium carbonate can be mentioned among the most common biomineralization agents of BIM process. Calcium carbonate precipitation by bacteria can often be induced and the type of mineral produced is substantially contingent upon environmental conditions. Denitrification, urea hydrolysis and metabolic conversion of organic compound, which are induced by microorganisms, are significant mechanisms of calcium carbonate precipitation that's why the process is called as microbially-induced calcium carbonate precipitation (MICP) [29].

In order to use MICP for metal recovery from electronic waste, the metal content in electronic waste must be dissolved. As a result of the bioleaching of electronic wastes, a leachate solution containing dissolved metal ions is obtained [30]. Metals in this solution are recovered via various chemical processes such as precipitation, ion exchange, solvent extraction, according to studies in the literature [31]. However, using MICP for metal recovery from leachate solutions appears to be a more environmentally friendly method as it will reduce the energy and chemical use in the recovery process. On the other hand, the use of microorganisms for metal recovery from electronic waste brings some difficulties. The most important of these is that the heavy metal content of electronic waste can be toxic to microorganisms above a certain threshold concentration. The high metal concentrations that the microorganisms are exposed to during the metal recovery process may cause microbial activity inhibition [32], bacterial lysis and thus low metal recovery efficiency [33]. Due to the poor adaptability of axenic cultures (pure cultures) to harsh environmental conditions [34], the use of non-axenic biogranules formed by the combination of various microorganisms might be more suitable for acclimation processes [35]. Since the acclimated non-axenic biogranules are reported to be more resilient to harsh environmental conditions [36], metal specific inhibitory concentration thresholds can be increased and thus the efficiency of microbial metal recovery process can be enhanced.

2. GENERAL INFORMATON

2.1. Waste Electrical and Electronic Equipment (WEEE)

Proportion of the WEEE in global waste composition have been increasing rapidly as a result of the population growth, economic growth and reckless consumption of electronic products, so that WEEE are considered among the most important environmental problems of the era. Recent studies revealed that e-waste is one of the fastest growing waste categories with an annual growth of between 3% and 5% [37]. Electrical and electronic equipment such as computers, mobile phones and cameras, which have become the necessities of modern life, turn into electronic waste when they complete their useful life. Factors such as changes in consumption habits as a result of the rapid development of technology, design and production of nondurable products by the producers to increase their sales, and the limited repair possibilities can be considered as the major reasons of the observed increase in e-waste generation [1].

When WEEEs are evaluated within the scope of circular economy, they can be considered as a source of secondary raw materials to natural resources due to their valuable material content. They also have a significant economic value because they contain high levels of precious metals such as Au, Ag, Ni and Cu.

2.1.1. Definition of WEEE

The definition and classification of WEEEs vary according to different organizations and researchers. While some organizations define e-waste as "user-discarded electronic devices from large household appliances to consumer electronics [38]", some defines it as an electrically operated device that no longer satisfies its current owner for its original purpose [39]. According to the United Nations, it is defined as “devices that are harmful to human and environmental health, contain toxic additives or dangerous substances such as mercury and lead and work with electricity” [40].

2.1.2. Types of WEEE

WEEE is generally divided into 4 main groups which constitutes approximately 95% of e-waste as large household appliances (Refrigerators, food freezers, dish washers, heat

pumps), small house appliances (Blender, kettle, oven, toaster), IT and telecommunication equipment and consumer equipment [41]. However, as shown in Table 2.1., the European Union has divided e-waste types into 10 categories in its Directive 2002/96/EC [2].

Table 2.1. Types of WEEE in accordance with EU Directive [40]

Category	**Label**	**Category**	**Label**
Large household appliances	Large HH	Electrical and electronic tools (with the exception of large-scale stationary industrial tools)	E&E tools
Small household appliances	Small HH	Toys, leisure and sports equipment	Toys
IT and telecommunications equipment	ICT	Medical devices (with the exception of all implanted and infected products)	Medical equipment
Consumer equipment	CE	Monitoring and control instruments	M&C
Lighting equipment	Lighting	Automatic dispensers	Dispensers

The valuable materials contained in WEEE often vary depending on the type, model, age and manufacturer of the EEE. For example, IT and telecommunications equipment contain more precious metals than household appliances. However, besides containing precious metals, WEEEs also contain metals such as Hg, Pb, Cr, which are highly toxic for the environment and human health. The average rates of valuable and toxic materials contained in WEEEs are given in Figure 2.1.

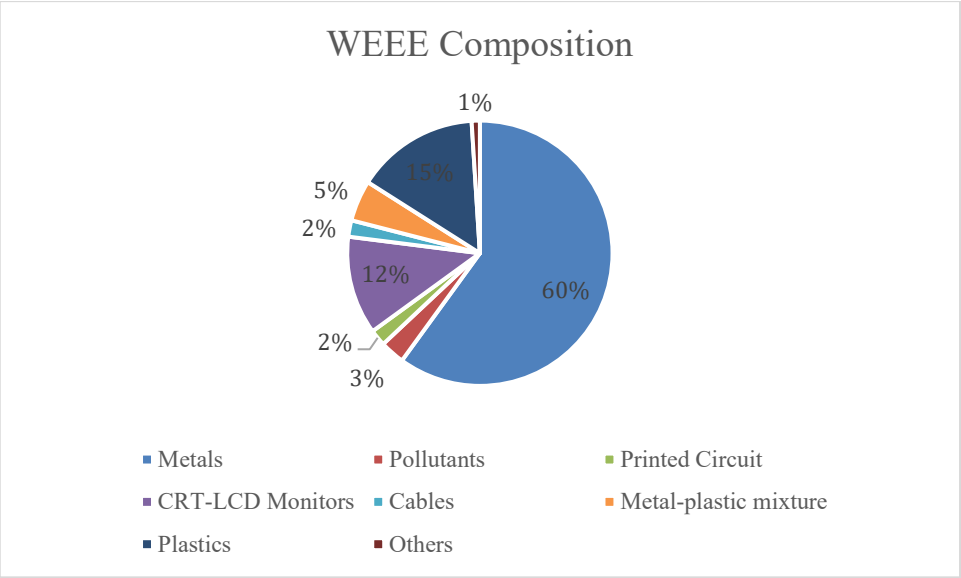

Figure 2.1. Material composition of WEEE [27]

The market value of precious metals contained in e-waste is estimated to be $14 billion. In addition, it is estimated that $10 billion worth of e-waste containing precious metals such as Au and Pt is generated every year [41].

2.1.3. Generation of WEEE

2.1.3.1. World Current Situation

When the current WEEE formation data is examined, e-waste formation, which was 41.8 million tons per year in 2014, reached 53.6 million tons per year in 2019 [41, 42] (Table 2.2.). WEEE production, which shows an average annual growth of 2 million tons, is expected to be 74.7 million tons in 2030 [41, 42]. However, after e-waste production, which has grown by about 2-3% to date, has grown by 6% in 2019, it is likely that much more e-waste will occur in the coming years than expected [41, 42].

Table 2.2. Amount of e-waste generated by waste types in 2019 [41]

WEEE Type	Amount (million ton)
Small Equipment	17.4
Large Equipment	13.1
Temperature Exchange Equipment	10.8
Telecommunication Equipment	6.7
Small IT	4.7
Lamps	0.9

WEEE produced per capita and total WEEE generated are increasing in all continents. The Asian continent, where countries with a large population such as China, Japan and India are located, has been the continent where the most electronic waste is produced in the world. WEEE production by continent is given in Table 2.3. [41].

Table 2.3. E-waste production by continent and its effects on global e-waste production [41].

Region	Total e-waste generation (MT)	Total Contribution (%)	E-waste Collected and Recycled (%)
Asia	24.9	46.45	11.70
Europe	13.1	24.44	42.50
Americas	12.0	22.39	9.40
Africa	2.9	5.41	0.9
Oceania	0.7	1.30	8.80

Although they have national e-waste policies, especially in developed countries in the Asian Continent, which prohibit the export of WEEE and make it mandatory to process it in their own licensed recycling and recovery facilities, the total amount of recycled waste remains at a very low level compared to the amount of waste generated [41].

After the Asian Continent, the most e-waste is generated in the Europe and the America. The amount of waste produced per capita per year in North and South American countries was reported as 12-13 kg [41] and thus the total amount of waste produced annually was calculated as 11-13 million tons [41]. The annual amount of WEEE in European countries has been kept steady around 12 million tons for the last six years by applying waste management strategies. In addition, according to official data, the amount of recycled WEEE in the USA was 1.2 million tons, while it was 5.1 million tons in Europe [41]. The main reason for this success of European countries that have managed to reduce the amount of waste produced per capita is that they develop strict WEEE management practices. Countries such as the USA and Canada have developed their own special legislation for e-waste management. The e-waste legislations implemented by Canada and the USA have given the responsibility for e-waste management more to the consumer than the producer [43]. As a result of this situation, the desired level of recovery and recycling cannot be achieved in e-waste management. European countries apply EU directives for e-waste management [41].

The continents of Africa and Oceania stand out as the continents with the lowest WEEE production. When 49 African countries are examined, Egypt, South Africa, Nigeria and Algeria are the African countries that produce the highest e-waste. However, unregistered practices are frequently carried out due to the incomplete WEEE legislations and insufficient control mechanisms in African countries [41].

Australia has been the country that produces the most e-waste among the 12 countries in the Oceania Continent, with an annual amount of 650 kilotons of e-waste. New Zealand is the second largest producer of e-waste with 96 kilotons per year [41]. As in the African Continent, many of the countries in Oceania have not established national WEEE legislation to conduct an efficient WEEE management and to prevent unregistered transactions. In addition, the Australian government enacted the National Television and Computer Recycling Plan (2011) which was aiming to increase the recycling rate of scrap televisions and computers to around 80% by 2027. It has been also prohibited to dispose of e-waste in landfills in Australia [41].

2.1.3.2. Turkey Current Situation

Due to the inadequacy of management systems and lack of social awareness, e-waste management cannot be carried out effectively, especially in developing countries [44]. In Turkey, which is among the developing countries, although there is a WEEE regulation for the collection, recovery and recycling of electronic waste, the e-waste recycling rate remains below the world average with 6% [45].

In 2010, 539 000 tons of e-waste was produced in Turkey and with an increasing trend this value reached to 847 000 tons in 2019 [41, 46]. In the study carried out by REC Turkey in 2010, the annual e-waste production was calculated as 0.27 kg/cap/yr. In the same study, it was predicted that the e-waste production value per capita would be 6.5 kg in 2020, but the annual e-waste production amount in Turkey has already reached 10.2 kg per capita in 2019 [41,47]. The amount of e-waste formed in Turkey between the years 2015-2019 is given in the Figure 2.2. As it is seen, only 3.2% of e-waste could be collected in Turkey in 2019. It is clear that the e-waste collection system needs to be improved in order to increase the recycling and recovery rate in Turkey.

In addition, in the report prepared by the European Commission (EC) in 2014, the amount of waste that may occur in Turkey in 2021 according to e-waste types is given in Figure 2.3. It seems that about 64% of the e-waste generated in Turkey consists of large and small household items. However, IT devices and monitors with high PCB content constitute a significant portion of e-waste in Turkey with 19%.

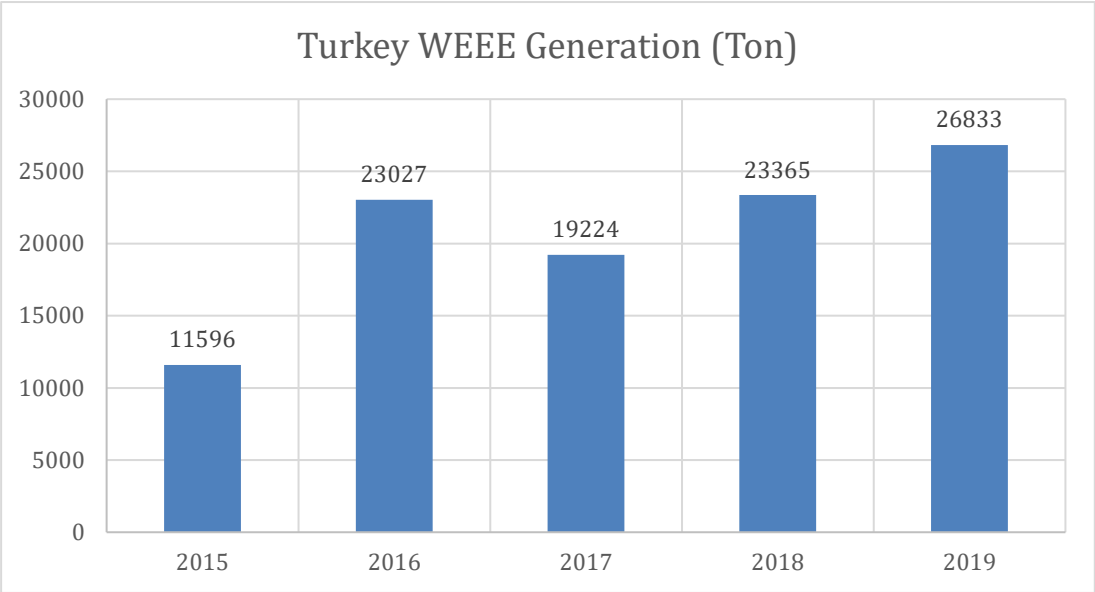

Figure 2.2. E-waste collection amounts by years in Turkey [48]

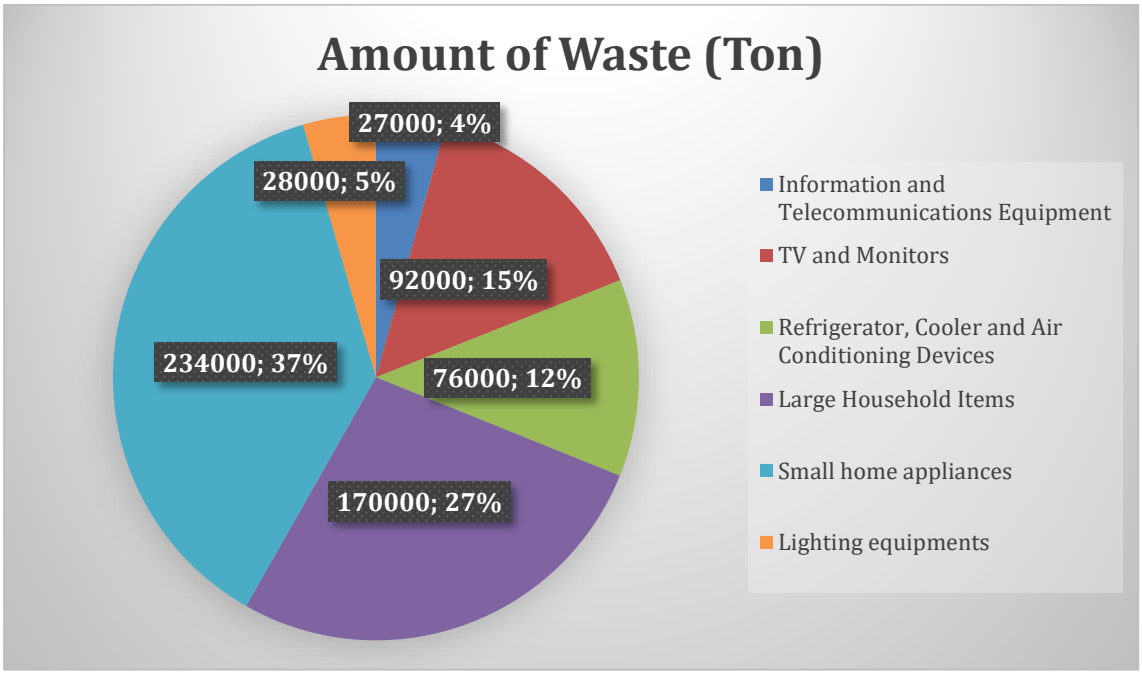

Figure 2.3. E-waste estimates by categories for Turkey in 2021 [49]

In 2021, the rate of unregistered transactions in e-waste management in Turkey is quite high, as is the case on a global scale. Very little of the e-waste generated is collected in landfills, which are the responsibility of municipalities. The most majority of e-waste is purchased free of charge or informally by small distributors and second-hand dealers and sold to processing facilities. In addition, a small portion of e-waste is collected by street collectors and sold to processing facilities. The most basic factors in the low e-waste recycling rate in Turkey are seen as informal transactions [50].

Turkey's e-waste collection and recycling rates seem to be insufficient compared to other developed countries. Therefore, Waste Collection Centers (WCC) seem to be the most suitable method in the efficient management of domestic e-waste for solution. Since the people should take their e-waste to the WCCs by their own means, it is important to raise awareness and encourage the public in this regard. Appropriate e-waste management methods currently applied in Turkey and recommended by the country's legislation are given in the Figure 2.4 [50].

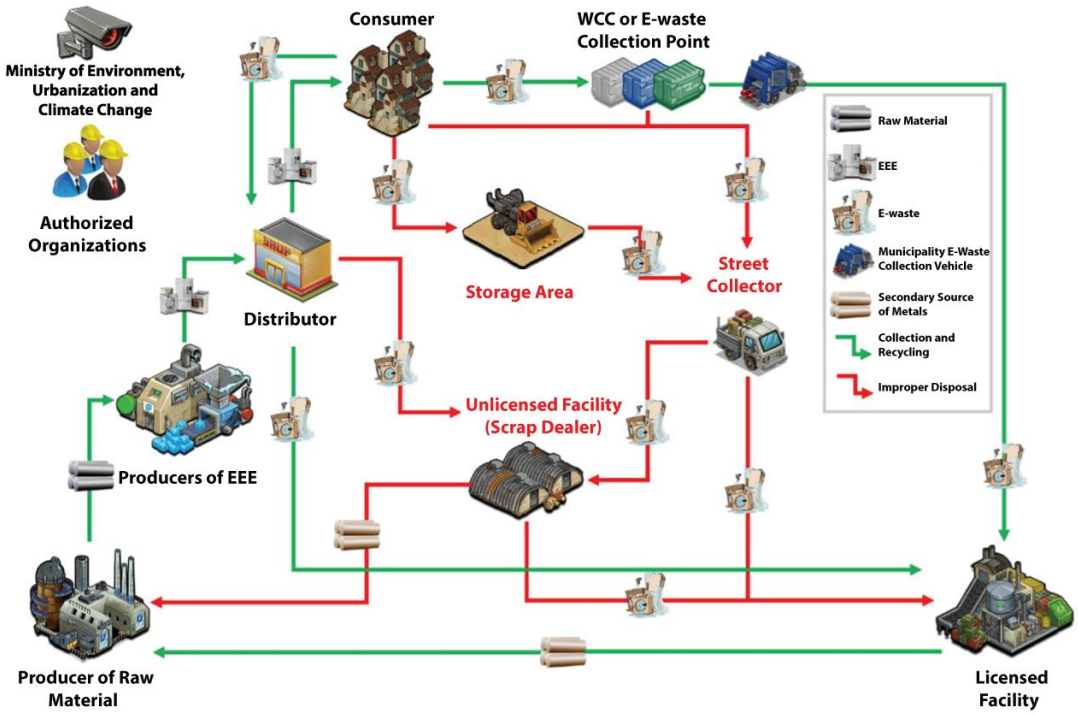

Figure 2.4. WEEE management proposed by the legislation and in practice in 2021; Green line indicates the legislation proposed, red line indicates the common practice [50]

The e-waste collected in WCCs is then taken to waste treatment facilities for physical pretreatment. Within the framework of certain standards, precious metal parts of e-waste are disassembled, shredded and sent to raw material manufacturing facilities for final recycling. Non-complex parts of e-waste such as iron, copper and plastic can be recycled simply by using these methods. However, the recovery of precious metals in printed circuit boards of devices such as mobile phones and computers is a complex process that requires high investment and technology. Currently, precious metal recovery processes from PCBs cannot be performed in Turkey. PCBs that are separated from the device they are in are collected and exported to different countries, primarily Germany, Belgium, France [50]. The inability to utilize semi-finished products with high precious metal content in processing facilities leads to serious employment and income loss.

Licensed WEEE processing facilities in Turkey reached 98 at the end of 2018 [50]. The high amount of WEEE, which is formed due to the population density, has made the establishment of WEEE processing facilities in Istanbul, Ankara and Kocaeli provinces widespread. However, some big cities such as Adana and Konya do not have e-waste processing facilities although they have high population and developed industry. The number of e-waste facilities currently serving in Turkey is given in the Table 2.4. according to the provinces they are located in.

Table 2.4. Licensed E-waste Recovery Facilities (2018) [50]

City	E-Waste Recovery Facility	City	E-Waste Recovery Facility
Ankara	25	Sakarya	2
İstanbul	13	Amasya	1
Kocaeli	13	Aksaray	1
Bursa	9	Balıkesir	1
Eskişehir	5	Düzce	1
Manisa	3	Hatay	1
Denizli	3	Kırıkkale	1
Bolu	3	Mardin	1
Antalya	2	Mersin	1
İzmir	2	Samsun	1
Konya	2	Tekirdağ	1
Nevşehir	2	Tokat	1
Niğde	2	Zonguldak	1

2.1.4 Management of WEEE

According to the waste management hierarchy, reducing the materials used in the production of EEE and controlling the consumption habits are the most important forms of e-waste management in order to prevent the generation of e-waste or reduce its amount. It is important that the reuse and recycling of the e-waste generated are carried out efficiently, taking into account environmental concerns.

The management of e-waste generated in households around the world is ensured by being thrown into the trash cans, collected by state-authorized organizations, and collected by informal companies and street collectors. Thanks to the official collection and recycling studies carried out by licensed companies and municipalities, valuable materials are recovered by using advanced technology, while effective control of environmentally harmful substances is ensured.

The use of these methods as a last resort should be encouraged in order to prevent the environmental burdens and economic losses caused by the waste storage and incineration options known as traditional methods. For example, Molto et al. have shown that serious polycyclic aromatic hydrocarbons and polychlorinated biphenyls emissions occur as a result of thermal disposal of mobile phones [51]. Widmer et al. (2005) stated that 70% of heavy metals found in landfills in the USA come from e-waste [40].

One of the most important issues that should be dealt with in e-waste management is e-waste export, especially implemented by developed countries. Developed countries generally export 50% of their e-waste to China, and the rest to countries such as Ghana, India, and Nigeria illegally [44]. It is known that the processes carried out in these countries, especially without suitable recycling technologies, contribute to global environmental pollution significantly [52]. For example, most of the waste in Agbogbloshie, Ghana, which is considered one of the largest e-waste landfills in the world, has been disposed of informally. In addition, recycling studies here are carried out without considering health and safety measurements and decent technological advances. Andrea et al. found in a study that recycling workers in Agbogbloshie are exposed to considerable amount of polychlorinated biphenyl [53].

Collection and recycling activities carried out by unlicensed persons and companies are generally carried out using inadequate and environmentally unfriendly methods (i.e. uncontrolled release of pollutants). However, the use of inappropriate methods in recycling causes a significant part of the valuable resources to cannot be recovered during the process. Only about 17.4% (9.3 Mt) of e-waste produced on a global scale in 2019 was collected by official organizations and the remaining 44.3 Mt was collected and recycled through informal means [41]. One of the most important reasons for this high rate is the informal transactions in Asian and African countries.

Due to the coexistence of precious metals such as Fe, Al, Au, Cu, Ni, WEEEs constitute a serious economic resource for scrap dealers, recovery and recycling companies. However, the use of strong acids such as HNO_3, H_2SO_4, HCl, for the extraction of heavy metals from WEEE cause emission of toxic gases and reactive compounds to the environment. Moreover, presence of brominated flame retardants and polychlorinated biphenyls in WEEE and production of toxic substances like polychlorinated dibenzo-p-dioxins, polychlorinated dibenzofurans, polycyclic aromatic hydrocarbons during the recycling process, significantly increase the adverse environmental impact of the recycling processes. In management of WEEE, emissions are classified into three main types; (i) pollutants in e-waste are defined as primary emissions, (ii) pollutants generated during recycling processes are defined as secondary emissions, (iii) emissions created by chemicals used for processing are defined as tertiary emissions [1].

2.2. Printed Circuit Board (PCB)

Printed circuit boards are one of the most basic components of most EEEs. It is produced by coating a thin layer of copper foil on the surfaces of a plate made of epoxy resin and glass fiber. The conductive paths of the circuits are made of copper to connect the electronic components to be soldered on [54]. PCBs are generally produced from varying concentrations of plastic, non-ferrous and ferrous metals [27].

PCB contents vary according to the year of manufacture, resource device and board type. PCBs produced in recent years contain much less metal concentration than PCBs produced in previous years. Integrated circuits produced with the combination of different types of circuits and electronic components are the PCBs with the highest metal content.

These types of PCBs turn into one of the most dangerous e-waste for the environment at the end of their useful life.

About 20% of the total weight of a typical laptop is PCB. At around 250-300 g, PCB has the third largest mass after display and battery [55]. The PCB contents of devices such as TVs and phones are also quite high. Table 2.5. shows the PCB percentages of EEEs by mass.

Table 2.5. PCB Ratios of EEE Types [56]

Resource Device	Amount of PCB (w/w)
Computer	19.23
TV	10.55
Phone	7.77
Radio	6.34
Calculator	5.12
Control Device	9.95
Video Recorder	3.86
Tape Recorder	6.14

PCBs' metal content is generally about 40% of the total mass. The copper used to manufacture PCB circuits accounts for about one-third (~13% of the overall) of the amount of metal used in a circuit. Other metals found in electrical components or used for brazing are precious metals such as Au, Ag, Ni Fe. In addition, there are rare elements with very high economic value such as 0.3% Ag, 0.1% Au and 0.03% Pd by weight. Depending on the current price situation of these three precious metals in the markets, it represents 80% of the economic value of PCBs, Table 2.6. gives the heavy metal concentrations in PCBs such as nickel, lead, copper which have negative effects on the environment [57].

Table 2.6. Metal percentage of PCBs [58]

Metal	Amount
Cu	10-26.8%
Al	1.3-4.8%
Pb	1-4.2%
Zn	0.2-2.2%

Ni	0.3-2.4%
Fe	1.22-8%
Sn	1-5.3%
Sb	0-0.4%
Au	80-1000 ppm
Pt	4.6-30 ppm
Ag	110-3301 ppm
Pd	10-294 ppm

PCBs contain electrical components such as resistors, integrated circuit chips, transformers, capacitors, in different sizes and compositions. Metal wires, usually made of copper or aluminum, are used to connect the components. In PCB production, semiconductors containing As, Sb, Se, Te, Ga, In, Ti, Si, Ge and Pb and Cd metals are used in solder connections [58].

When PCBs complete their useful life, they turn into e-waste just like the other EEEs. The copper and nickel contents of these waste printed circuit boards are 13-26 times higher than the concentrations found in natural metal ores. WPCBs with such high precious metal content are stated among the secondary metal sources possessing significant economic value [59].

In 2019, a total of 847000 tons of WEEE was collected in Turkey, of which 19% is made up of TV, information equipment and telephones. On average, the PCB content of IT, TV and telephone devices corresponds to approximately 12.52% of the mass. A PCB is composed of an average of 18.4% copper and 1.32% nickel. While the current price (October 2021) of 1 ton of nickel is 20215 dollars, 1 ton of copper is 10500 dollars. In the light of these data, the economic value of the copper content of WPCBs formed in Turkey in 2019 was 38.93 million dollars, while the wasted nickel value was 53.76 million dollars. As can be seen, every PCB that cannot be recovered is seen as a serious loss of economic value and secondary resource [41, 49, 56, 58].

2.3. Metal Recovery from PCBs

2.3.1. Physical Methods

In order to recover precious metals from WPCBs with complex structures and electronic components, it is necessary to remove toxic substances and non-metallic parts. Physical pre-treatments are needed to separate these parts and to classify valuable parts according to their metal content.

Physical processes are commonly the first step in metal recovery from WEEE. Technologies such as disassembly, size reduction, magnetic separation and Eddy-current separation have been developed according to the physical and chemical properties of the materials in WEEE. Physical separation processes are low-cost processes, but metal losses are between 10-35% in these processes [60]. The reason for the metal losses is that the metals that are not in the appropriate particle size for crushing processes cannot be separated from the plastic parts. In order to minimize metal loss in the WPCB recycling sector, physical processes are used only as a pre-separation process before pyrometallurgical, hydrometallurgical and bio-hydrometallurgical methods.

2.3.1.1. Disassembly

Firstly, different electronic components on WPCBs are separated, usually by disassembly method. In addition, as a result of the disassembly of WPCB components, the toxic components in the PCBs are prevented from entering the recycling process [61]. Components such as capacitors and batteries that are decomposed at this stage are processed in special recycling facilities due to the toxic heavy metal contents of these components [62]. Figure 2.5. shows how a TV-WPCB looks before and after disassembly.

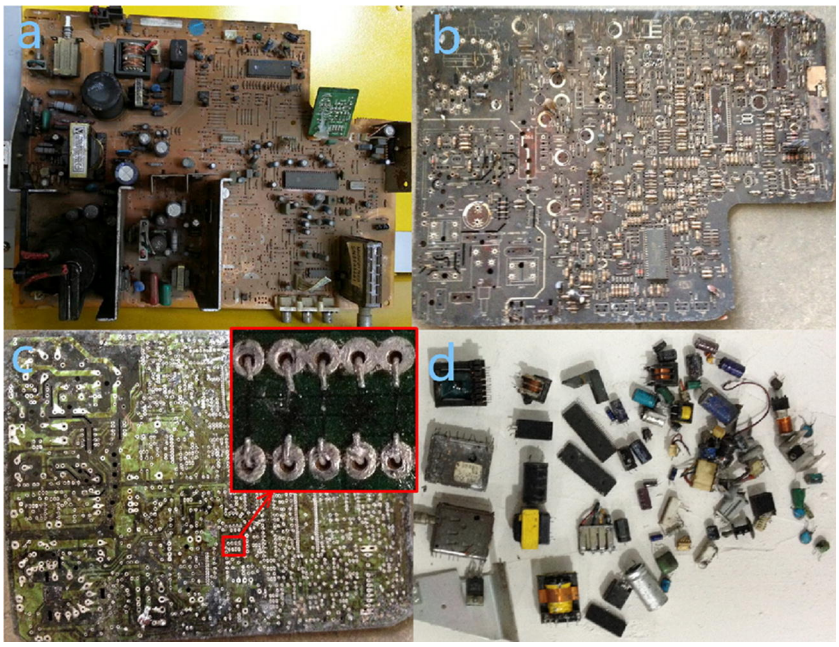

Figure 2.5. Photos of the TV-WPCB: (a) TV-WPCB (b) front side of the TV-WPCB after dismantling, (c) back of the TV-WPCB after dismantling, and (d) dismantled electronic components [63]

Disassembly can be performed manually, semi-automatically or automatically. Manual disassembly is the most preferred method in conventional applications. In automatic disassembly, a flexible algorithm is needed that can change itself by instantly evaluating the product condition. It has been reported that when this algorithm is developed properly, automatic removal will be the most economically feasible method [64].

In current conventional processes, WEEE recycling mostly starts with the separation/removal process. Removing hazardous parts and sorting reusable parts provide the most efficiency in further recycling activities. In the disassembly process, PCB, cable, battery and plastic parts are generally separated by hand. PCBs are then disassembled using additional separation processes at specialized recycling facilities [65].

During the disassembly process, not all parts of WEEE containing hazardous materials can be separated. In this case, some hazardous materials go through the crushing processes and blended with valuable recyclable materials, leading to a reduction of their recycling rate. [66]. As a result of these situations, disassembly is seen as the most important step in the PCB recycling chain for increasing the recycling efficiency, protecting resources and reducing environmental emissions [65].

2.3.1.2. Shredding and Size Reduction

After the removal of toxic materials, processes such as crushing, grinding and crushing are used to separate precious metals from coating materials such as glass fiber, plastic and resin and to bring the metals to the desired particle size. Equipments such as rotary crushers, disc crushers and hammer crushers are used for crushing and shredding operations [61].

The use of conventional crushers is not very efficient in the shredding process of PCBs produced in multilayers from copper wires, reinforced resin and glass fiber. It has been suggested that size reduction by trimming and cutting methods is more suitable for WPCBs. There is no fixed size fraction for the release of metals contained in PCBs, as in metal ores. Different size fractions are used for the release of different metals. For example, Zhang et al. revealed that ferromagnetic metals and copper in WPCB are completely free below 6 mm size, but larger sizes are needed for aluminum release [67].

In the size reduction processes of WPCB, 1-2 cm^2 pieces are cut first, usually with the help of grinders or granulators. It is then reduced to 5-10 mm with the help of a cutting or centrifugal mill equipped with a lower sieve. The most important disadvantage of this method is the formation of brominated and non-brominated phenol emissions when the WPCB temperature rises above 250 °C during impact and crushing [68]. In addition, another problem that occurs during the size reduction processes of WPCBs is the formation of fine dust, which is very difficult to evaluate during downstream processing.

Bio-recovery methods such as bioleaching are frequently used for metal recovery from WPCBs, and precipitate formation is common during these processes. Generally, this precipitate is expected to be composed of ferric hydroxides, while the precipitate formed during metal recovery from powdered WPCBs by bioleaching consists of Cu, Pb, Sn and Fe [69]. As a result of the precipitate being in this form, the separation of the residual WPCB powder and the precipitate becomes more difficult, making the recovery process more complicated [70].

Furthermore, if larger WPCB parts were used for metal recovery, the non-metal parts can also be easily recycled after the process. Therefore, it seems more appropriate to use larger pieces than powder WPCB in order to prevent precipitate contamination and make

the recycling process efficient. However, when bioleaching is applied on large pieces, the chemical coatings on the pieces prevent microorganisms from reaching the metals. To eliminate this problem, it is necessary to remove the chemical coatings before bioleaching [70].

2.3.1.3. Magnetic Separation

The method that allows metals with different magnetic susceptibility to be separated from each other in the appropriate magnetic field in WPCBs is called magnetic separation. Low-intensity drum magnetic separators are used for the recovery of non-ferrous metals and non-magnetic WPCB components [71].

The pieces formed after shredding and size reduction are fed onto the drum with a conveyor belt. Magnetic parts move by accumulating on the drum surface. Non-magnetic parts, on the other hand, fall in a parabolic trajectory due to gravity and centrifugal force. Due to the different magnetic poles, the pieces next to each other move by rotating and thus the non-magnetic pieces that are stuck between them are separated and fall [54].

Fragmented WPCB contains approximately 4.5-11% amount magnetic metal of its total weight [72]. In the magnetic separation process, while Fe and Ni accumulate in the magnetic fraction, Cu is accumulated in the conductive area [27]. However, with this method, metal species cannot be separated from their alloys.

2.3.1.4. Electrostatic Separation

In order to separate the non-ferrous metals and non-conductive materials contained in PCBs, the separation process using the different electrical conductivity properties of these components is called electrostatic separation. Basically, electrostatic separation is applied with three different method such as Eddy current separation, corona electrostatic separation and triboelectric separation [73, 74, 75].

In the Eddy Current method, which is generally used during the separation of metals such as Cu, Al, Pb and Zn, eddy currents are formed thanks to the voltage applied to the separators and these currents create a magnetic field [76]. WPCB parts fed on a rotating conveyor at the top are pulled onto the drum by the magnetic field. Other materials with weak electrical conductivity are not affected by the magnetic field and accumulate in the

collection section. The investment cost of the Eddy current separation method is high and the working efficiency is low for particle sizes smaller than 5 mm [71].

Corona electrostatic separators are used in the separation of metal and non-metal parts in materials with a particle size of 0.1-0.5 mm [77]. In addition, the triboelectric separator is used for plastic separation from materials with particle sizes smaller than 5 mm due to its low energy consumption and high processing capacity [78].

2.3.2. Hydrometallurgical (Chemical) Methods

Many base and precious metal ions from WEEEs can be recovered by extraction with hydrometallurgical methods using commercial chemicals. In order to obtain high metal recovery efficiency, it is crucial to use solvents suitable for the metals to be recovered and to apply pre-treatments to increase the efficiency. However, the use of chemicals and energy increases the cost of precious metal recovery from WEEEs by hydrometallurgical methods. Nevertheless, the recovery of precious metals such as rare earth elements (REE) by hydrometallurgical methods compensates for the high costs of the processes [79]. The precious and base metals that can be recovered by hydrometallurgical methods are given in Table 2.7. according to their classes.

Table 2.7. Metals that can be recovered by hydrometallurgical methods

Classification	Metal
Base Metals	Cu, Al, Ni, Zn, Fe, Sn
Precious metals	Au, Ag
Platinum Group Metals	Pd, Pt, Rh, Ir, Ru
Hazardous Metals	Hg, Pb, Cd, As, Sb
Rare Earth Elements	In, Te, Ga, Se, Ge, Ta

Hydrometallurgical methods are realized with the use of chemicals such as acid reagents, oxidizing agents in the aqueous medium. For example, acids such as HCl, H_2SO_4, $C_2H_2O_4$, are used to dissolve copper from WPCBs [54]. Name of leaching processes such as oxidative acid leaching, thiosulfate leaching, cyanide leaching, halogen leaching is given according to the type of solvent used in the recovery of base and precious metals from PCBs.

As PCB has a multi-layer structure and solvents cannot fully penetrate between these layers, metal losses between 10-35% ocurr during the leaching process. These losses can be reduced by performing size reduction processes before the leaching process. [80].

All of the purification processes such as solvent extraction, ion exchange, adsorption are performed following the leaching processes to release metals from WPCB surfaces and these type of processes are classified under hydrometallurgy [65].

2.3.2.1. Oxidative Acid Leaching

Mineral acids such as H_2SO_4, HCl and HNO_3 are widely used for extraction processes due to the flexibility of process control and scale-up advantages for metal recovery from WPCBs. [81]. While base metals such as Fe, Al, Zn are generally leached with dilute acids, precious metals are leached with concentrated strong oxidizing acids like HNO_3.

According to a study by Kumari et al., increase in pressure enhances metal dissolution [82]. The recovery efficiency was determined as 99% when Cu, Ni, Fe metals were reacted with 2.4 M H_2SO_4 at 150 °C and 20 bar oxygen pressure for 90 minutes. It has been determined that when chemical reagents such as $CuCl_2$ and H_2O_2 are added to the process for Cu leaching, the efficiency increases even more [82]. Moreover, Oh et al. revealed in their study that different chemical concentrations can dissolve metals selectively. In the study, 95% of Cu, Fe, Zn, Ni, and Al were dissolved with 2 M sulfuric acid and 0.2 M hydrogen peroxide. Ag and Au were dissolved with 0.2 M ammonium thiosulfate, 0.02 M copper (II) sulfate and 0.4 M ammonium hydroxide at 100% and 95% rate, respectively [83].

Furthermore, HCl acid leaching is widely used for the extraction of metals such as Ni, Al, Fe, Zn, Ag from WPCBs [84]. The chemical reactions of solid Al, Zn, Ni, Fe, Ag metals during the leaching process with HCl are given in Eqn. (1-5).

$$2Al_{(s)} + 6HCl_{(aq)} \rightarrow 2AlCl_{3\,(aq)} + H_{2\,(g)} \quad (1)$$

$$Zn_{(s)} + 2HCl_{(aq)} \rightarrow ZnCl_{2\,(aq)} + H_{2\,(g)} \quad (2)$$

$$Ni_{(s)} + 2HCl_{(aq)} \rightarrow NiCl_{2\,(aq)} + H_{2\,(g)} \quad (3)$$

$$Fe_{(s)} + 2HCl_{(aq)} \rightarrow FeCl_{2\,(aq)} + H_{2\,(g)} \quad (4)$$

$$2Ag_{(s)} + 2HCl_{(aq)} \rightarrow 2AgCl_{2\,(aq)} + H_{2\,(g)} \quad (5)$$

2.3.2.2. Cyanide Leaching

Cyanide leaching has been used in the mining industry for many years to separate Au from primary Au ores. Cyanide was used as a liquefier in approximately 875 Au and Ag mines that were actively operated in 2000 [85]. Cyanide extraction of Au in the ore is an electrochemical reaction and that is given in Eqn. (6-7) [86].

$$4Au + 8CN^- \rightarrow 4Au(CN)_2^- + 4e \quad (6)$$

$$O_2 + 2H_2O + 4e \rightarrow 4OH^- \quad (7)$$

As a result of the cyanide leaching process carried out in the pH range of 10-10.5, it was determined that the extraction efficiency of precious metals was higher than base metals. The highest activity was observed in Au metal, followed by Ag, Pd and Pt, respectively [86].

Since WPCBs contain significant amounts of Au and Ag, cyanide leaching can be used to recover precious metals from WPCBs. However, Cu content dissolution of WPCB causes excess amount of cyanide consumption. In addition, CuO and $Cu(OH)_2$ layers formed on the particle surface, due to the 23.4% (w/w) Cu content of WPCB, may adversely affect the dissolution of precious metals [87]. Furthermore, the CN^- leaching process in WPCB recycling is quite slow [88].

Considering the reasons such as CN^- pollution from accidents in Au mines, aforementioned operational inefficiency in precious metal recovery from WPCBs due to high consumption of CN^-, and the hazardous of WPCB recycling facilities that use cyanide due to the prohibition of high cyanide use in urban areas on a global scale, alternative techniques to cyanide leaching are being investigated. There is a need to use more suitable hydrometallurgical techniques such as thiourea. Moreover, instead of hydrometallurgical recovery methods with high chemical consumption and high energy needs, bio-hydrometallurgical methods which proposes a more sustainable and bio-based

solution for extraction and recovery of metals should be prioritized in the approaching bioeconomy era.

2.3.2.3. Thiosulfate Leaching

Thiosulfate ($S_2O_3^{-2}$) leaching process is suggested as an alternative to cyanide due to its low environmental impact, low corrosivity, high selectivity and economically feasibility for the recovery of precious metals such as Au and Ag from WPCBs [89]. Since thiosulfate decomposes easily in an acidic environment, thiosulfate leaching is carried out in the pH range of 9.0-10.5 [90]. In order to perform Au extraction in alkaline thiosulfate solution quickly and efficiently, it is necessary to add a catalyst such as Cu(II) and NH_3 to the solution [91]. When Cu(II) and NH_3 are used as a catalyst in thiosulfate leaching of Au from solid form, the reaction that will take place is given in Eqn. (8-9). The $Cu(NH_3)_4^{+2}$ species in the solution extract electrons in the cathodic part of the Au surface and are directly reduced to $Cu(NH_3)_4^{+}$. Then, ammonia or thiosulfate ions react with Au ions and $Au(NH_3)_4^{+2}$ or $Au(S_2O_3)_2^{-3}$ species occur.

$$Au + 5S_2O_3^{-2} + Cu(NH_3)_4^{+2} \rightarrow Au(S_2O_3)_2^{-3} + 4NH_3 + Cu(S_2O_3)_3^{-5} \quad (8)$$

$$Cu(S_2O_3)_3^{-5} + 8NH_3 + \frac{1}{2}O_2 + H_2O \rightarrow 2Cu(NH_3)_4^{+2} + 2OH^- + 6S_2O_3^{-2} \quad (9)$$

Due to the high reagent and thiosulfate consumption, the thiosulfate leaching method might not be an economical and efficient technique for the recovery of precious metals from WPCBs, despite its potential environmental benefits. Appropriate additional chemicals and proper pretreatment process can improve operating conditions and obtain a more efficient thiosulfate leaching for metal recovery from WPCBs [91].

2.3.2.4. Thiourea Leaching

The use of thiourea for metal extraction is more environmentally friendly and less toxic compared to traditional leaching methods, and in this method leaching of gold and silver reaches 99% efficiency levels [92]. As seen in Eqn. (10-11), thiourea transforms Au and Ag into soluble form by forming cationic complexes in acidic medium.

$$Au + 2SC(NH_2)_2 + Fe^{+3} \rightarrow Au(SC[NH_2]_2)_2^{+} + Fe^{+2} \quad (10)$$

$$Ag + 2SC(NH_2)_2 + Fe^{+3} \rightarrow \ Ag(SC[NH_2]_2)_2^+ + Fe^{+2} \quad (11)$$

In leaching processes, Fe^{+3} is generally used as an oxidizer. It has been proven that the addition of extra Fe^{+3} to the process in thiourea leaching process can increase the extraction efficiency up to 4 times [93]. However, when excessive Fe^{+3} is added to the system, Fe^{+3} oxidizes thiourea and consumes thiourea, and as a result, the leaching efficiency may decrease [94].

Thiourea is very sensitive to pH changes and decomposes easily when the pH drops below 4.3 [95]. Thiourea leaching is generally carried out in the 1-2 pH range. Thanks to the extremely acidic environment, metals such as Fe, Cu, Ni, Zn in WPCBs can also be extracted [93].

2.3.3. Bio-hydrometallurgical (Biological) Methods

The method in which microorganisms are used to extract metal from metal ores and electronic waste is called bio-hydrometallurgy [96]. The adverse environmental effects of bio-hydrometallurgy are less than those of hydrometallurgy. Since it also enables metal recovery from low grade and complex ores, the number of studies in this field has been increasing day by day [97]. Commercial metal extraction from ores by bio-hydrometallurgical methods was first performed in a Cu mine in Chile in the 1980s. Today, 15% of the global Cu production and 5% of the Au production are provided by bio-hydrometallurgical methods [96]. In addition to Cu and Au, biohydrometallurgy has been extensively investigated and applied for extraction of Ni, Zn and Co.

Table 2.8. List of metal recovery efficiencies from WPCBs

No	Recovery method	Microorganism used	Metal recovery (%)	Operation conditions			Reference
				pH	°C	Day	
1	Acidophilic Bioleaching	*Acidithiobacillus ferrivorans* *Acidithiobacillus thiooxidans*	Cu – 98.4	1.0–1.6	23	7	[98]

2	Cyanogenic Bioleaching	*Pseudomonas fluorescens* *Pseudomonas putida*	Au – 44.0	7.3–8.6	30	2	[98]
3	Acidophilic Bioleaching	*Acidithiobacillus* sp.	Cd – 93 Cu – 53 Ni – 48.5 Zn - 48	2.0–3.0	37	15	[99]
4	Cyanogenic Bioleaching	*Chromobacterium violaceum*	Au – 22.5	9.5	30	8	[100]
5	Acidophilic Bioleaching	*Acidithiobacillus ferrooxidans* *Leptospirillum ferrooxidans* *Acidithiobacillus thiooxidans*	Cu – 83	1.7	35	5	[101]
6	Cyanogenic Bioleaching	*Pseudomonas Chlororaphis*	Cu – 52.3 Ag – 12.1 Au – 8.2	7.0	25	3	[102]
7	Fungal Bioleaching	*Aspergillus niger* MXPE6 *Aspergillus niger* MX7	Au – 87 Cu – 24 Ni – 0.6	4.4	28	14	[103]
8	Cyanogenic Bioleaching	*Chromobacterium violaceum*	Cu – 24.6 Au – 11.31	10.0–11.0	30	8	[104]
9	Bioleaching	*Pseudomonas fluorescens*	Au – 54	9.0	30	56 h	[105]
10	Thiourea bioleaching	*Acidiplasma* sp.	Au – 98 Ag – 14	1.5	45	2	[106]

Reasons such as the reduction of easily extractable ore deposits, the extraction of low-grade and complex ores from deeper deposits, the acceleration of electronic waste production day by day are seen as the driving force in the development of bio-hydrometallurgical techniques. The importance of biological methods, which are developed to reduce the environmental effects created by the high chemical and energy needs of the conventional methods used by the mining and recycling sectors, within the framework of the circular economy, is increasing in the current situation.

According to the interaction between metals and microorganisms, bioprocessing techniques have been named differently, such as biosorption, bioleaching, bioprecipitation, bioaccumulation [107]. For instance, metal extraction from ores and e-waste is defined as a bioleaching process in the literature. In addition, the process of accumulating organic or inorganic pollutants by living organisms or using their own metabolic activities is called bioaccumulation. Moreover, the process of removing the pollutants from the environment by precipitating various metabolites produced by some microorganisms as a result of their metabolic activities is called bioprecipitation.

2.3.3.1. Biosorption

The process of removing substances through binding of metal ions with proteins present on the cell surface from the solution using microorganisms such as bacteria, fungi and algae is called biosorption [108]. It has been widely used in recent years, especially in metal recovery from WEEEs, metal removal from wastewater and electroplating applications due to its features such as simple processing, reusability and high metal recovery [109, 110].

The mechanism of biosorption is realized by the adsorption of metal on biosorbents by electrostatic interactions rather than interactions such as chemical reactions and ion exchange [91]. It has been proven that extracellular proteins play an important role in the biosorption process using microorganisms. For example, 1 mg of extracellular protein obtained from *Tepidimonas fonticaldi sp.* can adsorb 9.7 mg of gold. In addition, in the study carried out to treat the wastewater of the PCB production factory, 71% of the gold in the wastewater was removed by using the extracellular proteins. [111]. Furthermore, significant progress has been made in recent years as a result of the studies carried out to improve the adsorption capacity. For example, *E. coli* suspension treated at 90-100 °C temperature realised biosorption process 7 times faster than untreated suspension [112]. Thanks to the increased zeta potential and free amino acids on the cell surface as a result of thermal treatment, the biosorption efficiency has increased.

2.3.3.2. Bioleaching

Metal solubilization using microorganisms from WEEEs and ores is called bioleaching. In the ores, metals in sulfur and oxide forms are solubilized as metal cations [107]. Then,

the purity of dissolved metals is increased by using techniques such as solvent extraction, adsorption, membrane separation, and selective precipitation [107]. Bioleaching, which is successfully used for the extraction of valuable metals such as Cu, Ni, Zn, Co, U, is also known as bio-oxidation. For example, CuS_2 is oxidized to $CuSO_4$ by microorganisms and metal ions dissolve and mobilize in the aqueous phase [107].

Due to the scarcity of natural metal resources, bioleaching technology is gaining importance day by day for metal recovery from electronic wastes, which are seen as secondary metal resources. Bioleaching process is seen as an environmentally friendly technology in e-waste management in order to prevent leakages due to e-waste and to recover the metals back into the economy [113].

Microorganism species used in bioleaching process are divided into two main groups as chemolithotrophs and chemoorganotrophs according to their energy source preferences. Microorganisms that use inorganic electron donors such as hydrogen, iron and sulfur as energy sources in the low pH range are called chemolithotrophs. In addition, chemolithotrophs are divided into 3 groups as thermophilic, moderately thermophilic and mesophilic according to their optimal growth temperature. Thermophiles (60-80 °C) usually consist of archaea, while mesophiles (28-37 °C) and intermediate thermophiles (40-60 °C) are usually bacteria [114]. Microorganisms that use CO_2 as carbon source are called chemolithotrophic autotrophs, while microorganisms that use organic carbon as carbon source are called chemolithotrophic heterotrophs. Fungi that use organic carbon as an energy source, such as fungi and cynogenic microbes, are called chemoorganoheterotrophs.

Chemolithotrophs generally tend to grow in highly acidic (2.0 pH) conditions. The most preferred chemolithotrophs for bioleaching, such as *Acidithiobacillus ferrooxidans* and *Acidithiobacillus thiooxidans* bacteria, oxidizes reduced sulfur compounds (S_8, $S_2O_3^{-2}$ and H_2S or polysulfide) to SO_4^{2-} or Fe^{+2} to Fe^{+3} [115, 116].

Fungi, which are considered as chemoorganotrophic, consume organic carbon and turn it into organic acid, while cyanogenic microbes produce HCN. These produced products react with metals and metal extraction takes place [34].

The process, which is generally carried out at a pH range of 3.0-7.0 and at a temperature of 25-35°C, using organic acids such as gluconic, citric and oxalic acids produced by fungal species such as *Aspergillius niger* and *Aspergillius flavus*, is called fungal bioleaching [117,34].

The most commonly used bacterial species in the cyanogenic bioleaching process, which is generally carried out in the pH range of 7.0-11.0 and at a temperature of 25-35°C, are as follows; *Pseudomonas fluorescens*, *Pseudomonas aeruginosa*, *Pseudomonas putida*, *Chromobacterium violaceum*, *Bacillus megaterium*, *Pseudomonas chlorophis*, *Pseudomonas aureofaciens* and *Escherichia coli* [118]. In addition, *Marasmius oreades*, *Clitocybe sp.* HCN-producing fungi species such as *Polysporus sp*. are also preferred for bioleaching [119].

Acidophilic (Chemolithotrophic) Bioleaching: In bioleaching processes using acidophilic microorganisms, Fe^{+2} is oxidized to Fe^{+3} and sulfur is oxidized to sulfuric acid by contact and non-contact mechanisms. Protons from the resulting ferric iron and sulfuric acid dissolve metals from ore and e-waste.

Previously, it was thought that bioleaching occurred only by contact and directly microbial enzymatic decomposition of ores, but today it has been revealed that metal dissolution occurs via ferric iron produced by microorganisms, similar to the non-contact mechanism. [120]. Bacteria adhere to edges, corners and cracks on the ore surface through extracellular polymeric substances (EPS) [121]. Fe^{+3} in EPS, consisting of Fe^{+3} and glucuronic acid complex, is reduced to Fe^{+2} by removing an electron from pyrite. Then, glucuroinic acids come into equilibrium with dissolved Fe^{+3} ions and take new Fe^{+3} from the solution. In this way, six electrons are repeatedly removed from the pyrite by EPS. As a result of the reaction, the sulfur part of the pyrite is released as thiosulfate, while the metal part passes into the water as a cation. $S_2O_3^{-2}$ formed in the EPS layer is oxidized to H_2SO_4 and elemental sulfide via polythionates $S_nO_6^2$.

Non-contact bioleaching is carried out by free-living bacteria. Fe^{+2} ions in the solution are oxidized to Fe^{+3} by these microorganisms and also free sulfur species (S_8, $S_2O_3^{2-}$, H_2S) are converted to H_2SO_4. Metal ions and sulfur species in the ore are released by EPS around the cell [122].

Bioleaching mechanisms occur in two mechanisms as thiosulfate and polysulfide which are given in Figure 2.5. Bioleaching process of some sulfidic ores, whose valence bonds are derived only from orbitals and not affected by acid dissolution, takes place via thiosulfate, where only Fe^{+3} extraction occurs [120]. Some sulfidic ores that dissolve with both sulfuric acid and Fe^{+3} are extracted by polysulfide [120]. The bioleaching mechanisms by thiosulfate and polysulfide pathways are shown in Figure 2.6.

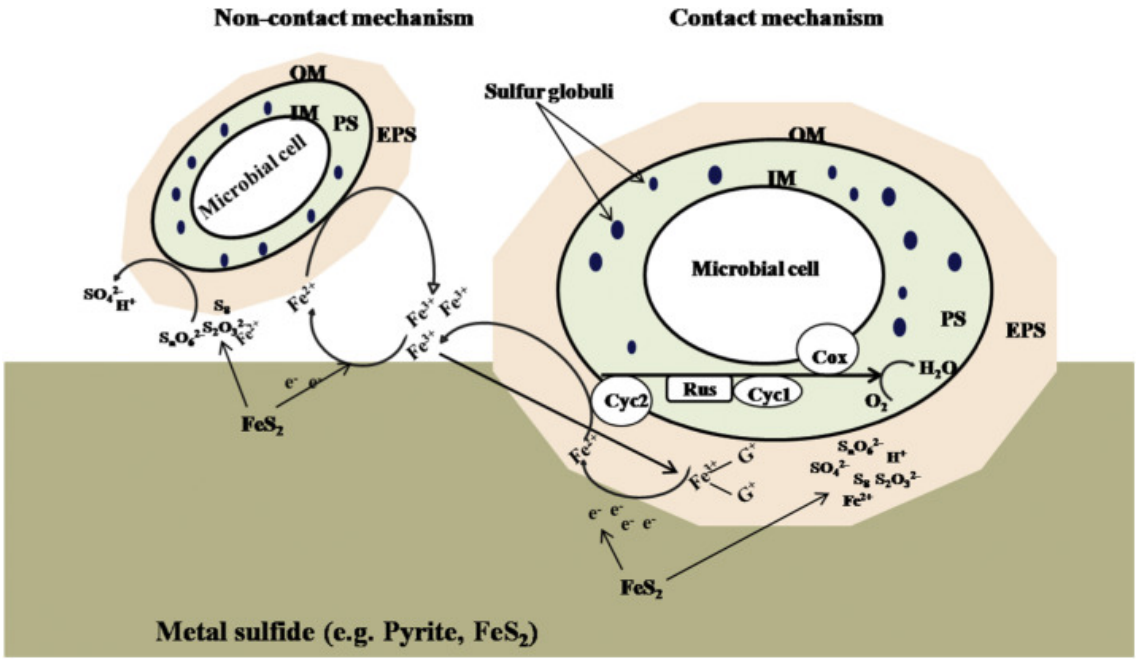

Figure 2.6. Contact and non-contact mechanisms of bioleaching [123]

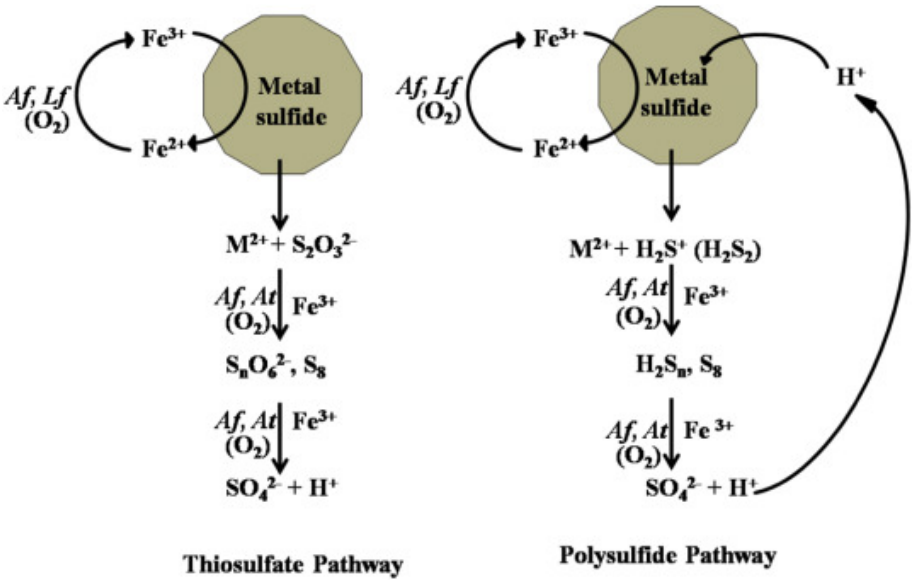

Figure 2.7. Metal extraction by thiosulfate and polysulfide mechanisms [123]

Fungal (Organotrophic) Bioleaching: Fungi that produce organic acids such as gluconic, citric, and oxalic acids are also frequently used in bioleaching applications. Metal extraction with organic acids produced by fungi takes place through acidolysis, complexolysis, redoxolysis and bioaccumulation [124]. The process of solubilization of metal ions as a result of the reaction of protons in organic acids produced by fungi with the ore surface is called acidolysis. For example, the solubilization of nickel metal by acidolysis is given in Eqn. (10).

$$NiO + 2H^{+} \rightarrow Ni^{+2} + H_2O \quad (10)$$

Organic acids and amino acids produced by fungi carry out the complexolysis reaction by binding protons and complexes to metal ions dissolved as a result of the acidolysis reaction. Metal extraction by complexolysis is given in Eqn. (11) [124].

$$Ni^{+2} + C_6H_8O_7 \rightarrow Ni(C_6H_5O_7)^{-} + 3H^{+} \quad (11)$$

Moreover, the microbial oxidation and reduction of metals is called redoxolysis. In Eqn. (12), the enzymatic oxidation of manganese is given.

$$MnO_2 + 2e^{-} + 4H^{+} \rightarrow Mn^{+2} + 2H_2O \quad (12)$$

Furthermore, the process of accumulation in the cell by binding to various functional groups such as hydroxyl, carboxyl, amine, phosphate and sulfate is called bioaccumulation. *Aspergillus* sp. and *Penicillium* sp. genus fungi are known to have high aptitude for the bioaccumulation process [34, 124].

Cyanogenic (Organotrophic) Bioleaching: Cyanogenic bacteria and fungi, which use organic carbon as an energy source and produce HCN, are used for metal recovery from ores and e-waste. Metals interacting with cyanide transform into complexes with good water solubility and chemical stability [118].

The HCN production reaction realized by consuming glycine by cyanogenic bacterial species such as *Pseudomonas putida*, *Pseudomonas florosence*, *Chromobacterium violaceum* is given in equation 14. [125]. The produced HCN is used for the extraction of metals such as Au, Ag, Cu, Zn from metal ores, but also it is used for the recovery of

these metals from WEEEs [126]. The gold extraction reaction with HCN is given in Eqn. (13-14).

$$NH_2CH_2COOH + O_2 \rightarrow HCN + CO_2 + 2H_2O \quad (13)$$

$$4Au + 8CN^- + O_2 + H_2O \rightarrow 4Au(CN)_2^- + 4OH^- \quad (14)$$

Metal Recovery via Bioleaching from E-Waste: Metal recovery from e-waste, sludge and slag by bioleaching method has become increasingly common in recent years [127, 128, 129]. However, in the process of metal extraction with bioleaching, the addition of these extra substances might be required because there could be lesser amount of iron and sulfur in WEEEs than metal ores.

In the literature, bioleaching is carried out in three different ways as one-step, two-step and spent medium step [124]. The process, which is carried out by adding microorganisms and the material to be removed at the same time to the environment, is called one-stage bioleaching. In two-stage bioleaching, the microorganism is grown separately, and then material is added to the microorganism culture that begins to produce oxidant. [124, 130].

It has been reported that two-step and spent medium step bioleaching processes, where microbial organic acid production and microbial growth are higher in the absence of waste, are more efficient in metal recovery compared to one step bioleaching [131]. In addition, microbial growth could not be obtained in some studies due to the toxicity caused by the presence of heavy metal ions in the environment during microbial growth in the one step bioleaching process [124]. In addition, the spent medium step process seems to be more suitable especially for industrial scale applications, so that the microbial community is not affected by metal toxicity and can produce organic acids for a longer period of time.

The extraction efficiency of the species produced by microorganisms differs according to the metal type to be extracted. It turned out that while Fe^{+3} is more efficient at Cd extraction from Ni-Cd batteries, sulfuric acid is more efficient for Li recovery from Li-ion batteries [132, 133]. In addition, metal recovery efficiency from WEEEs can be increased by using a catalyst. For example, Gu et al. examined Cu recovery from WPCBs, they obtained 74% Cu extraction with only *Acidithiobacillus ferrooxidans* in the catalyst-

free process, while they obtained 84% Cu extraction in the process they used *Acidithiobacillus ferrooxidans* with graphene as a catalyst. As a result of the study, it was determined that when the appropriate dose of graphene was added to the process, it showed good compatibility with *A. ferrooxidans* [134].

Different organic acids produced by the fungal species used in the bioleaching process affect the solubility of metals differently. For example, in a study in which citric acid was used as a leaching agent, the extraction efficiencies of metals in Li-ion batteries were reported as 99.99% Cu, 65% Al, 45% Co, 38% Ni [34]. In another study where gluconic acid was used as a leaching agent for metal extraction from scrap electronics, it was reported that 8% Cu, 43% Al, 100% Ni and 100% Sn could be recovered [34].

The bioleaching process is the first step in metal recovery from WEEEs. In addition to traditional methods such as precipitation, ion exchange, and solvent extraction, new biological methods such as bioadsorption, bioflotation, and bioreduction are used to selectively convert dissolved metals into solid form after bioleaching [31].

Limitations of Bioleaching: While the bioleaching process has many advantages over hydrometallurgical and pyrometallurgical methods, it also has several disadvantages;

- Low process speed [135]
- Insufficient suitability for metal recovery from high-grade ores and WEEEs [136]
- The negative effects of toxic metals on microorganism activity [137]
- Additional iron and sulfur cost for WEEEs with low iron and sulfur content [138]
- Low metal recovery efficiency from hard-to-process and durable WEEE [139]
- The accumulation of Jarosite and iron hydroxide on the ore surface reduces the diffusion of leaching agents to the ore surface and decreases the metal recovery efficiency [140]
- WEEE grinding cost [141]

The negative effects of toxic metals on microorganisms can be reduced by acclimation of the microorganisms to the metals to be extracted [142]. In addition, the use of naturally occurring nutrient sources for microorganism incubation instead of commercially available microbial nutrient sources and the addition of low-grade pyrite or pyrite-containing coal to the process instead of commercial iron and sulfur sources can reduce

the cost of the process. [143]. Moreover, the low metal recovery efficiency due to the durable structure of WEEEs can be increased by using suitable catalysts [134].

2.3.3.3. Bioprecipitation (Biomineralization)

Microbial technologies are used for metal recovery from wastewaters or leachate formed as a result of dissolving metals in electronic waste [144]. One of these technologies that provides selective metal recovery for low cost and industrial scale applications is bioprecipitation [145].

Precipitation of dissolved metal ions by interacting with microbial metabolites such as sulfur, hydroxide and carbonate is called bioprecipitation. Precipitation occurs when these agents produced by microorganisms change the ionic balance of the solution medium [146]. The efficiency of the metal recovery process by bioprecipitation is highly dependent on the pH and the metal concentration in the solution. The high chemical consumption to adjust the appropriate pH range is seen as the most important disadvantage of the process [147].

Metal Sulfide Precipitation: Biogenic sulfur production occurs through the use of oxidized sulfur compounds as electron acceptors by sulfate-reducing bacteria such as eubacteria and archaea. Biogenic sulfur formed during the reduction of sulfate compounds can precipitate metal ions [148]. Bioprecipitation reactions of metal ions are given in Eqn. (15-16).

$$2CH_2O + SO_4^{-2} \rightarrow H_2S + 2HCO_3^- \quad (15)$$

$$Me^{+2} + HS^- \rightarrow MeS\,(\downarrow) + H^+ \quad (16)$$

(Me^{+2} – metal cation)

The Metal Sulfide Precipitation (MSP) mechanism consists of biogenic hydrogen sulfide production with SRB and metal sulfide precipitation as a result of the interaction of the produced H_2S and metal. The most important parameters affecting the MSP process are; Metal sulfide ratio, pH, sulphate source, COD/SO_4^{-2} ratio [149].

The most important advantage of bioprecipitation is the selective recovery of metals from polymetallic leachates. Cao et al. had used MSP mechanism for the recovery of metals from leachate containing Cu, Ni, Mg and Fe. As a result of the study, Cu, Ni and Fe metals precipitated as metal sulfide compounds at pH 7.0, while Mg remained soluble [150]. According to Sethurajan et. al., selective Zn recovery with biogenic sulfides is possible from the leaching residues containing high Fe and Zn [149].

Microbiologically Induced Calcite Precipitation: Microbial induced calcium carbonate precipitation is based on the mechanism of calcium precipitation with microorganisms during microbial activity [151]. The MICP mechanism takes place by varying the amount of dissolved calcium in the environment as a result of metabolic pathways that produce alkalinity and dissolved inorganic carbon, such as urea hydrolysis, nitrate reduction (denitrification), photosynthesis, sulfate reduction, methane oxidation [152, 153, 154, 155, 156, 157, 158].

In the MICP process, the alkalinity of the aqueous medium changes due to the microbial production of CO_3^{-2} in various metabolic activities, and in the presence of Ca^{+2}, $CaCO_3$ precipitation occurs [159]. During the induction process by microorganisms, increasing the adsorption capacity on the cell surface. Thanks to the large number of negative charges in bacterial cell walls, divalent metal ions that can precipitate with calcium carbonate can be separated from water [160].

Although carbonate formation can be achieved by various processes such as denitrification, photosynthesis, and ammonification, MICP with urea hydrolysis is the most widely used technique [161]. MICP is usually induced by enzyme activities that facilitate mineral formation. As a result of the reactions affected by the urease enzyme, which is widely used in MICP, the pH rises and carbonate precipitation occurs as shown in Figure 2.8. [162]. MICP reactions realized by the mechanism of urea hydrolysis are given in Eqn. (17-22).

$$CO(NH_2)_2 + H_2O \rightarrow NH_2COOH + NH_3 \quad (17)$$

$$NH_2COOH + H_2O \rightarrow NH_3 + H_2CO_3 \quad (18)$$

$$NH_3 + H_2O \rightarrow NH_4^+ + OH^- \quad (19)$$

$$2OH^- + H_2CO_3 \rightarrow CO_3^{-2} + 2H_2O \quad (20)$$

$$Ca^{+2} + \text{Cell} \rightarrow \text{Cell - } Ca^{+2} \quad (21)$$

$$\text{Cell - } Ca^{+2} + CO_3^{-2} \rightarrow \text{Cell - } CaCO_3 \quad (22)$$

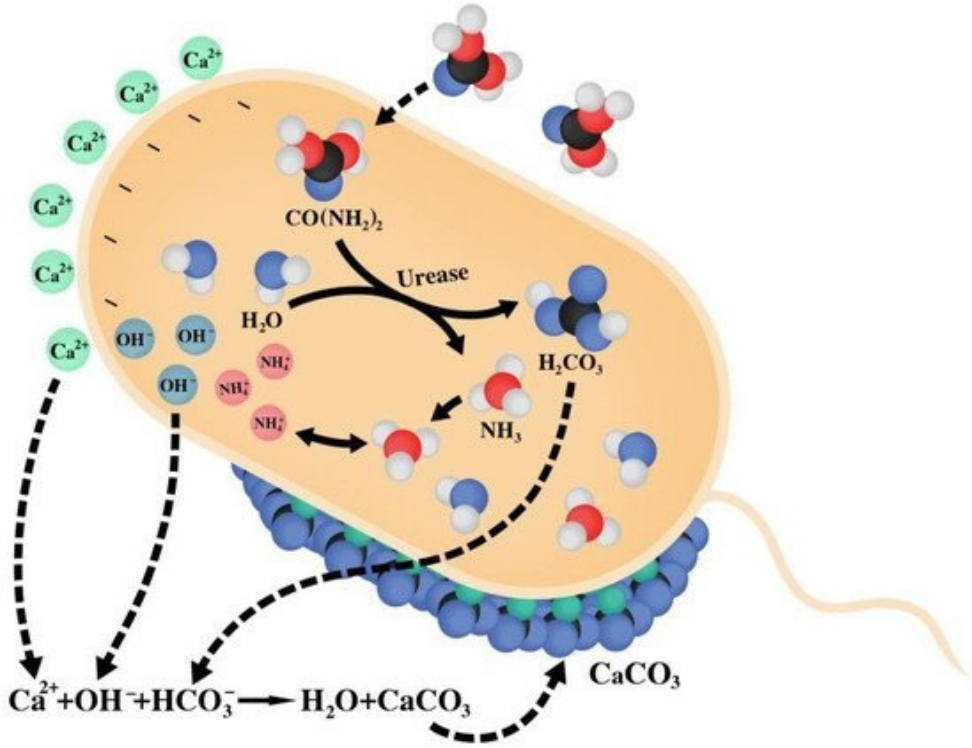

Figure 2.8. MICP mechanism through urea hydrolysis [163]

In the MICP mechanism with denitrification, microorganisms reduce nitrate to nitrogen gas and produce carbonate. If there is sufficient Ca^{+2} in the medium, MICP occurs [164]. MICP reactions with denitrification mechanism are given in Eqn. (23-27).

$$2HCOO^- + 2NO_3^- + 2H^+ \rightarrow 2CO_2 + 2H_2O + 2NO_2^- \quad (23)$$

$$HCOO^- + 2NO_2^- + 3H^+ \rightarrow CO_2 + 2NO + 2H_2O \quad (24)$$

$$HCOO^- + 2NO + H^+ \rightarrow CO_2 + 2N_2O + 2H_2O \quad (25)$$

$$HCOO^- + 2N_2O + H^+ \rightarrow CO_2 + N_2 + 2H_2O \quad (26)$$

$$Ca^{+2} + CO_2 + H_2O \rightarrow CaCO_3 + 2H^+ \quad (27)$$

Carbonate ions formed by urea hydrolysis and denitrification mechanisms can interact with dissolved divalent metal ions in the aqueous medium and depending on their K_{sp} value they may precipitate as metal carbonate compounds. Eqn. (28-29) shows how the precipitation process of carbonates formed by microbial induced urea hydrolysis, denitrification or photosynthesis occurs in the presence of metal in the environment.

$$Cu^{+2} + OH^{-} + HCO_3^{-} \rightarrow CuCO_3 + H_2O \qquad \text{Ksp: } 1.4\times10^{-10} \qquad (28)$$

$$Ni^{+2} + OH^{-} + HCO_3^{-} \rightarrow NiCO_3 + H_2O \qquad \text{Ksp: } 6.6\times10^{-9} \qquad (29)$$

In the literature, metal removal efficiencies of up to 98% were obtained in MICP studies using urea hydrolysis. For example, Jalilvand et al. performed MICP study with urea hydrolysis for metal recovery from heavy metal contaminated mine soil. As a result of the study, 96.25% Pb, 71.3% Cd and 63.91% Zn were removed from the environment as metal carbonate compounds [165]. Again, in a study conducted by Maity et al. for metal removal from contaminated soils, 95.93% Pb, 73.45% Cd and 73.81% Zn removal were obtained [166]. In addition to the prevalence of metal carbonate precipitation studies with MICP using urea hydrolysis in the literature, the lack of metal removal studies using the denitrification mechanism is striking.

According to studies in the literature, in most heterotrophic MICP mechanisms, approximately equal amount of substrate is required for 1 mole of biomineral production. However, while 1 mol of HCO_3 can be produced with 1 mol of urea in the mechanism realized by urea hydrolysis, 2 mol of CO_2 can be produced with 1 mol of acetate in the denitrification mechanism [167]. In this context, more metal precipitation can be achieved by the denitrification mechanism for equal substrate concentrations.

In addition, studies are carried out on biogranules that produce biominerals with the denitrification mechanism on the inside and generally with urea hydrolysis on the outside, where both mechanisms are carried out together. For example, Erşan et al., in their study with non-axenic cultures, showed that biomineral production can increase more when the two mechanisms are used together for biomineral production [168].

2.4. Biogranulation

Microorganism consortia formed by cell-to-cell interactions physically and chemically under aerobic or anaerobic conditions are called biogranules which is given in Figure 2.9. Biogranules consisting of different bacterial species and millions of bacteria are formed as a result of the loss of individual motility of each bacteria in the granule [169]. Due to their dense and strong structure and good settling properties, biogranules are seen to be more resistant to high pollution load compared to conventional activated sludge [170, 171]. In granular systems, decomposition of the substances and pollutants depends on the enhanced synergistic substrate consumption and product transfer between various microorganisms that are enriched in different layers of the compact structure of the biogranules according to the redox potential of their preferred metabolic pathway.

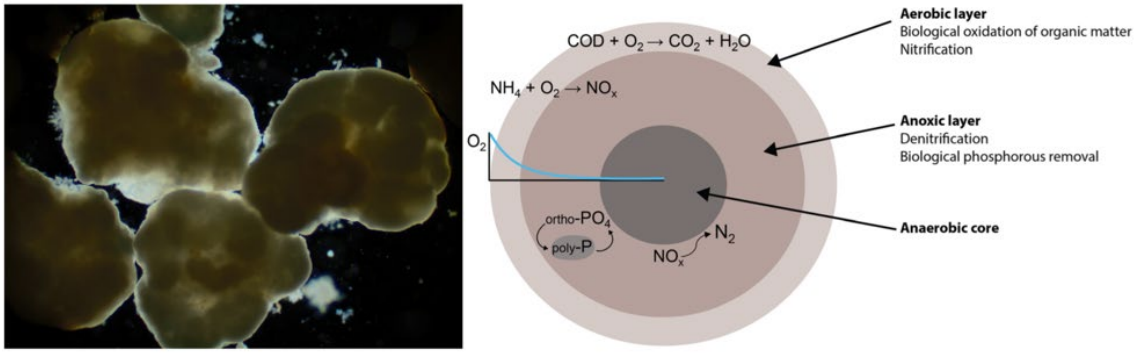

Figure 2.9. Schematic drawing and microscopic image of aerobic granule [172]

Aerobic granular sludge sytems are suitable for treatment of both low and high strength wastewaters [173]. In addition, aerobic granular systems avoid the use of several biological treatment units (anaerobic, anoxic, aerobic tanks) that occupy massive area in wastewater treatment plants. Moreover, due to their compact structure biogranules can be separated from the liquid in a very short time and thus avoids the need for a secondary settling tank. Overall, these systems occupy less area than conventional activated sludge process, save about 20–25% of the operational costs and 23–40% of the electricity costs [174].

Aerobic granules were observed to provide the most efficient growth in the sequencing batch reactor (SBR) [175]. As in anaerobic granulation, long initiation period seems to be an important disadvantage in aerobic granulation. Slow aerobic granulation process

leads to negative results such as foam formation, poor settling characteristics and inefficient treatment performance of pollutants such as COD, P, N [176].

It is known that the granulation process that is applied in wastewater with high pollutant load takes longer times varying based on the strength of the water. For example, in a study of Fulazzaky et al., process that was conducted with palm oil production facility wastewater, granule formation was not observed after 190 days [177]. In addition, in a study conducted by Cetin et al. at high Mixed Liquor Suspended Solids (MLSS) and high suspended solids concentrations, they grew mature granules of 600 μm in diameter at day 44. The presence of high MLSS destabilized the system, resulting in smaller mature granules and formation of irregular filamentous granules [178].

2.4.1. Aerobic Granules Formation

Biogranules are considered as dense and compact microbial aggregates with a spherical structure. Biofilm development plays an important role in aerobic granule growth [179]. Granulation generally consists of 4 stages: 0-30 days of cell to cell attachment, 30-60 days of microbial aggregation, 60-200 days of pre-maturation and post-maturation [180]. Cell to cell attachment stage plays an important role in granule formation. Factors such as surface hydrophobicity, charge neutralization, hydrodynamic shear force and EPS release are defined as primary factors [180]. The optimal levels of these factors enhance the interaction between microorganisms and prepare the environment for microbial aggregation. Performing the first stage of the granulation process under suitable conditions (i.e. controlling primary factors) can shorten the granulation time. In addition, factors that have less effects on the granulation process than primary factors such as organic loading rate (OLR) and solid retention time (SRT) are called secondary factors [181].

Compared to flocs, aerobic granules have a more regular, dense and strong microbial structure. It is also known that they have better settling abilities than flocs. In addition, EPS accumulated around the granules forms a shield that protects the granules from the highly toxic effects of pollutants. Thanks to these advanced features, they are more resistant to high pollutant loads and can remove different pollutant loads in the same environment thanks to their complex microbial diversity [182].

2.4.2. Factors Affecting Aerobic Granule Formation

2.4.2.1. Substrate Composition

Granular structure and species diversity are directly related to the type of carbon source. Biogranule growth was obtained with different substrates such as glucose, acetate, ethanol, methanol, formate, phenol and synthetic wastewater [183, 184, 185, 186]. While filamentous and less stable granules were obtained in granulation with glucose-containing substrate, more compact and stable granules were obtained in granulation when acetate was used as the main carbon source. In addition, although strong granules were obtained as a result of using phenol as a substrate, the granulation time was prolonged [187].

In some studies carried out in recent years, propionate has been used as a carbon source. Despite the long cultivation time, strong granules were obtained that can be used for a long time without disintegration [188]. However, it has also been revealed that substrates containing high concentrations of propionate can inhibit granule formation [189].

The ratio of chemical oxygen demand to nitrogen has important effects on the granulation process. The COD/N ratio affects the physiochemical and microbial properties of the granules, causing significant changes in the granule size [190]. A study by Liu et al. suggested a significant reduction in granule size when the COD/N ratio was set below 5 [191].

Luo et al., on the other hand, investigated the effects on aerobic granules by adjusting the COD/N ratio as 1,2,4 in three different ways. 1 and 2 COD/N ratios caused a decrease in the physical properties and nitrification abilities of the granules. In fact, 1 COD/N ratio caused a decrease in the EPS ratio of the granules, leading to granule fragmentation [192].

In addition, the high COD/N ratio of the substrate may cause filamentous bacterial growth and granule fragmentation. In another study, filamentous but large granules with a COD/N ratio of 10-30 were obtained, while small but more stable granules were obtained between 2-5. In the study, the optimal COD/N value was determined as 7.5 [193].

2.4.2.2. Organic Loading Rate

Organic loading rate (OLR) is used to provide granule formation and stability in the granulation process [194]. Aerobic granules can be grown in a wide OLR scale between

2.5-15 kg COD. $m^{-3}.d^{-1}$ [195]. Although the effect of OLR on aerobic granulation is low, it does affect the physical properties of the granules. For example, in a study by Liu et al., as a result of raising OLR from 3 kg COD. $m^{-3}.d^{-1}$ to 9 kg COD. $m^{-3}.d^{-1}$, the granule size increased from 1.6 mm to 1.9 mm [196]. It is known that OLR is ineffective in the formation of the rounded structure of granules, but it affects the properties such as sludge volume index (SVI), biomass density and weight.

In their granulation studies carried out in the range of 4.8-18 kg COD. $m^{-3}.d^{-1}$, Long et al., obtained stable granules by using OLR values below 15 kg COD. $m^{-3}.d^{-1}$ [197]. In another study with 0.54 kg COD/ $m^{-3}.d^{-1}$ OLR, it was reported that biomass was broken down and thus granulation did not occur [198].

In addition to these, OLR can be adjusted with volume exchange ratio. In most laboratory studies, the volume exchange ratio is usually adjusted between 50-75% [199, 200].

2.4.2.3. Hydrodynamic Shear Force

Hydrodynamic shear force (HSF) and feast-famine feeding regimes play an important role in the aerobic granulation process with SBR. HSF affects the bacterial species clustered in the biofilm as well as the structural and functional properties of the biofilms.

In SBR tanks, the HSF value is calculated by dividing the aeration rate by the cross-sectional area of the tank and is often referred to as the up-flow superficial air velocity. In order to obtain granulation in SBR tanks, the lower limit value of up-flow superficial air velocity was stated to be 1.2 cm/s [183]. At higher aeration rates, rounder and more compact granules were obtained [184].

Moreover, it was reported by Tay et al. that HSF, which usually originates from aeration bubbles, positively affects aggregation by increasing EPS production and intercellular cohesion [183]. As HSF increases the EPS production, it indirectly contributes to granule formation by increasing the cell surface hydrophobicity. In this context, stronger and more compact granules were obtained in the reactors operated with high HSF values [201].

2.4.2.4. Settling Time

In the SBR system, the biomass is precipitated at the end of successive cycles before the treated water is discharged from the reactor. By setting a short settling time, a hydraulic selection pressure is created on the microorganisms [202]. As a result, bacteria that settle quickly continue to grow in the reactor, while bacteria with poor settling characteristics are wash-out with the effluent.

In addition, long-term settling time causes excessive floc formation and increase of filamentous bacteria in the reactor [203]. Qin et. al. investigated aerobic granulation by operating the reactors with two distinct settling periods of 5 minutes and 15 minutes. Their findings indicated that while granule formation was observed in the settling time of 5 minutes, mixed sludge with high suspended solids density was obtained in the settling time of 15 minutes [204]. In another study, which was performed by setting the settling time to 3 minutes, compact granules with rapid settling properties (SVI: 23 ml/g) were obtained [205].

Furthermore, a small amount of granules is obtained as a result of the process, as the settling time, which is set for a short time at the initial stage of the reactor operation, adversely affects bacterial growth. Nevertheless, a settling time of 1 minute seems sufficient for mature granules [183].

2.4.2.5. Hydraulic Retention Time

HRT and settling time create hydraulic selection pressures which control aerobic granulation performance [206]. The frequency of removal of solids in the reactor during the SBR cycle time is called the wash frequency. This wash frequency is related to the hydraulic retention time (HRT) of a given rate of change. HRT is typically calculated by dividing the reactor volume with the volume of effluent discharged in specific time period from the reactor.

Short HRT and short settling time create very strong selection pressure on biomass. For example, in a study performed by Zhang et al., the granulation process was carried out by adjusting the cycle time of 30 minutes and the settling time of 1 minute. The granules formed at the beginning of the process were completely fragmented due to high selection pressure at the end of 2 days of operation [207]. For this reason, HRT and settling time

should be adjusted in a balanced way in order to create appropriate selection pressure on biomass.

Moreover, it is known that excessive biomass formation in the reactor reduces the granulation efficiency. In order to keep the biomass amount in the sludge in balance, the SRT value depends on the HRT and settling time adjustment [208]. For example, in a study by Liu et al., HRT was set at 1.5 hours and settling time as 2 minutes, and these conditions caused a short SRT value in the process. This prevented the formation of slow growing bacteria such as nitrifying bacteria [209].

2.4.2.6. Solid Retention Time

The removal of substrates such as nitrogen and phosphate by aerobic granules is highly dependent on the sludge retention time (SRT) [210]. Regular removal of excess sludge from the reactor stimulates biomass conversion and new cell growth. This transformation increases the removal performance by making growth stimulus nutrient consumption faster [211].

In addition to affecting the substrate removal performance of SRT granules, it also affects their physical properties. One of the main problems of the granulation process is the growth of filamentous organisms [212], which adversely affects the settling properties of the sludge. High SRT value supports filamentous organism growth. Therefore, regular removal of excess sludge is necessary to prevent the proliferation of filamentous organisms [213].

Although quite different values are reported in the studies, it is accepted that the appropriate SRT value for aerobic granules is approximately 2-30 days at medium and low temperatures (16-20 °C) and 8-10 days in warm (27-40 °C) environments [214, 215].

According to the study of Beun et.al., during the granulation in an SBR, SRT usually increases from 2 days to 30 days initially. Afterwards, the SRT value, which drops to 17 days, stabilizes in 9 days as the granules begin to mature [216]. In another study by Lin et al., small-sized but compact granules were obtained at a 10-day SRT [217]. In this context, a stable reactor can be operated with different SRT values under different operating conditions.

2.4.2.7. Feast-famine Operation

SBR operation for aerobic granulation typically consists of feeding period, aeration period, settling of biomass and removal of the supernatant. Bacteria growing in SBR are subject to periodic feast-famine conditions under the influence of substrate change in the environment. Due to the rapid depletion of substrate during the reaction period, microorganisms experience a period of starvation [183]. The aeration process takes place in two stages. The first stage is the nutrient decomposition also known as the feast period. It is followed by the famine period due to the absence of nutrients. During this starvation period, the hydrophobic properties of bacteria increase and they tend to adhere to each other [183]. The main reason for the formation of these hydrophobic properties is the consumption of EPS by granules during the starvation period [218]. As a result of decreasing EPS, the electrostatic balance changes and microbial aggregation becomes easier.

Microorganisms that enter the famine period in proper time produce denser and stronger granules [219]. Wang et al. obtained aerobic granules in SBR with two different cycle times of 3 and 12 hours. As a result of the study, it was determined that the granules grown in 12-hour cycles had larger granule size and stronger granule strength than 3-hour cycles [220]

2.4.2.8. Extracellular Polymeric Substances

Extracellular polymeric substances (EPS), mostly composed of polysaccharides and proteins, are biopolymers produced by microorganisms [221]. EPS affects microbial aggregation positively by enabling bacterial cells to adhere to each other [222]. EPS and bacterial cells are interconnected by interactions such as hydrophobic interactions, ion bridging interactions, and polymer entanglement that trigger granulation [223]. In addition, it is known that high HSF increases EPS production [224].

One of the most important factors affecting EPS formation in aerobic granulation is OLR. Rusanowska et al. carried out granulation studies at three different OLR values: 0.78 kg COD. m^{-3} .d^{-1}, 1.16 kg COD. m^{-3}.d^{-1} and 1.53 kg COD. m^{-3}.d^{-1}. They obtained the highest EPS amount at the lowest OLR value [225]. Considering that the lower OLR value in

general will increase the fasting time, granules that are fasted for longer produce more EPS.

Moreover, differences in COD/N ratio cause significant changes in EPS composition. Shi et al. investigated the amount of EPS in the two different reactors with COD/N ratios of 20 and 10. As a result of the study, they obtained more EPS with low COD/N ratio [226].

Furthermore, water salinity affects EPS production. In the granulation study conducted by Corsino et al. in a wastewater containing more than 20 mg NaCl/L salt, it was determined that 90% of the EPS consisted of tightly-bound EPS (TB-EPS) [227]. TB-EPS is known to be the main EPS composition that increases zeta potential and hydrophobicity and improves aggregation between sludge cells [228].

Rhodocyclaceae, *Xanthomonadaceae*, *Sphingomonadaceae*, *Meganema* and *Devosia* species in the granules are denitrifying bacteria that provide nitrogen removal as well as taking an active role in EPS production. Therefore, EPS producing bacterial species also have an important role in the nutrient removal performance of aerobic granules [229].

Cell aggregation can be increased by polymeric interactions created by high EPS amount. In addition, it can be said that aggregation is low in the presence of low EPS. The amount of EPS increases during the growing phase of granule cultivation process, but remains constant in mature granules [230]. High EPS production can provide rapid granulation as well as increasing granule stability [206].

2.4.2.9. Presence of Ca^{+2} and Mg^{+2} Ion in Feed

As a result of the studies, it has been reported that divalent and trivalent cations such as Ca^{+2}, Mg^{+2}, Fe^{+2}, Fe^{+3} form a bridge with EPS in the granulation process and positively affect the agglomeration of microorganisms. It is known that Ca^{+2} and Mg^{+2} divalent cations can accelerate the granulation process by reducing the start-up time [231]. In addition, it has been revealed that divalent metals contribute to granule formation by providing self-immobilization of microorganisms [232].

Jiang et al., obtained granulation in 32 days and in 16 days with wastewater that does not contain Ca^{+2} and with wastewater containing 100 mg/L Ca^{+2}, respectively. In addition, EPS amount and settling properties of granules fed with Ca^{+2} containing wastewater were

higher [233]. Furthermore, Li et al. reported that the positive effect of using Mg^{+2} on the granulation process was slightly less than that of Ca^{+2} [234].

2.4.2.10. Dissolved Oxygen, pH and Temperature

Dissolved oxygen (DO), temperature and pH are important parameters in biogranulation reactors. In the granulation process, aerobic granules were obtained at the lowest concentration of 0.7-1.0 mg/L DO, while granulation was achieved successfully at >2 mg/L DO [235].

The effects of pH and temperature on the process efficiency in the anaerobic granulation process have been frequently investigated in the literature [236]. However, due to the fact that these parameters in aerobic granulation are not as effective as in anaerobic granulation, studies on this subject are lacking in the literature.

Growth of aerobic granules with the SBR system is usually carried out at room temperature (20-25°C) [237]. The efficiency of aerobic granulation below and above room temperature continues to be investigated in the literature. For example, De Kreuk et al found that in a reactor operated at 8°C, filamentous organisms grew excessively and destabilized the granules [237]. However, in the granulation studies performed by Halim et al. at 50 °C, they succeeded in obtaining mature and stable granules with a diameter of 2-5 mm [238].

2.4.2.11. Seed Sludge

In anaerobic granulation, the properties of the seed sludge significantly affect the formation of anaerobic granules. However, information on the effect of seed sludge quality on granulation in aerobic granulation is limited. In aerobic granulation, the quality of the seed sludge affects the microbial activity, surface properties and settling characteristics [239].

Since the seeding sludge affects the microbial committee during granule cultivation, it also affects the substrate removal performance of the granules [240]. For example, Erşan et al. obtained granules in separate reactors with two different seed sludges taken from membrane bioreactor (MBR) and conventional activated sludge (CAS). As a result of the study, it was determined that the granules obtained with MBR sludge were more resistant

to high OLR, had a more compact and smooth shape, and also had higher substrate removal performance [241].

Moreover, Verawaty et al. revealed that the mixture of crushed granules and biomass flocs shortens the initiation time of the granulation process without affecting the nutrient removal performance [242].

2.4.3. Metal Recovery with Aerobic Granules

In recent years, aerobic granules have been used frequently for heavy metal removal from wastewater. Thanks to its properties such as high adsorption capacity, large surface area and strong physical structure, biogranules are seen as a suitable biosorbent for heavy metal removal [243]. Heavy metal adsorption with aerobic granules takes place both on the granule surface and in the inner region of the granules due to the porous structure of the granule [244]. Moreover, it is quite easy to separate the granules from the liquid phase.

Liu et al. used aerobic granules for heavy metal adsorption for the first time and the reported successful Cd adsorption from industrial wastewater [245]. In addition, Xu et al. reported that Ni biosorption increased in the pH range of 2-6 and the highest removal was obtained at pH 6 [246].

Ni biosorption performances of aerobic and anaerobic granules were investigated by Li et al. [247]. As a result of the study, it was revealed that the EPS amount of anaerobic granules was higher than aerobic granules. It has been observed that anaerobic granules provide more Ni biosorption thanks to the adsorption potential provided by the high EPS amount [247]. Feng et al. investigated the removal performance of aerobic granules grown with the addition of Ni. An increase in COD removal efficiency was observed after increasing the Ni ion concentration from 0 to 1 mg/L. I It was found that while feeding at 5 mg/L Ni level, the COD value in the effluent increased and COD removal efficiency decreased. However, a significant decrease in COD removal efficiency was observed during 10 mg/L Ni feeding [248].

Cu (II) removal using aerobic granules has also been frequently investigated in the literature. Xu et al. reported that aerobic granules could remove Cu (II) up to 246.1 mg /g (mass of granule). Zhang et al., on the other hand, observed that stable granules could be formed at Cu (II) concentrations between 0.5mg/L to 3 mg/L with low SVI. However, it

was found that microbial activity of granules was impaired at higher Cu (II) concentrations [249].

2.5. The Goal and the Scope of the Thesis

As seen in the literature research, WPCB recycling is not implemented in Turkey. Therefore, it is clear that hydrometallurgical and biohydrometallurgical methods need to be explored and integrated into the local electronic waste recycling industry. Hydrometallurgical methods are widely used for recycling processes in European and developed countries around the world. However, due to the high chemical and energy consumption required by hydrometallurgical methods, the importance of biohydrometallurgical methods, which are seen as more environmentally friendly processes, is increasing day by day.

The bioleaching process, which is becoming widespread today, seems to be the most efficient and environmentally friendly biohydrometallurgical method. However, physical or chemical methods still continue to be used to purify the mixed metal content of leachates formed after bioleaching. In this context, the use of biogranules, which are more resistant to high heavy metal concentrations than isolated pure culturesa, as a metal purification method has been theoretically found suitable to make WPCB recycling a fully biological process.

Literature studies on metal recovery from WPCBs by biohydrometallurgical methods have generally focused on Au, Ag and Cu metals. Despite the high economic value of Ni metal, studies on Ni recovery from WPCBs in the literature are insufficient.

Biogranules produce carbonate through many different mechanisms such as urea hydrolysis, denitrification, photosynthesis, and sulfate reduction, and these carbonate ions interact with the dissolved metals in the environment and enable their separation from the liquid in the form of metal carbonates. It seems theoretically more appropriate to perform biomineralization process using both urea hydrolysis and denitrification mechanisms to increase the amount of generated carbonate ions. There is information in the literature that acclimation of microorganisms with the target metal for selective bioleaching processes might increase the recovery efficiency.

In accordance with the aforementioned needs and the advances in microbial metal recovery, in this thesis study, the use of mature granules acclimated to Ni exposure was investigated for selective Ni recovery from a synthetic metal leachate solution. In order to propose a completely biohydrometallurgical and complementary approach for metal recovery from WPCBs, the composition of the synthetic metal leachate solution was defined based on a previous study that investigated bioleaching of metals from WPCBs.

3. MATERIALS AND METHODS

Although aerobic granules are frequently used for metal recovery from wastewater, they have never been used before to extract metals from multi-metallic leachate resulting from bioleaching process. Within the scope of the thesis, it was aimed to investigate whether it is possible to selectively recover the nickel metal from the synthetic leachate solution prepared based on the available information in literature. In experimental studies, firstly aerobic granules were produced from a dry seed and then biomineralization experiments were carried out using the obtained granules. General thesis working scheme is given in the Figure 3.1.

Thesis Work Chart

Installation of SBR

↓

Enrichment of Microorganism

↓

Granulation Period

↓

Nickel Acclimation Period

↓

Biomineralization

Figure 3.1. Thesis working scheme

3.1. Experimental Procedure of Biogranulation

The granule cultivation was carried out under SBR operating conditions in a plexiglass cylindrical reactor with a length of 76 cm, a diameter of 4.5 cm and a volume of 1.2 L. The reactor was operated in 4 cycles of 6 hours, consisting of 1-hour of simultaneous feed/draw period to replace 50% of the reactor content, 2-hours of anoxic period and 3-hours of aerobic period. An automatic time controller was used to control aeration and feeding.

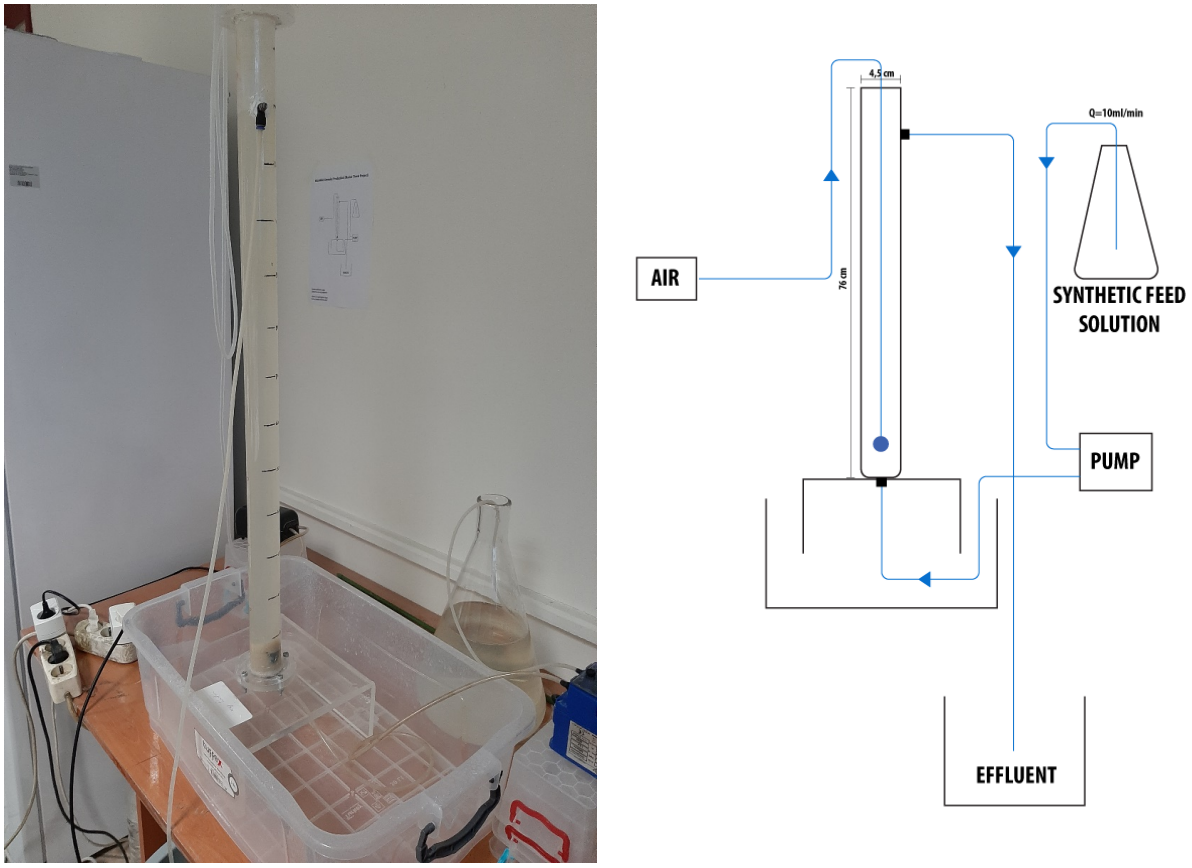

Figure 3.2. SBR setup

Dry powder (<200 µm) composed of denitrifying spores were used as initial seed for cultivation of biogranules. The HRT value was set to 12 hours. While aeration was carried out with an air pump, the feed with a flow rate of 10 ml/min was provided by a peristaltic pump through the valve located at the bottom of the reactor. The reactor setup is given in Figure 3.2.

3.1.1. Seed

In a previous study by Sonmez and Erşan (2022), spores were obtained as a result of drying and sieving denitrifying granules grown with Beet-sugar processing water [250]. Sonmez and Erşan used Beet-sugar processing water with a high pH value in order to select resilient bacteria (to alkaline pH, high temperatures) in the biogranules which were further used in highly alkaline concrete environment [250]. The granulation reactor in this thesis study was seeded with 2 g of dry powder (particle size < 200 µm) containing denitrifying spores previously cultivated by Sonmez and Erşan.

3.1.2. Nutrient Solution

In a study performed by Erşan et al., aerobic granules were obtained by adjusting the COD/TAN ratio to 1500/200. In the same study, the reactor was fed by diluting the nutrient solution in half until the VSS value rose above 2000 mg/l [251]. Based on this study, the reactor was initially set up with dry powder of denitrfying spores and fed with 4-times diluted nutrient solution for 2 weeks. Next, the reactor was fed with 2-times diluted nutrient solution until the VS concentration reached 2500 mg/L. The reactor, which reached a VS value of 2500 mg/L on day 68, was fed with the synthetic nutrient solution without any dilution and the content of the undiluted nutrient solution was given in Table 3.1.

Table 3.1. Nutrient solution content

Chemical	Concentration	Chemical	Concentration
CH_4N_2O	1000 mg/L	Yeast Extract	240 mg/L
$MgSO_4.7H_2O$	90 mg/L	$NaNO_3$	508 mg/L
KH_2PO_4	60 mg/L	NaCl	600 mg/L
$Ca(NO_3)_2 \cdot 4H_2O$	150 mg/L	CH_3OH	1.3 ml/L

In parallel with the work of Sonmez and Erşan, the minimal nutrient solution was free of micronutrients [250]. Different from the previous study, the nutrient solution contained 1 g/L of urea and 0.24 g/L yeast extract to enrich urea hydrolyzing microorganisms in the granular biomass. The main reason for using minimal nutrients was to reduce the operational costs in full-scale processes. In traditional biogranulation processes, trace elements and nutrients such as yeast extract are used to increase granulation efficiency and accelerate granulation [252]. In this study, it was tried to reduce the cost of granule production by completely excluding micronutrients and minimizing the supplied yeast extract.

3.1.3. Enrichment of the Nitrate Reducing Urea Hydrolyzing Bacteria from Dry Seed and Acclimation Period

The settling time was initially set to 30 minutes for the enrichment of the bacteria and to prevent the wash-out of the newly grown culture from the reactor. As the amount of bacteria started to increase in the reactor, the settling time was gradually reduced to 15 and 5 minutes to increase the selective pressure on microorganisms and thus wash-out the poorly settling microbial flocs. As of the 103rd day, the settling time was completely

removed from the operation, maximizing the selection pressure on the grown culture. the important details of the operational conditions of the reactor at different time intervals were summarized in the Table 3.2.

Table 3.2. Operational parameters whilst cultivation of biogranules

Operation Days	OLR (kg COD/ m^3-d)	NLR (kg NO_3 -N/ m^3-d)	ULR (kg Urea/ m^3-d	Anoxic Period (min)	Aerobic Period (min)	Settling Period (min)
1-13	0.77	0.05	0.5	180	150	30
14-16	1.54	0.10	1	180	150	30
17-67	1.54	0.10	1	180	165	15
68-102	3.08	0.20	2	180	175	5
103-159	3.08	0.20	2	180	180	-
160-244	3.08	0.41	2	180	180	-

3.1.4. Acclimation of biogranules to Ni

It was reported in several studies that most of the microbial communities are susceptible to heavy metal concentrations and their metabolic activites may be inhibited when the threshold values are exceeded [253]. However, the feeding of low doses of metal to the system during the cultivation of microbes and gradually increasing the exposed metal concentrations before the actual exposure conditions provides both an increase in the activity of microorganisms and resilience against the toxic effects of higher concentrations [254].

Furthermore, in the studies carried out to provide metal recovery from e-waste by bioleaching process, it was revealed that the pre-adaptation of the microorganisms with the metal desired to be recovered increases the selective metal recovery efficiency [255]. In addition, Huang et.al. revealed that acclimated microorganisms before the process had higher metal recovery efficiency [256]. Therefore, in this thesis work, in order to acclimate the produced mature granules to Ni exposure for selective nickel recovery, nickel concentration in the feed solution was gradually increased as given in Table 3.3. If nickel was given with other metals, the toxicity tolerance level of the granules to other metals would also increase, but this would not provide an advantage for selective nickel recovery.

Table 3.3. Nickel concentrations fed into the reactor and their starting day

Operation Day	196	201	214	231
Nickel Concentration	1 mg/L	2 mg/L	3 mg/L	4 mg/L

3.1.5. Determination of Biogranulation Performance and Microbial Activity

During the granulation process, the development of the microbial granules was investigated by monitoring TSS, VSS, SVI, wet particle size and microscopic surface properties of the agglomerates. Moreover, the operational parameters and microbial activity was assessed by regular monitoring of pH, DO, chemical oxygen demand (COD), NO_3-N, total ammonia nitrogen (TAN) concentrations in the nutrient solution, at the end of the anoxic period and at the end of the aerobic period.

The TAN generated due to urea hydrolysis and the COD consumed through nitrate reduction and aerobic oxidation in anoxic and aerobic periods over a cycle were monitored. In order to accurately determine the urea hydrolysis and carbon consumption perforrmances of the biogranules, samples were taken at four different time points; from feed solution (t=0 min), from the effluent of the previous cycle (t=0 min), at the end of the anoxic (t=180 min) and the aerobic periods of the new cycle (t=360 min). In regular monitoring of the reactor, operation was plug flow during feed/draw period (first hour of anoxic period) and completely mixed during the aerobic period. TAN and COD samples were taken from the effluent point from the reactor at the end of the anoxic and the aerobic periods.

Bacterial aggregates with a radius of at least 200 microns are considered as biogranules in the literature [184]. In addition, it has been reported that the system reaches a granular structure when the SVI30 value falls below 50 ml/g [257]. In their study, Sonmez and Erşan accepted that the granulation process was completed when the SVI_{30}/SVI_5 ratio reached 85% [250]. Accordingly, in this thesis study, it was tried to reach these values before the nickel acclimation stage.

At the end of the granulation period (granule percentage > 85%) and during the acclimation of granules to Ni exposure, kinetic analyzes were performed to picture the

performance of microbial community before and after the acclimation. Kinetic analyses were conducted by taking samples every 15 minutes during a cycle to examine the microbial activity of the granules, and the samples were analysed to determine the changes in TAN, COD and NO_3-N concentrations. As described above, in normal operation, granulation reactor was fed from the bottom of the reactor and the feed solution passed through the granular sludge layer during the feed/draw period. In order to avoid the effect of the plug flow operation and thus the sampling point on determination of microbial activity, the reactor was operated in completely mixed mode during the kinetic analysis.

In addition, size distribution analysis was carried out to examine the change in granule size during the granulation period and during the gradual increase in nickel concentration of the feed solution. In addition, the size distribution of the granules used in the biomineralization experiment was also determined.

3.1.6. Analytical methods

Methods for the analyses conducted during regular monitoring of the biogranulation reactor and during the kinetic analyses are described below.

pH: Daily measurements were made with a pH meter (Hanna HI98190, USA). The pH meter is calibrated at regular intervals over 2 different pH points (acidic and neutral).

DO: Daily measurements were made with a DO meter (Hanna HI98193, USA). The DO meter was calibrated with 2 points as zero oxygen solution and oxygen concentration in the air.

TSS & VSS: Total suspended solid and volatile suspended solid values were determined according to the 2540 D, E coded standard methods [258].

SVI: SVI_{30} values was calculated twice a week according to the standard methods with code 2710 D. The duration of the method was changed to 5 minutes to determine SVI_5 as previously described by Liu et.al. [257].

Granule Percentage: The formuladescribed by Liu et.al. which is given in Eqn. (31) was used to determine the granule percentage of the reactor [257].

$$Granulation: \frac{SVI_{30}}{SVI_5} x\ 100 \quad (31)$$

COD: The COD analyzes of the filtered samples were carried out twice a week with the reactor digestion method approved by the EPA with a measuring range of 100-1000 mg COD/L (Hach LCI 400).

TAN: The reaction of urea to ammonia as a result of microbial activities is given in Eqn. (17-19). Thanks to the conversion of urea to ammonia, TAN analyzes were carried out in order to determine the urea hydrolysis efficiency in the thesis study. The TAN analyzes of the filtered samples were carried out twice a week according to the standard methods coded 4500-NH_3 Step-B, C. As the titrant, 0.02 N sulfuric acid was used in the titration process.

NO_3-N: NO_3-N concentrations of the filtered samples were determined with HACH, LCK 340 test kits.

Average Granule Size: Samples were taken while the reactor was fully mixed in the aerobic period. The samples, which were dropped on the glass surface with the help of a dropper, were visualized with 100x magnification of a light microscope. The granule images in the microscope were taken with a 25 Megapixel camera. Then, with the imageJ program, 8-9 granules were selected randomly from each image and the granule sizes were measured. After performing the same procedure for 20 photographs, average granule sizes were determined.

Statistical Analysis: Deviations and accuracy of the data were analyzed by SigmaPlot software's one way ANOVA calculation.

3.2. Experimental Procedure of Nickel Recovery from Bio-leachate Solution via Biogranules

3.2.1. Setup of Biomineralization Experiment

While preparing the bioleachate solution, the metal mass percentage of the laptop WPCBs obtained by Işıldar (2016) and the immobilization percentages of the metals as a result of the bioleaching process performed on electronic scrap materials by Brandl et. al. with *A.niger* fungi were used [16, 20]. Thanks to these data obtained from the literature, the

metal concentrations of the polymetallic bioleachate solution that may occur after the bioleaching process of 1 g laptop WPCB could be determined (Table 3.4).

Table 3.4. Metal content of a laptop WPCB [16, 20]

Metal	**Al**	**Cu**	**Pb**	**Ni**	**Zn**
Scrap Metal Content (mg/g)	19.8	176.1	2.2	5.7	4.5
Metal mobilization percentage	%43	%8	%97	%100	%100
Amount of dissolved metal (mg/L)	8.51	14.09	2.13	5.7	4.5

In order to control the effect of heavy metal toxicity on biogranules and to determine whether selective Ni recovery occurs via MICP in synthetic leachate solutions at different concentrations, 4 different bioleachate solutions: 1:20, 1:10, 1:5 and 1:2.5 were prepared (Table 3.5).

Table 3.5. Starting metal concentrations of biomineralization

Conc. / **Metal**	**1/20 (mg/L)**	**1/10 (mg/L)**	**1/5 (mg/L)**	**1/2.5 (mg/L)**
Al	0.43	0.85	1.70	3.40
Cu	0.70	1.41	2.82	5.64
Pb	0.11	0.21	0.43	0.85
Ni	0.29	0.57	1.14	2.28
Zn	0.23	0.45	0.9	1.80

Microbial granules for the batch experiments were harvested from the biogranule reactor on day 311. The VSS:TSS ratio of the harvested biogranules was 62%. Harvested biogranules were first separated from the liquid media via centrifugation. Then, the granules were washed once with tap water and the supernatant was removed by centrifugation. These granules were used for further batch tests.

In batch tests, 100 mL serum bottles were used. In each batch the bacteria concentration in the form of biogranules was set to ~3000 mg/L. In order to induce microbial production

of carbonate in synthetic leachate solutions given in Table 3.5, each solution was supplemented with nutrients providing the final nutrient concentrations of 1 g/L urea, 100 mg/L NO_3-N and 1542 mg/L COD. In the absence of Ca^{2+} ions, the metals were expected to act as the metal ions in carbonate precipitation. The batch reactors for biomineralization experiment were given in Figure 3.3. Each batch was prepared in triplicate.

Figure 3.3. Batch reactors for the biomineralization tests

In order to verify that the metals in the bioleachate solution precipitated due to the effect of the granules, abiotic control batches were prepared. Initially, the air in the headspace of the batches (10 mL) and the dissolved oxygen in the medium were not removed. However, processes were carried out at anoxic operational conditions by completely sealing the bottles with rubber stoppers. Therefore, the process was initially carried out under microaerobic conditions until the initial dissolved oxygen was depleted, then the rest of the process took place under anoxic conditions.

All the prepared bottle reactors were operated at 25°C on a 100-rpm shaker for a total of 6 hours. At the end of the 3rd hour and the 6th hour, samples were taken from the reactors to determine the dissolved metal concentrations inside the reactors. In addition, COD, TAN and NO_3-N analyzes were performed with the samples taken from the reactors to determine the microbial activities of the biogranules during the biomineralization process.

3.2.2. Analytical Methods for Determination of Metal Biomineralization Performance

In order to examine the biogranule activity in the bioleachate solution, COD, NO_3-N and TAN analyses were conducted on each sample according to the methods given in section 3.1.6. In addition, samples were analysed with ICP-MS device to determine the dissolved metal concentration that could not be separated from the leachate solution via bioprecipitation.

ICP-MS analyzes were performed based on EPA 200.2 (Sample preparation procedure for spectrochemical determination of total recoverable elements) and EPA 6020 (Multi-elemental determination of analytes by Inductively Coupled Plasma-Mass Spectrometry, ICP-MS in environmental samples) methods. For the calibration studies performed for the analysis, the solutions were prepared using Agilent (27 element mix: 8500-6940 2A and 8500-6940 Hg) and the obtained calibration curves are given in Annex-I. All samples were analyzed as triplicate and mean values were used in the thesis study.

The carbonate content of the precipitates was determined by using a test setup described by Kardogan et al. [259]. In this setup, which is given in Figure 3.4., 10 M H_2SO_4 was added to the reactors to dissolve the carbonate precipitates. Formed gas bubbles due to the latter were trapped inside the vacuumed headspace of a water column and the carbonate content was calculated by using Eqn. (32).

$$P.V = n.R.T \quad (32)$$

$$KH = PCO_2 / [CO_2] = 29.41 \text{ atm/M} \quad (33)$$

$$\text{Metal-}CO_3 + H_2SO_4 \rightarrow \text{Metal-}SO_4 + CO_2\uparrow + H_2O \quad (34)$$

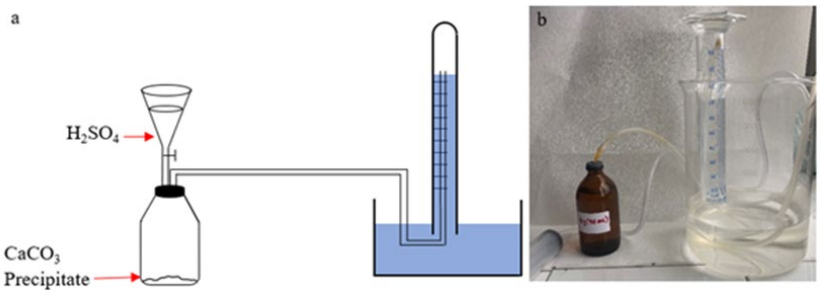

Figure 3.4. (a) Schematic representation of the CO_3^{2-} quantification method; (b) Experimental set up of CO_3^{2-} quantification [258].

4. RESULTS AND DISCUSSION

4.1. Granulation and Nickel Acclimation Stage

The reactor, which was inoculated with spores, was fed with diluted concentrations of the nutrient solution until the volatile solid (VS) value reached 2500 mg/L. During this time, analyzes were not performed to evaluate treatment performance, but total solid (TS) and volatile solid values were determined. The TS-VS changes during the enrichment of bacteria inside the reactor, are given in Figure 4.1.

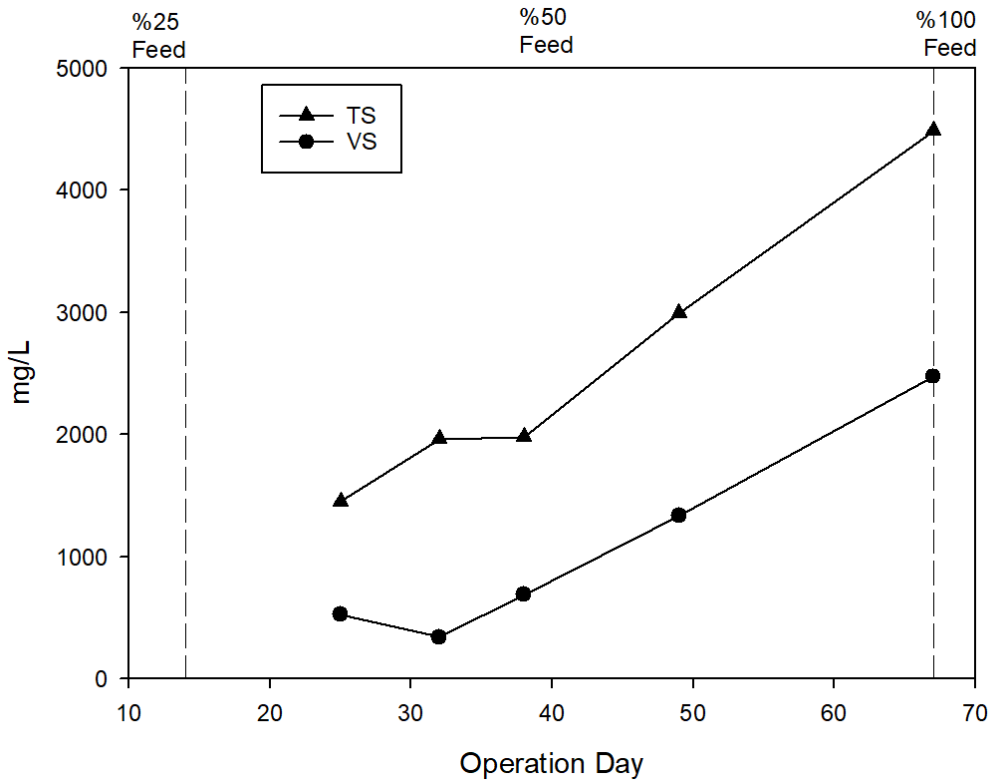

Figure 4.1. TS-VS values during the enrichment of bacteria from seed

During the enrichment stage, the VS/TS ratio gradually increased and reached to 55% as shown in Figure 4.2. As the VS concentration was over 2500 mg/L and VS:TS ratio was higher than 55% on day 67, the reactor was further operated without diluting the feed solution given in Table 3.1.

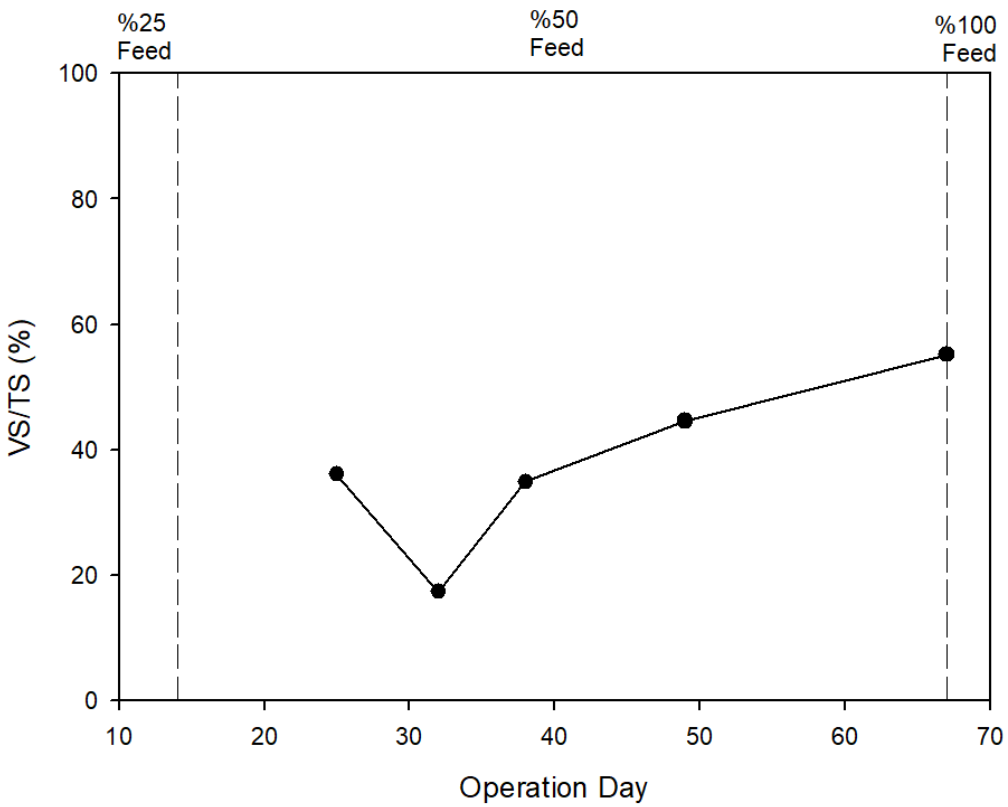

Figure 4.2. VS/TS ratio before %100 feeding

Parameters pH, DO, TSS-VSS, NH_4-N, floc/granule size distribution were monitored regularly until stable and mature granules were obtained. When these parameters became steady, the carbon oxidation, nitrate reduction and urea hydrolysis performances of the microbial community were evaluated by kinetic analyses of a single cycle. In order to assess the effect of Ni on the activity of microbial community kinetic measurements were conducted before and after the acclimation period to Ni exposure.

During the acclimation period, nickel feed was provided to the reactor by gradually increasing the Ni concentration of the feed solution from 1 mg/L to 4 mg/L and regularly monitoring the performance parameters. After the reduction in the granule sizes, which were examined regularly, the nickel feeding was stopped at 4 mg Ni /L level. Results of the kinetic analysis before and after the acclimation period was compared among each other. Each operation stage, except the enrichment period, was represented with a letter (Table 4.1) in the graphs of the operating parameters.

Table 4.1. Letters representing each of the operational periods in performance figures

Granulation Period (100 mg NO_3-N/L)	Granulation Period (200 mg NO_3-N/L)	1 mg/L Ni Feeding	2 mg/L Ni Feeding	3 mg/L Ni Feeding	4 mg/L Ni Feeding
A1	A2	B	C	D	E

4.1.1. pH

Recorded pH values in the feed solution, during anoxic period and aerobic period at all operational conditions of the reactor are given in Figure 4.3.

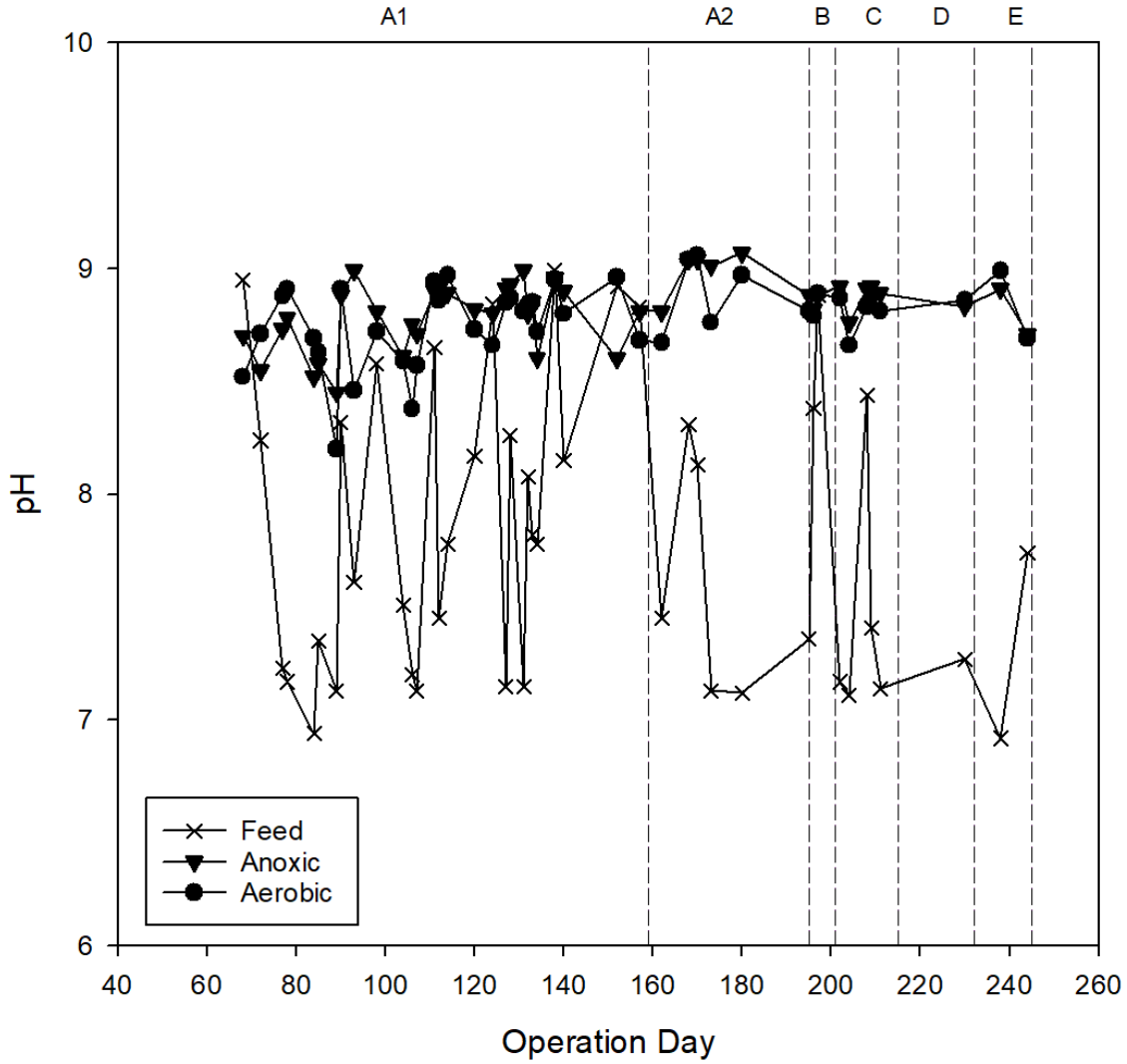

Figure 4.3. pH change during reactor operation; A1) Granulation period (100 mg NO_3-N/L), A2) Granulation period (200 mg NO_3-N/L) B) 1 mg/L Ni feeding period, C) 2 mg/L Ni feeding period, D) 3 mg/L Ni feeding period, E) 4 mg/L Ni feeding period

The main reason feed pH is so unstable is that nutrient solutions begin to degrade over time. Spontaneous microbial activities in the nutrient solution cause urea hydrolysis which raise the pH of the feed. While the pH value of the freshly prepared nutrient solution was 7.3 on average, the pH value of 3-days old nutrient solutions could exceed 8. However, this situation did not significantly affect the pH values at the end of the anoxic and aerobic periods.

The pH value measured at the end of the aerobic period was generally around 8.7-8.9 on average. The anoxic pH value was recorded as 8.8 on average. During the reactor operation, a slight increase in pH values is observed both at the end of the anoxic period and at the end of the aerobic period from the 70th day to the beginning of 1 mg/L Ni acclimation period. This was attributed to the NO_3-N reduction and urea hydrolysis performed by biogranules, as both processes produce alkalinity. According to a study by Wang et al., a pH value above 7 is sufficient for metal carbonate precipitation [253], and in this thesis study pH values were always above 8.

4.1.2. Dissolved Oxygen

DO values were measured regularly during the reactor operation and are given in Figure 4.4. While the average DO value was 5.5 mg/L in the aerobic periods of the cycles, it was 0.17 mg/L in the anoxic periods. Recorded values confirmed that the anoxic and aerobic periods were successfully achieved in the reactor. It was observed that the Ni acclimation step did not significantly affect the DO concentration in the reactor.

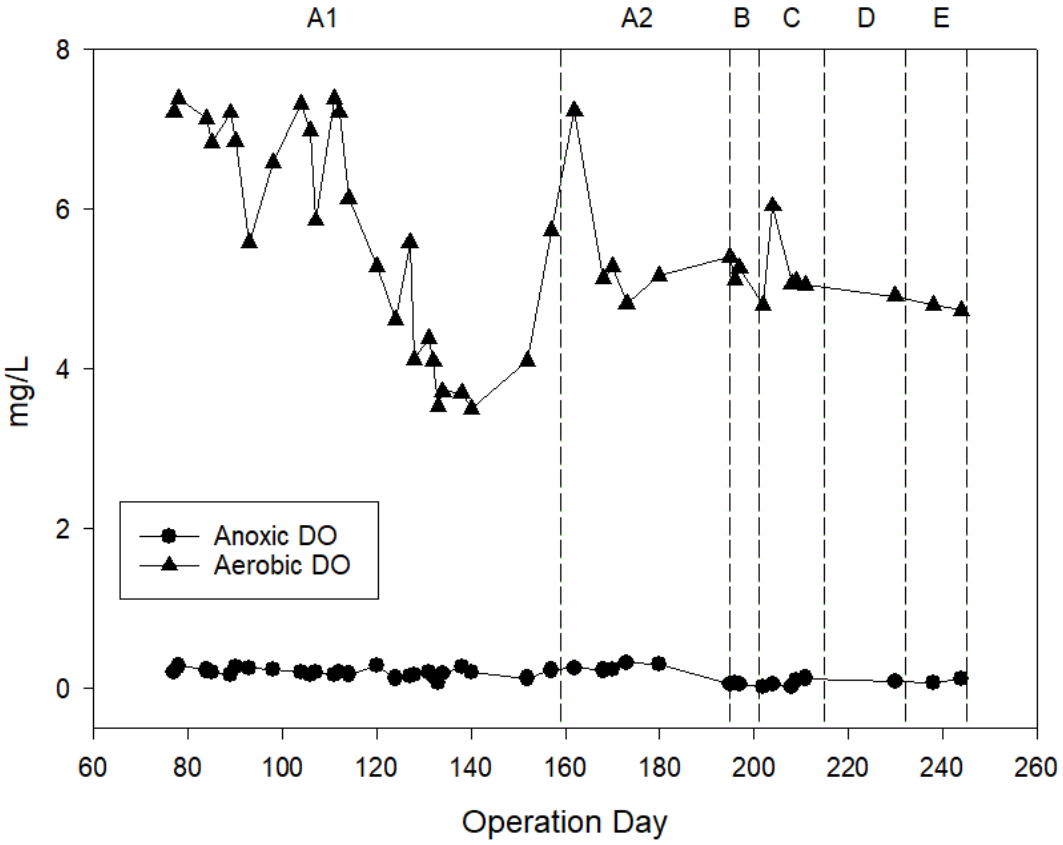

Figure 4.4. DO change during reactor operation; A1) Granulation period (100 mg NO_3-N/L), A2) Granulation period (200 mg NO_3-N/L) B) 1 mg/L Ni feeding period, C) 2 mg/L Ni feeding period, D) 3 mg/L Ni feeding period, E) 4 mg/L Ni feeding period

4.1.3. TSS-VSS

As seen in Figure 4.5, the VSS value in the reactor could only reach around 6500 mg/L until the 157th day. From day 159, the concentration of NO_3-N in the nutrient solution was doubled (200 mg NO_3-N/L). As a result of denitrifying bacteria reaching more $NO_3 - N$, microbial activity increased and thus microbial growth as well. After the nitrate increase in the feed, the VSS value doubled within 2 weeks.

Feng et al. investigated the simultaneous nitrification and denitrification activities of aerobic granules under 1, 5 and 10 mg/L Ni exposure. While 1 mg/L Ni stimulated nitrification and COD degradation activities, these activities were inhibited when the Ni concentration was increased to 10 mg/L Ni. The highest nitrification and COD degradation activities were observed during 5 mg/L Ni feeding. In addition, inhibition of denitrification activity was observed at all Ni concentrations [248]. In this context, as a result of feeding low concentrations of Ni to the reactor, Ni accelerated the growth of

microorganisms by creating a trace element effect. However, 3 mg/L Ni feeding negatively affected the biogranule stability as the major core community in the biogranules were denitrifying bacteria. This negative effect on denitrifying core community might have caused disintegration of biogranules. The latter caused wash-out of VSS from the reactor due to the hydraulic selective pressure in the reactor (no settling period).

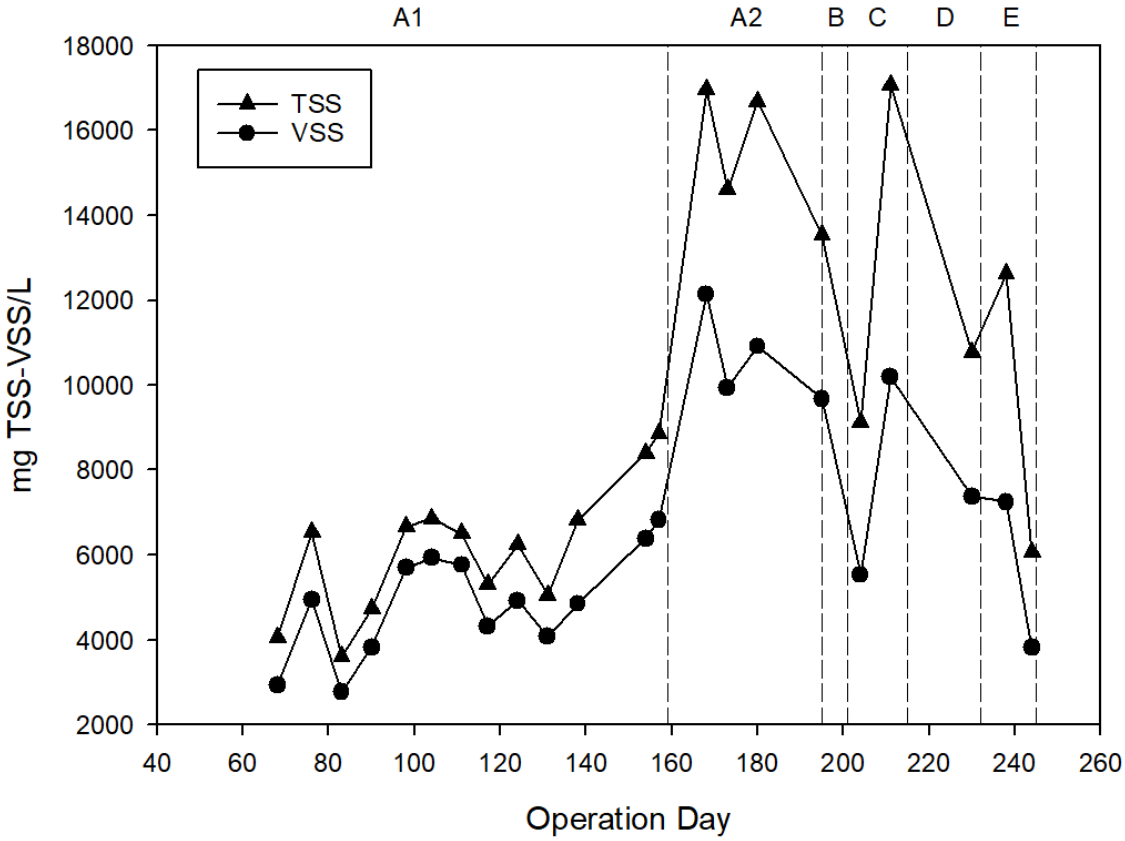

Figure 4.5. TSS-VSS change during reactor operation; A1) Granulation period (100 mg NO_3-N/L), A2) Granulation period (200 mg NO_3-N/L) B) 1 mg/L Ni feeding period, C) 2 mg/L Ni feeding period, D) 3 mg/L Ni feeding period, E) 4 mg/L Ni feeding period

In order to determine the bacterial content of the biogranules in the reactor, the VSS/TSS ratio was calculated and given in Figure 4.6. According to the VSS/TSS ratio data, a maximum microbial density was obtained with of 88% on the 111th day. In addition, it was determined that the granules, which were examined with a microscope in this period, had small sizes but very compact shapes.

Granular compactness and stability mainly depend on microbial growth rate [250]. It is known that granules obtained in operational conditions promoting slow growth rate are

stronger and more compact than granules obtained with systems with fast growth rate [260]. Therefore, it was also possible that the increase in the amount of flocs during the Ni acclimation period was due to the trace element effect of Ni on growth rate of the bacteria in the reactor. Both disintegration of the existing granules and the increase in growth rate might lead to boost of flocs and formation of loose unstable granules.

One of the most important parameters increasing the microbial growth rate is OLR [261]. For instance, in a study by Moy et al., granulation was performed with different OLRs. According to the results of the study, it was determined that the granules obtained at low OLR had a high density of filamentous bacteria and a loose structure. In the granulation performed at high OLR, granules with a more irregular structure with folds and crevices on the surface were obtained [262]. The formation of floc is significantly higher in granulation reactors with high OLR and therefore high growth rate. In this context as a result of doubling the NO_3-N concentration, the VSS raise was observed due to excessive formation of floc. The stability of the reactor, which was also monitored through the abundance of compact granules, has been deteriorated due to this increase.

As a result of the microscope examination of the samples taken from the sludge in the reactor, it was observed that the compact structure of the granules began to deteriorate during the Ni feeding process, and at the same time, nickel-carbonate compounds were found in the sludge in crystalline form. Hence, accumulating $NiCO_3$ crystals in the reactor increased the TSS value, causing a decrease in VSS/TSS ratio.

Barros et al. reported that the VSS/TSS ratios started to decrease slowly as a result of the accumulation of inorganic calcium compounds in the reactors where they grew biogranules [263]. Moreover, in another study by Ren et al., it was reported that excessive $CaCO_3$ accumulation had a negative effect on the microbial activities of biogranules. It has been shown that CaCO3 compounds accumulated on the granule surface prevent substrate entry into the granule core and impair the microbial activity of microorganisms in the granule core [264]. In this context, it can be said that $NiCO_3$ compounds accumulated as a result of Ni feeding cause a decrease in the TSS/VSS ratio of the reactor.

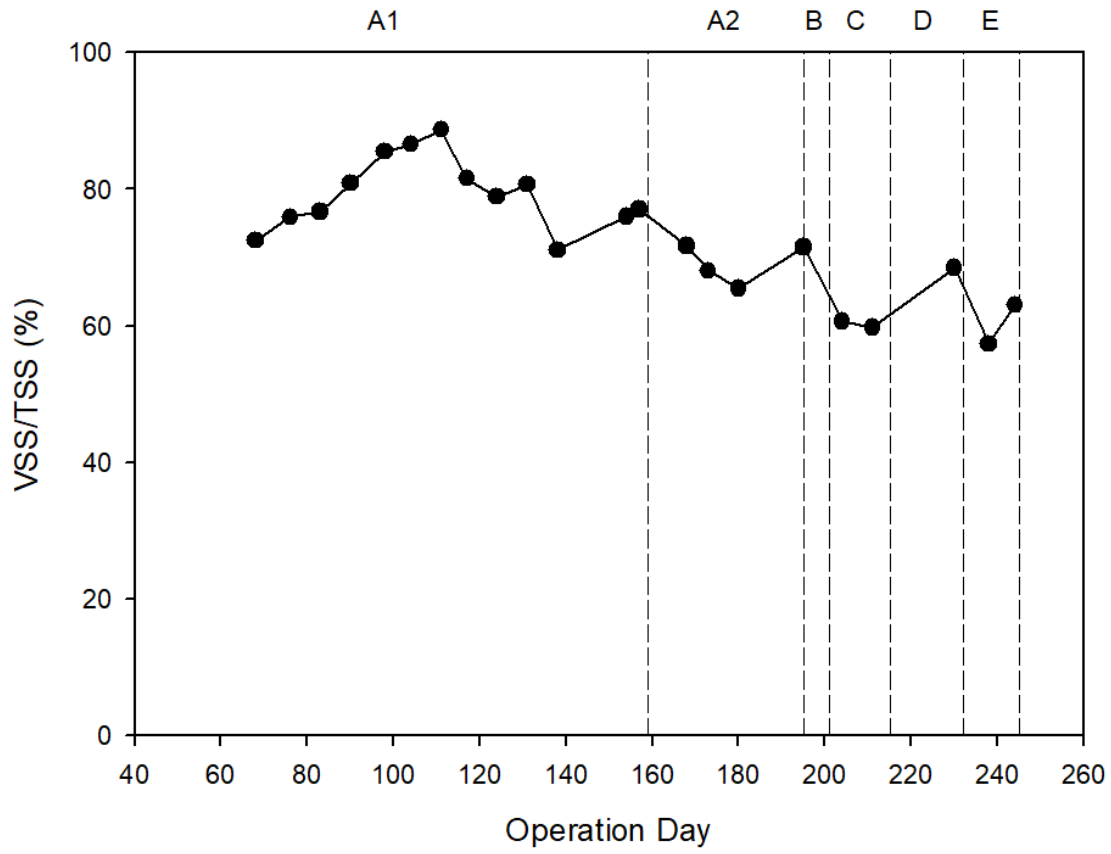

Figure 4.6. VSS/TSS ratio change during reactor operation; A1) Granulation period (100 mg NO_3-N/L), A2) Granulation period (200 mg NO_3-N/L) B) 1 mg/L Ni feeding period, C) 2 mg/L Ni feeding period, D) 3 mg/L Ni feeding period, E) 4 mg/L Ni feeding period

4.1.4. Sludge Volume Index

The sludge volume index values which indicates the settling characteristics of the granules were measured regularly. While the reactor was operating in the aerobic period with full stirring, aeration was stopped for 30 minutes to calculate the SVI_5 and SVI_{30} values. SVI values at the 5th and 30th minutes were calculated and given in Figure 4.7.

It was described that in granular sludge reactors, SVI_{30} value over 150 ml/g is an indication of the abundance of bulk and filamentous bacteria. [265]. In this study, since the seed of the biogranulation reactor was the powder obtained from a granular reactor with good settling characteristics [250], the SVI_{30} value of the reactor was recorded as slightly above 50 ml/g immediately after the enrichment period (enrichment period: Day 0 - 68). SVI_{30} value decreased even more during the granulation period. Between Day 79

and Day 201 SVI_{30} was under 50 ml/g which revealed that the reactor content was fully granular biomass.

The SVI_{30}/SVI_5 ratio is another good indicator of the granulation level of the reactor during the granulation period (when SVI_{30} is close to or larger than 50 ml/g) [257]. However, it should be noted that the sensitivity of this measurement decreases significantly when the system is completely granular, because in fully granular systems, SVI_5 value might change rapidly due to granule disintegration or increase in floccular biomass while SVI_{30} does not change significantly as the overall composition is still mostly granular. The former cause significant changes in the granule percentage (Figure 4.7) which do not truly represent the reactor content. Considering this sensitivity, it can be claimed that in fully granular systems (when SVI_{30} < 50 ml/g and VSS:TSS ratio > 75%) SVI_{30}/SVI_5 values are only significant to detect granule disintegration and floc formation but they are less meaningful in terms of determination of granule percentage until the SVI_{30} value reach above 50 ml/g. In stage A2, due to the increase of NO_3-N in the feed solution, floc formation and microbial activity increased. In the same period, the SVI_{30} value did not change significantly (Figure 4.7). The main reason for this seems to be that the mature granules in the reactor continued to sweep part of the newly formed flocs. As seen in Figure 4.7, in stage A2, SVI_5 value slightly increased with the increase in floc formation and as a result the SVI_{30}/SVI_5 ratio decreased abruptly although the SVI_{30} value was way below 50 ml/g which was an indication that the system was mostly granular (See section 4.1.8). These observations confirmed that the SVI_{30}/SVI_5 ratio is more meaningful during the granulation stage rather than full granular stage. Increase in SVI_5 further continued with the further disintegration of granules during acclimation period operated for Ni exposure.

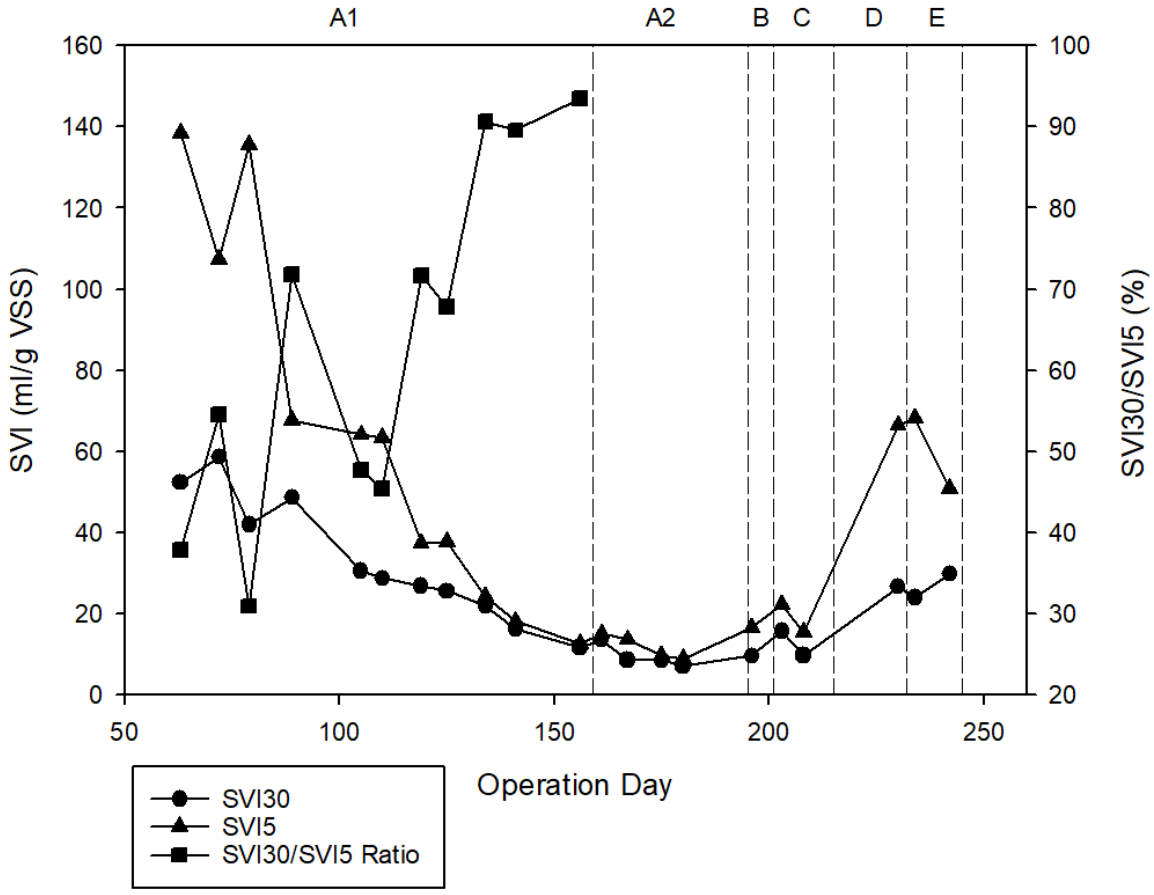

Figure 4.7. SVI change during reactor operation; A1) Granulation period (100 mg NO_3-N/L), A2) Granulation period (200 mg NO_3-N/L) B) 1 mg/L Ni feeding period, C) 2 mg/L Ni feeding period, D) 3 mg/L Ni feeding period, E) 4 mg/L Ni feeding period

4.1.5. Granular Size Distribution

The granule size, which affects the specific surface area and cohesion of the granule, determines the performance of the whole process by affecting the microbial activity and granule performance by causing differences in substrate and oxygen permeability [266].

In this context, granule size distribution analyzes were performed at different stages of granule growth as seen in Figure 4.8. In the distribution analysis performed on the 133rd day, the presence of granules from 0.2 mm to 3.5 mm was detected. In this period, the rate of granules with a diameter higher than 0.2 mm was determined as 95.78%. In addition, the SVI30 value of the reactor was determined as 22 ml/g so the reactor content was fully granular. However, as can be seen in Figure 4.9. larger granules did not have a compact structure.

On the 147th day, round and compact granules were obtained compared to the previous analysis. However, the granules, which were in large sizes before, were getting compacter at this stage. The density of 0.2-0.6 mm diameter granules was 58% and 69% on days 133 and 147, respectively, which revealed a significant increase in compactness. Moreover, the rate of granules with a diameter higher than 0.2 mm was determined as 98.91% in this period.

In the distribution analysis performed on the 171st day, the granule density with a diameter of 0.4-0.6 mm had the highest rate with 53%. Also in this period, the rate of granules with a diameter higher than 0.2 mm was determined as 100%. A slight increase in the diameters of the granules also positively affected their microbial activity. The reactor, which had 70% urea hydrolysis on the 133rd day, showed 77% urea hydrolysis performance on the 171st day. It can be said that the increase in the microorganism density in the anoxic zone in the granule core and the doubling of the NO_3-N feeding in the same period cause this increase in urea hydrolysis.

In the last distribution analysis before the Ni acclimation process, 70% of the biogranules have a diameter of and 0.2-0.4 mm. In this period, the SVI_{30}/SVI_5 ratio reached its highest with 90%. Although the granule sizes obtained in this thesis study were smaller than those reported (1.4-3.4 mm) in previous studies [267, 268], when the settling characteristics, microbial activities and microscopic images were concerned, it was quite clear that mature stable granules were obtained.

Moreover, some of the recent studies revealed that when low strength wastewater was used, granules which has smaller diameter size were obtained (0.2-0.9 μm) [269]. In the granulation study performed by Czarnota et al., granules were obtained with two different OLR values. Smaller diameter granules were formed in the reactor fed with low OLR [261]. In the study of Du et al., granules were obtained in two separate SBR reactors fed with different NLR. In the reactor fed with low NLR, smaller diameter but rather compact granules were obtained with a slower granulation process [270]. In this context, small but highly compact granules were obtained with minimal nutrient feeding, which was used to reduce granule production costs in the thesis study.

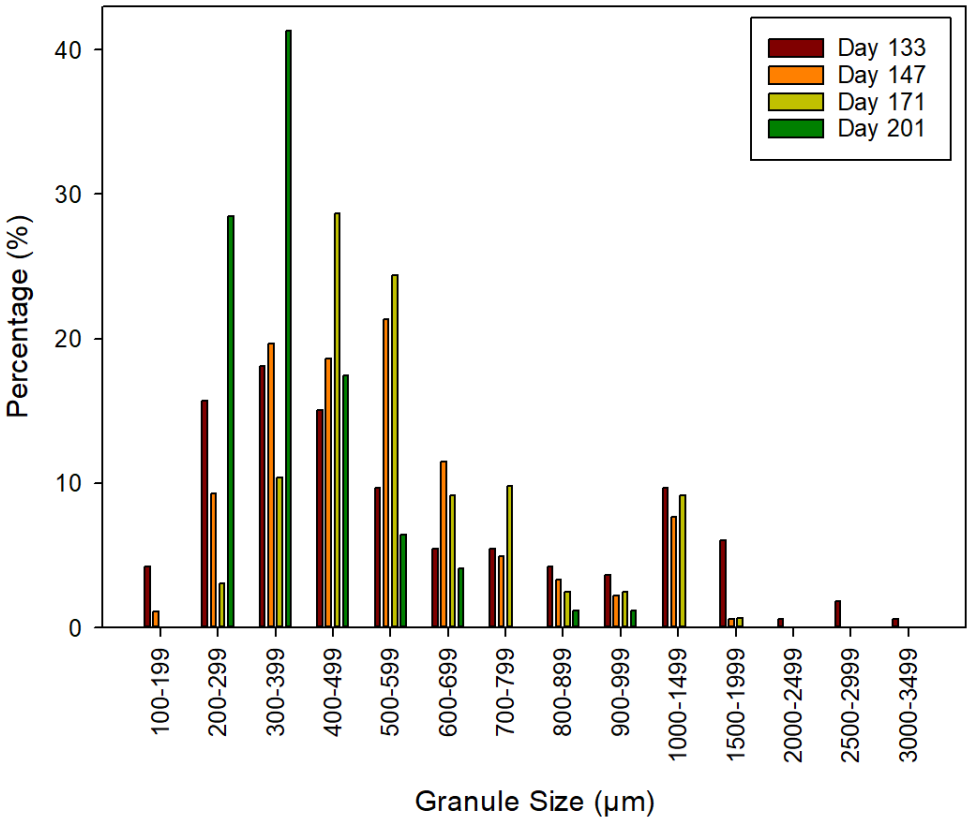

Figure 4.8. Change of granule size distribution between days 133 and 201

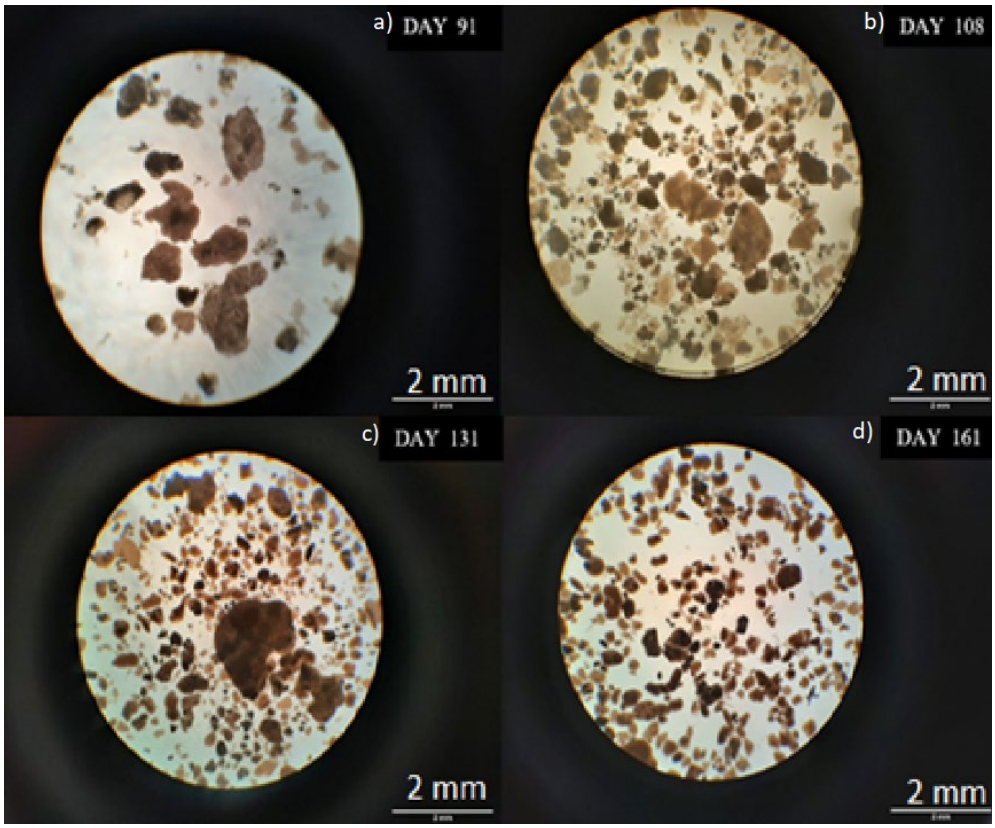

Figure 4.9. Granule size alteration of granulation stage; a) Day 91, b) Day 108, c) 131, d) 161

The size distribution analysis data achieved before each increase in the Ni dose during the acclimation stage are given in Figure 4.10. According to the size distribution analyzes performed at the end of each metal increase in the Ni acclimation period, the proportions of granules larger than 0.2 mm were determined as 98.15%, 87.21%, 86.63% and 74%, respectively. Although low Ni concentration played an important role in the increase in VSS, it caused a decrease in the granule sizes as seen in Figure 4.11. As a result of the size distribution analysis performed on day 244, the percentage of the granules with a diameter of 0.2-0.3 mm was 60% and the percentage of the flocs smaller than 0.2 mm was 26%. In addition, the disintegrated granules with poor settling properties were washed-out from the reactor during feed/draw period as there was no settling period before the feed/draw period. The wash-out caused a significant loss of VSS. Based on these data, the acclimation process was stopped at a Ni level of 4 mg/L to recover the granular biomass.

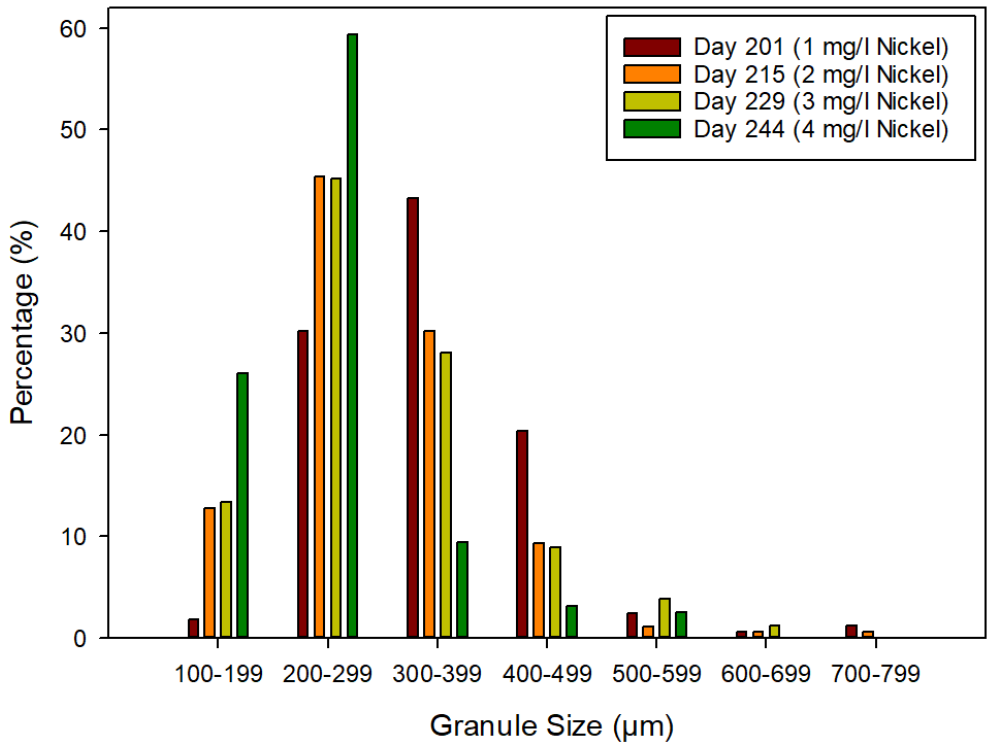

Figure 4.10. Change of granule size distribution in accordance with Ni feeding concentrations; Day 201: end of 1 mg/L Ni Feeding, Day 215: end of 2 mg/L Ni Feeding, Day 229: end of 3 mg/L Ni Feeding, Day 244: end of 4 mg/L Ni Feeding

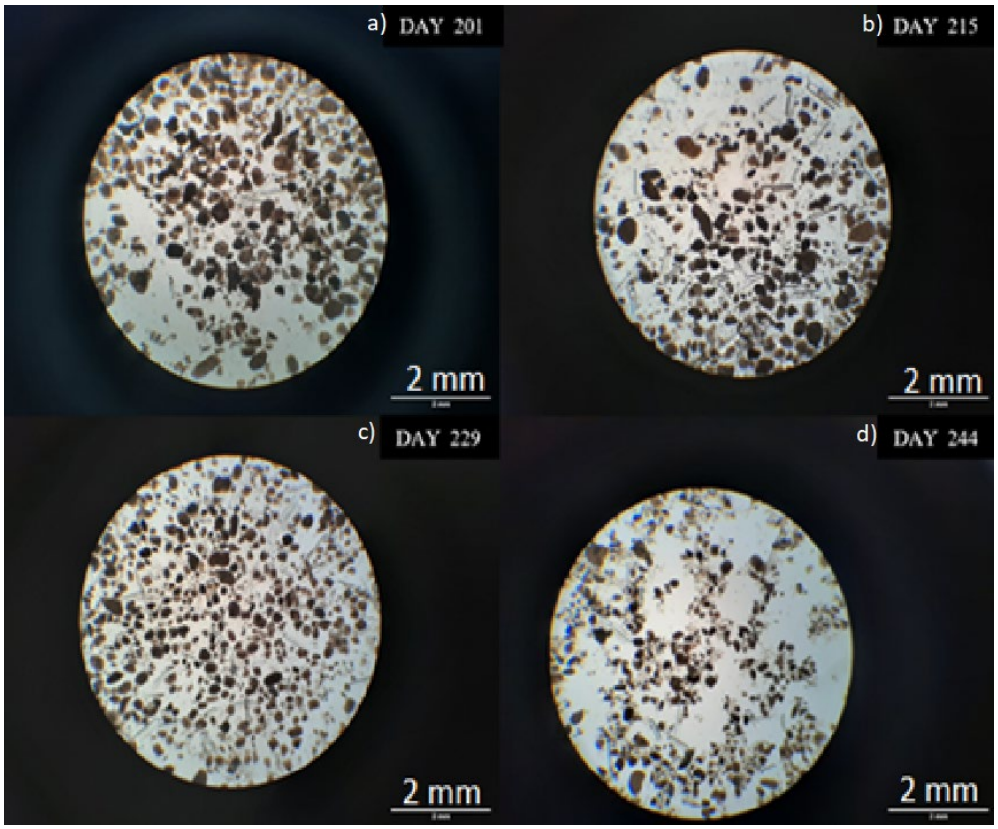

Figure 4.11. Granule size alteration during acclimation to Ni exposure; a) Day 201 (1 mg/L Ni feeding), b) Day 215 (2 mg/L Ni feeding), c) Day 229 (3 mg/L Ni feeding), d) Day 244 (4 mg/L Ni feeding)

4.1.6. Urea Hydrolysis

Urea was used as a nitrogen source in the granulation process. Urea hydrolysis efficiency of granules grown in aerobic and anoxic periods are given in Figure 4.12. Urea hydrolysis efficiencies were calculated by monitoring the variation of total ammonium nitrogen (TAN) concentrations over cycles.

TAN formed as a result of urea hydrolysis accumulates in the reactor. In case of nitrification activation in the system, only TAN measurements are not sufficient to monitor urea hydrolysis. In cases where nitrification is present, nitrite and nitrate measurements are performed, and urea hydrolysis is calculated over mass balance. For this reason, it was checked whether there was nitrification in the reactor during the aerobic period. Since neither ammonia oxidation nor nitrification occurred during the aerobic period, urea hydrolysis could be determined by monitoring the change in TAN concentration in the reactor.

In this context, the theoretical maximum TAN concentration that can occur in the reactor as a result of 100% urea hydrolysis was calculated as 466.7 mg/L and this value was obtained on the 207th day. Average urea hydrolysis throughout the steady reactor operation in stage A (days between 140-180) was 70.28±8.51% and the effluent TAN concentration was 417.03±14.14 mg/L. In addition, urea hydrolysis performances of all different operating periods are given in Table 4.2.

Table 4.2. Urea hydrolysis performance of reactor in different operation period

Period	**TAN Con. Anoxic Period (mg NH_4-N/L)**	**TAN Con. Aerobic Period (mg NH_4-N/L)**	**Anoxic Urea Hydrolysis (%)**	**Aerobic Urea Hydrolysis (%)**	**Total Urea Hydrolysis (%)**
Granulation (Day 70-140)	246.99±97.36	292.53±114.89	28.12±16.44	25.87±16.44	53.99±29.78
Granulation (Day 140-180)	360.28 ±27.27	417.03±14.14	48.17±8.01	41.95±17.02	70.28±8.51
1 mg/L Ni Feeding	360.45±9.14	424.95±5.54	53.82±1.59	55.68±7.79	79.63±3.17
2 mg/L Ni Feeding	326.77±48.98	466.20±24.76	43.69±16.51	100±13.88	100±8.54
3 mg/L Ni Feeding	379.56±0	423.11±0	52.70±0	35.44±0	69.46±0
4 mg/L Ni Feeding	344.40±2.80	396.20±9.80	56.33±1.64	46.69±10.28	76.89±3.61

2 mg/L Ni feeding increased the urea hydrolysis efficiency to 100±8.54% in the reactor. Mugwar reported in his doctoral study that the addition of low concentrations of Zn increased enzyme activity [271]. Similar to this situation, it can be said that Ni feeding has the same effect up to a certain concentration. In addition, according to the results obtained, the optimum Ni feed for microbial enzyme activity seems to be 2 mg/L. However, it is clear that further research is required to determine at which Ni concentrations the enzyme activity is best affected.

The major influence of Ni was observed on the aerobic microbial community as the positive effect on urea hydrolysis was only valid under aerobic conditions. Baltar et al. investigated the effects of metals such as Fe, Ni, Cu, Zn on the growth of heterotrophic

microorganisms in the marine water environment. As a result of the study, it was revealed that especially Fe significantly increased microbial growth [272]. In this context, it can be said that the Ni feeding carried out in the thesis study has the same effect.

When the periods in a cycle are compared among each other in terms of urea hydrolysis performance, 48.17±8.01% of the urea was hydrolyzed on average in the anoxic period, while this rate was around 22.11±10.27% in the aerobic period. The total urea removal was around 48.23±23.01% before doubling the NO_3-N concentration on Day 159, the total urea removal reached around 70.28±8.51% after the NO_3-N increase (Table 4.2). In the light of these data, it can be claimed that the bacteria hydrolyzing urea under anoxic conditions via nitrate reduction were more abundant in the granule compared to the bacteria hydrolyzing urea under aerobic conditions. This observation was significant as most of the urease positive bacteria reported in literature are strict aerobes [273]. Our findings revealed that considerable urea hydrolysis under anoxic conditions is also possible which can enhance the MICP yield of the community.

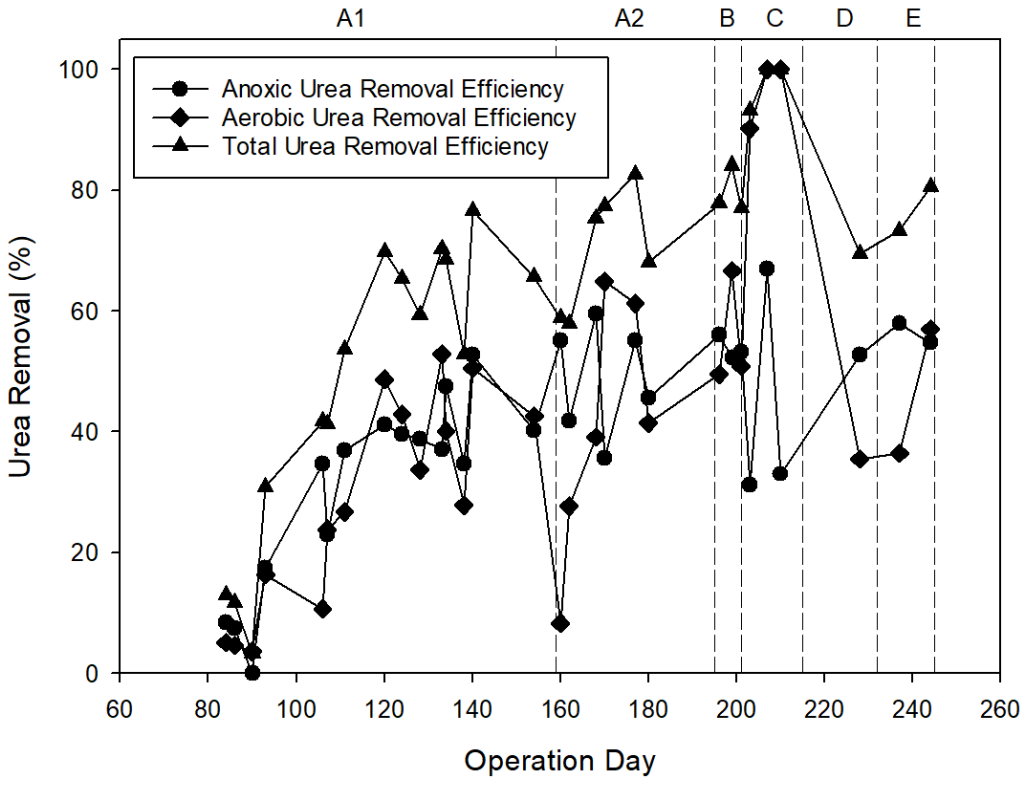

Figure 4.12. Urea removal variation during reactor operation; A1) Granulation period (100 mg NO_3-N/L), A2) Granulation period (200 mg NO_3-N/L) B) 1 mg/L Ni feeding period, C) 2 mg/L Ni feeding period, D) 3 mg/L Ni feeding period, E) 4 mg/L Ni feeding period

4.1.7. Organic Carbon Oxidation

COD values were measured by taking samples from the end of the anoxic and aerobic periods in a cycle and recorded values are given in Figure 4.13. As can be seen in Figure 4.14. of the reactor, as a result of the COD analyzes starting on the 166th day, the carbon oxidation activity ranges between 87-99%. According to these data, the amount of COD in a cycle was almost completely consumed at the end of the cycle.

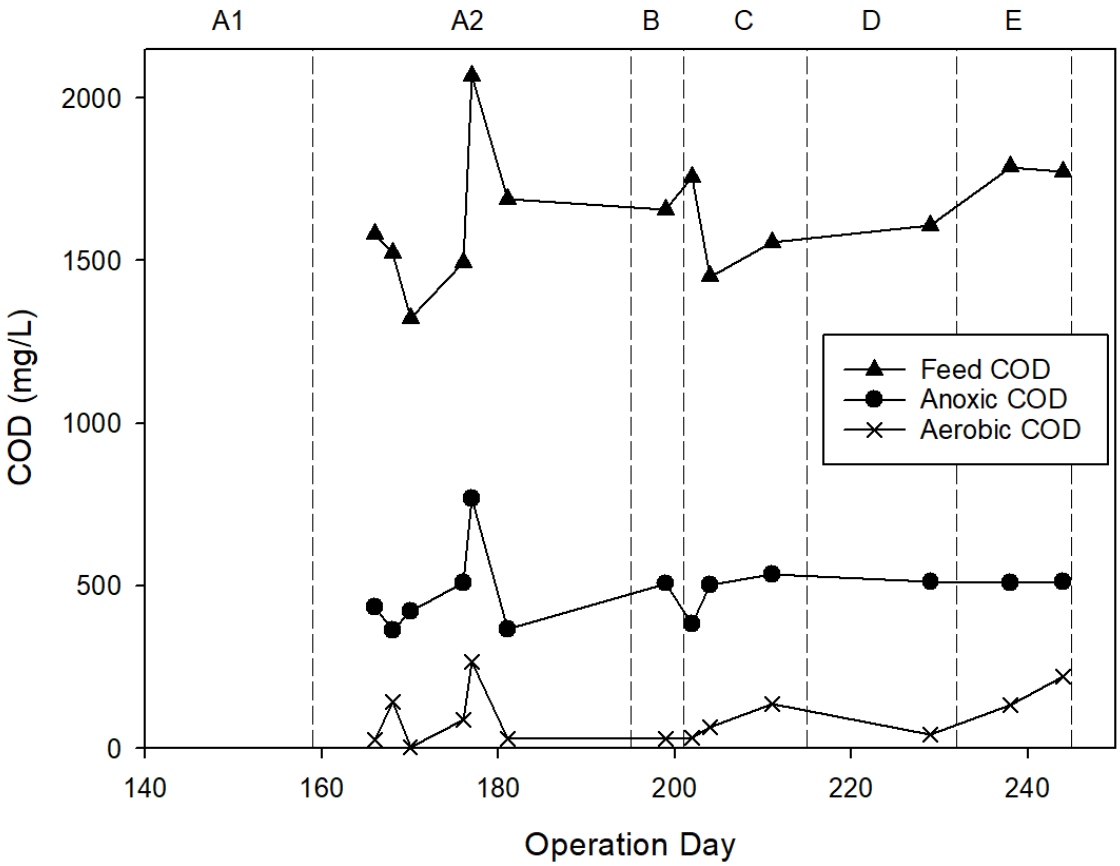

Figure 4.13. COD values at the end of the anoxic and aerobic periods throughout the operation; A1) Granulation period (100 mg NO_3-N/L), A2) Granulation period (200 mg NO_3-N/L) B) 1 mg/L Ni feeding period, C) 2 mg/L Ni feeding period, D) 3 mg/L Ni feeding period, E) 4 mg/L Ni feeding period

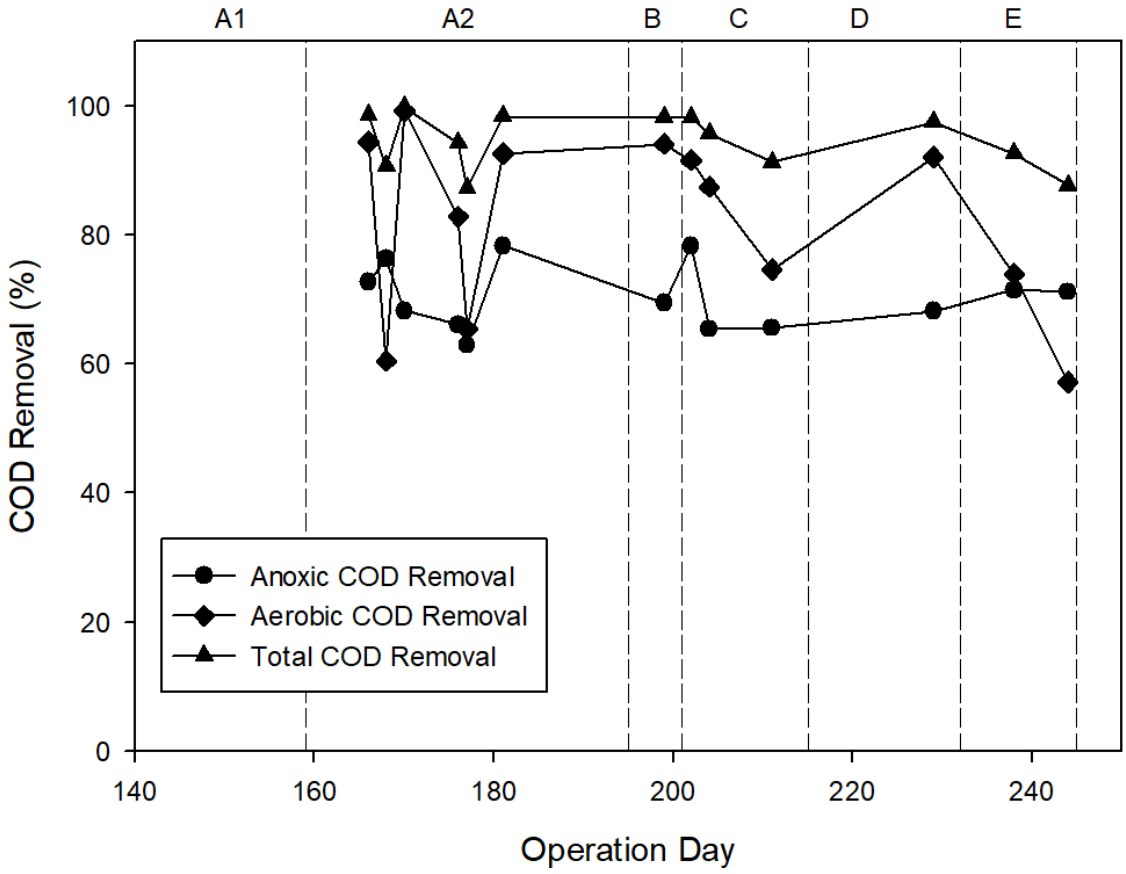

Figure 4.14. Evolution of COD consumption in anoxic and aerobic periods throughout the operation; A1) Granulation period (100 mg NO_3-N/L), A2) Granulation period (200 mg NO_3-N/L) B) 1 mg/L Ni feeding period, C) 2 mg/L Ni feeding period, D) 3 mg/L Ni feeding period, E) 4 mg/L Ni feeding period

4.1.8. Nitrate Reduction Activity

Oxidized nitrogen compounds might be used in various microbial processes such as nitrate reduction, dissimilatory nitrate reduction to ammonia (DNRA) or annamox. In order to verify that the nitrate reduction was coupled with carbon oxidation rather than annomox, on day 157, the culture inside the reactor was tested in a separate batch reactor for nitrate reduction activity. The nitrate reducing activity of 6819 mg/L initial VSS concentration was analyzed in a medium containing 100 mg/L NO_3-N and 1542 mg/L COD. The system was operated as a batch reactor under anoxic conditions with intermittent mixing for 3 hours. Samples were taken at 1-hour intervals and filtered.

NO_3-N and COD concentrations were examined and given in Figures 4.15 and 4.16. According to the results of the analysis, the COD/N ratio was found to be 6.94 in the

optimal range. According to the studies carried out in the literature, annamox can generally be used in the treatment of wastewater with a low COD/N ratio. The most suitable COD/N ratio for the Annamox mechanism to work is values below 0.5 [274]. In addition, annamox bacteria could be obtained up to 2.7 COD/N ratio by providing different conditions [275]. In the light of this information and experimental data, it is revealed that there is no annamox mechanism in the reactor.

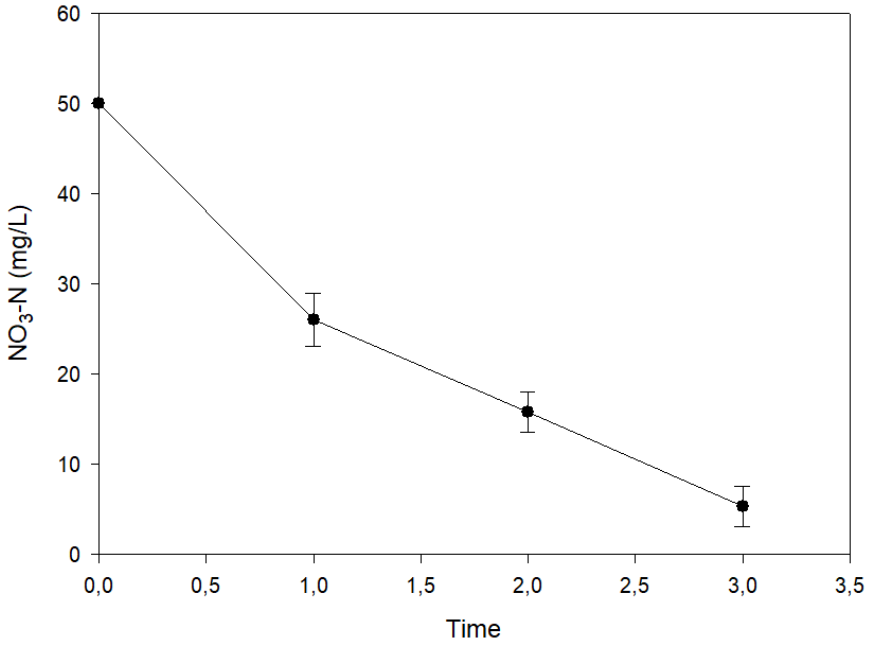

Figure 4.15. NO_3-N variation during batch test under anoxic operation condition

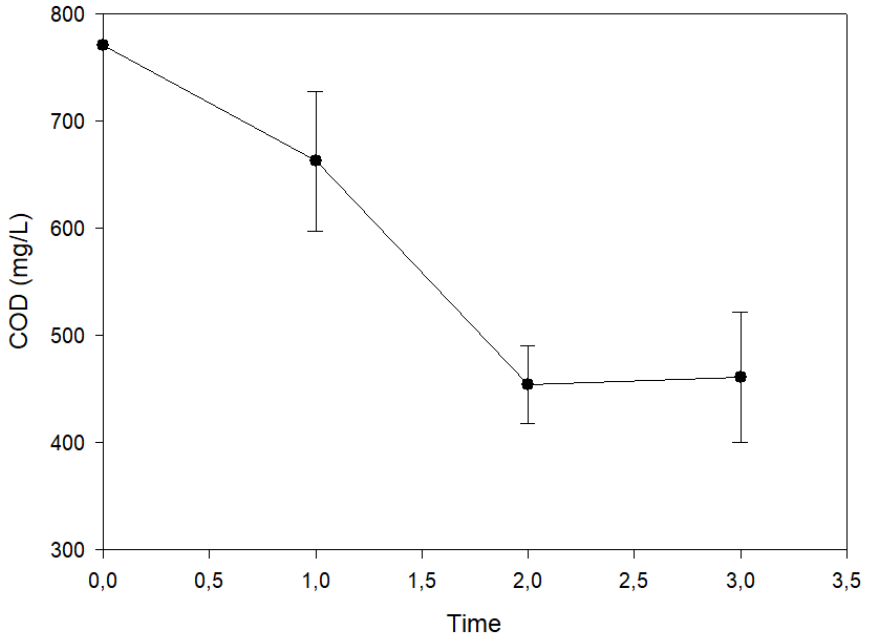

Figure 4.16. COD variation during batch test under anoxic operation condition

4.1.9. Microbial Activity of the Mature Biogranules

The biodegradation kinetics of substrates in a bigoranulation reactor provides information on microbial activities, simultaneously occuring processes (e.g. simultaneous nitrification and denitrification) and duration of feast-famine conditions [209].

Since the feeding was carried out in the form of plug flow in the SBR operating system, in order to avoid the effect of sample location, the kinetic analysis was carried out on the 180th day under completely mixed operational conditions. Samples were taken from the reactor in 15-minutes intervals, filtered, and NH_4-N, NO_3-N and COD analyzes were performed. As seen in Figure 4.17, the NH_4-N concentration increased rapidly at the beginning of the cycle. As shown in Figure 4.18, 64% of urea hydrolysis occurred in the first 3 hours in the anoxic period, while this rate obtained at the level of 69.32% in the aerobic period.

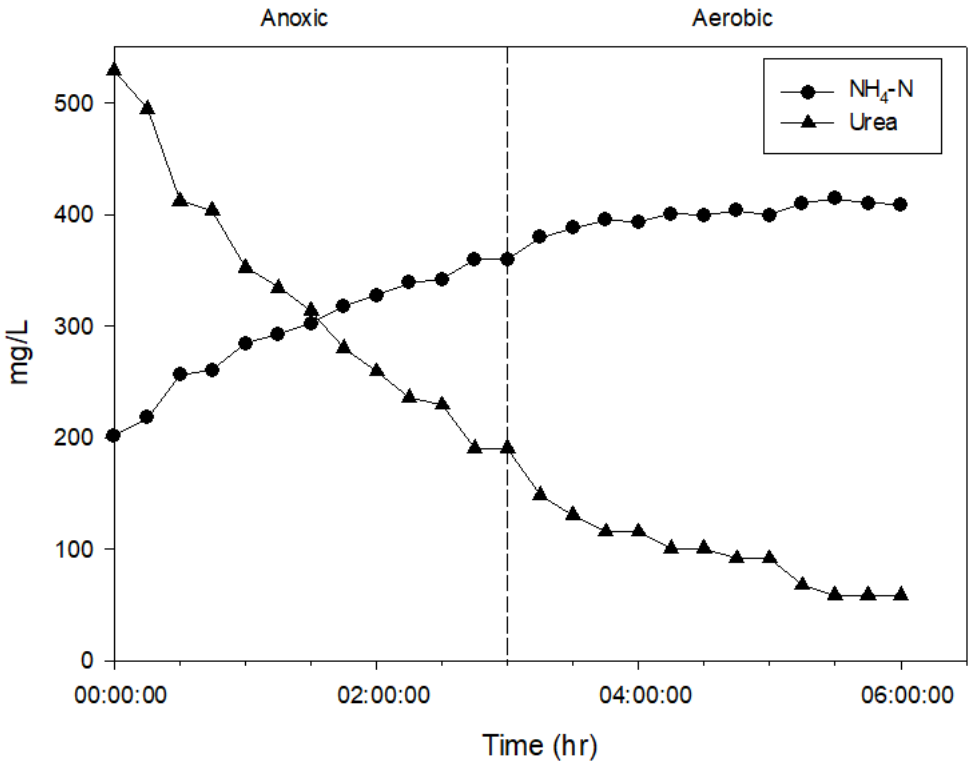

Figure 4.17. Variation of urea and NH_4-N and Urea concentrations in a cycle

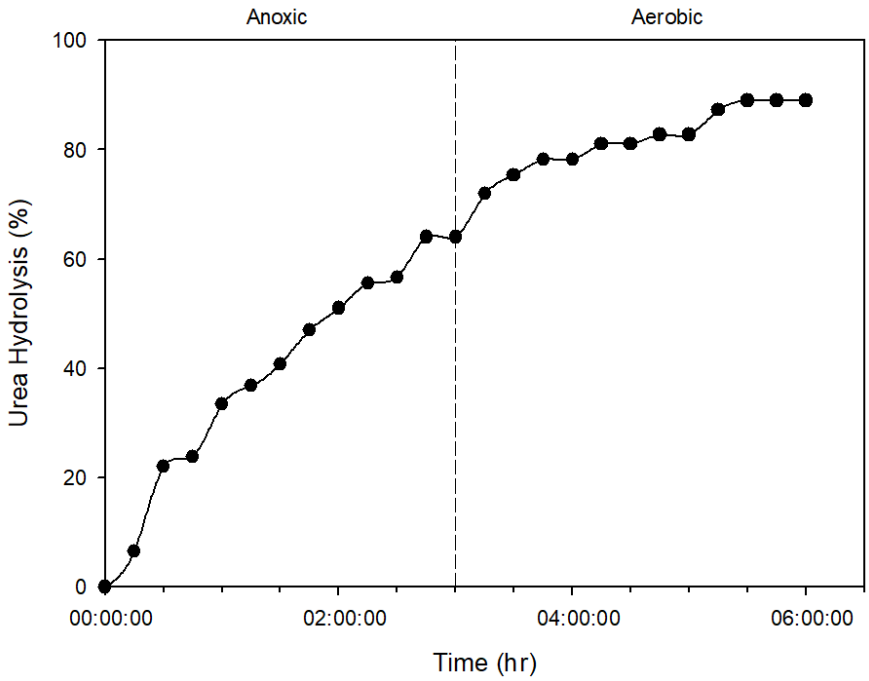

Figure 4.18. Urea removal variation in a cycle

According to the results of the kinetic analysis, 85% of the NO_3-N amount was reduced in the first 2 hours of the anoxic period. At the end of the anoxic period, NO_3-N in the reactor was completely reduced by microorganisms. The NO_3-N reduction activity in a single cycle was given in Figure 4.19.

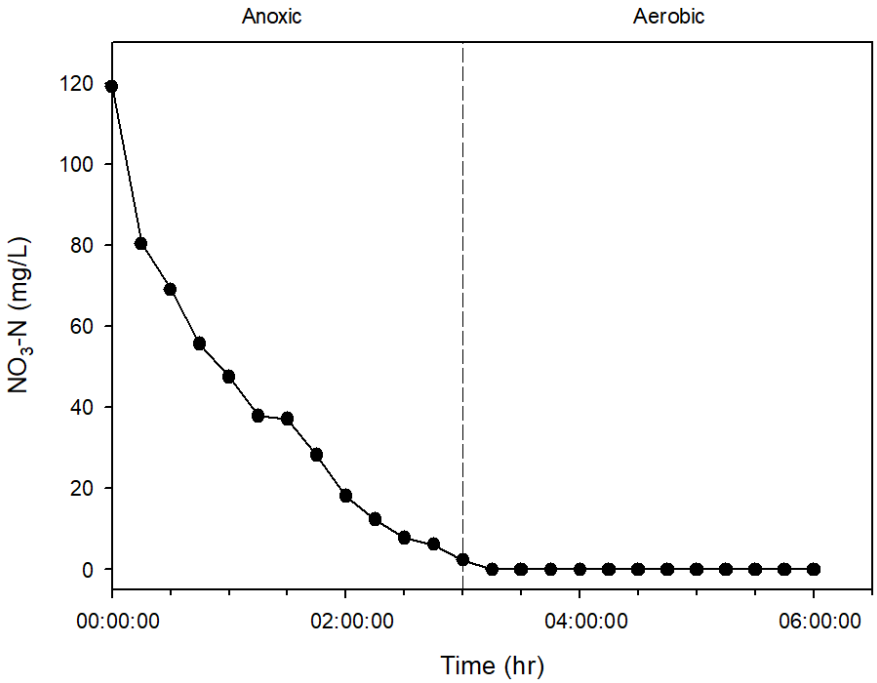

Figure 4.19. NO_3-N concentration variation in one cycle

As seen in Figure 4.20, 70% of the organic carbon was oxidized at the end of the anoxic period. The removal of a significant part of the COD in the anoxic period enabled the famine period in the aerobic period. At the end of the aerobic period, 95% of the COD amount was removed and only 50 mg/L COD remained in the reactor as shown in Figure 4.21. With the kinetic analysis data, it was understood that the reactor was ready for the Ni acclimation stage.

The COD/N ratio is one of the most important parameters affecting the size, shape and strength of the granules grown. As a result of the kinetic analysis experiment, the COD/N consumption was found to be 9.6 in one cycle. Considering that the low COD/N ratio limits the microbial activities of denitrifying bacteria [276], carbonate production is accomplished successfully by the denitrification mechanism of the granules.

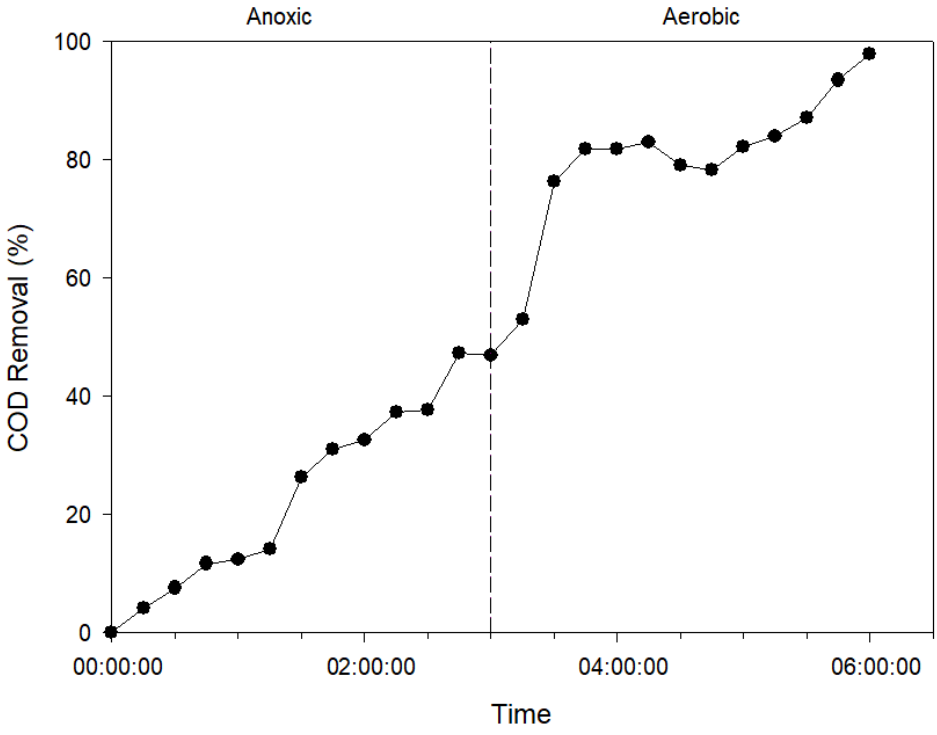

Figure 4.20. Oxidation of organic substrate in a single cycle

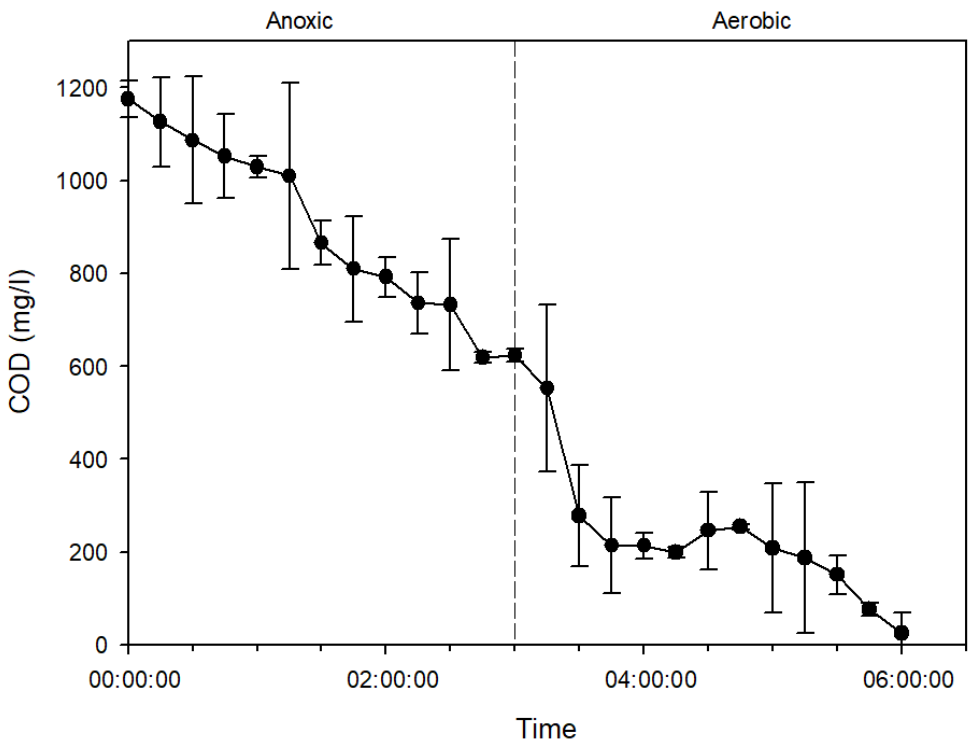

Figure 4.21. COD concentration variation in one cycle

4.1.10. Kinetic Analysis of Nickel Acclimation Stage

Kinetic analysis was carried out to examine the change in the microbial activities of the granules as a result of Ni feeding into the reactor. Due to the detection of deterioration in granule structures on day 244, kinetic analysis was performed to examine granule performances. The same kinetic analysis method that was carried out for the mature granules was performed again.

Despite the deterioration in granular structure and significant loss of VSS, urea was completely converted to ammonia in the beginning of the aerobic period, as seen in Figure 4.22 and 4.23. In addition, NO_3-N was completely consumed at the end of the anoxic period, as shown in Figure 4.24.

As seen in Figure 4.25, only 25 mg/L COD remained in the reactor as a result of the kinetic analysis. Moreover, as shown in Figure 4.26, the COD oxidation efficiencies in the anoxic and aerobic periods were 47% and 84%, respectively.

Taking all things into the consideration, although Ni feeding increased the activity of the microorganisms like a trace element, crystal nickel compounds accumulating in the reactor caused deterioration of granule structure and reduction of granule sizes.

In order to compare the microbial performances of the granules in both the steady operation with mature granules and Ni acclimation periods, the specific activity values are calculated and given in Table 4.3. Since NO_3-N is completely depleted before the aerobic period in both stages, NO_3-N reduction specific activity was only determined for anoxic periods. In addition, organic carbon oxidation and urea hydrolysis performances in the aerobic period increased 1.39 and 1.15 times, respectively, after Ni addition.

Table 4.3. Specific activity of biogranules in different operation conditions

Specific Activity (g substrate/ g VSS-h	**Anoxic Period (Mature granules)**	**Anoxic Period (Nickel Acclimation)**	**Aerobic Period (Granulation Kinetic)**	**Aerobic Period (Nickel Acclimation Kinetic)**
NO_3-N	0,004	0,009	NA*	NA*
COD	0,017	0,070	0,018	0,025
NH_4-N	0,010	0,039	0,004	0,005
*NA: Not applicable				

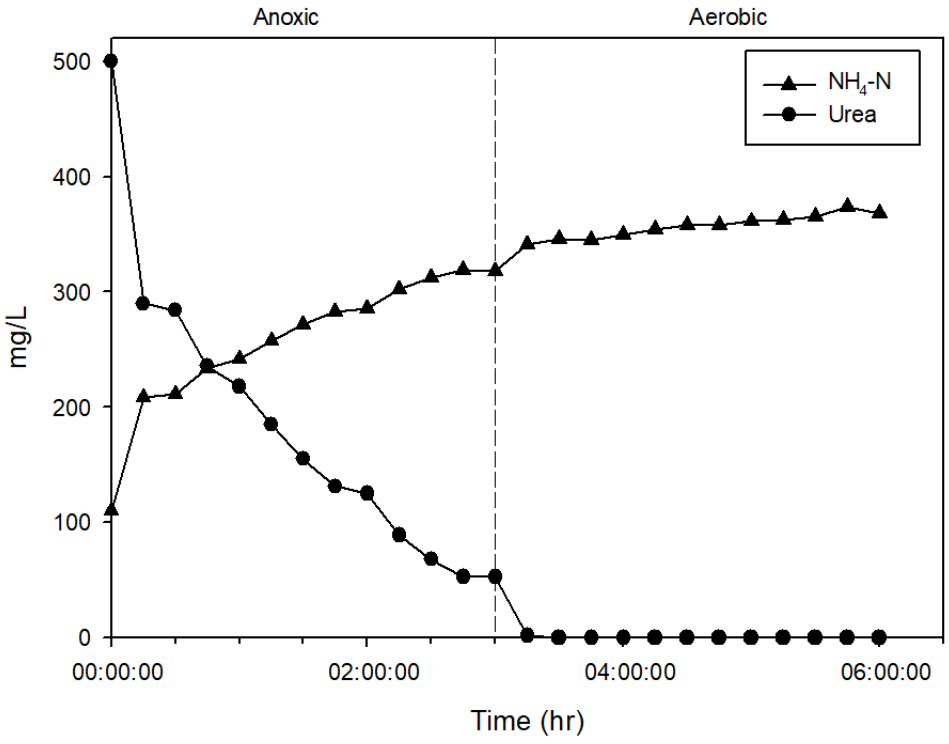

Figure 4.22. Variation of urea and NH_4-N concentrations in a cycle with 4 mg/L Ni feeding

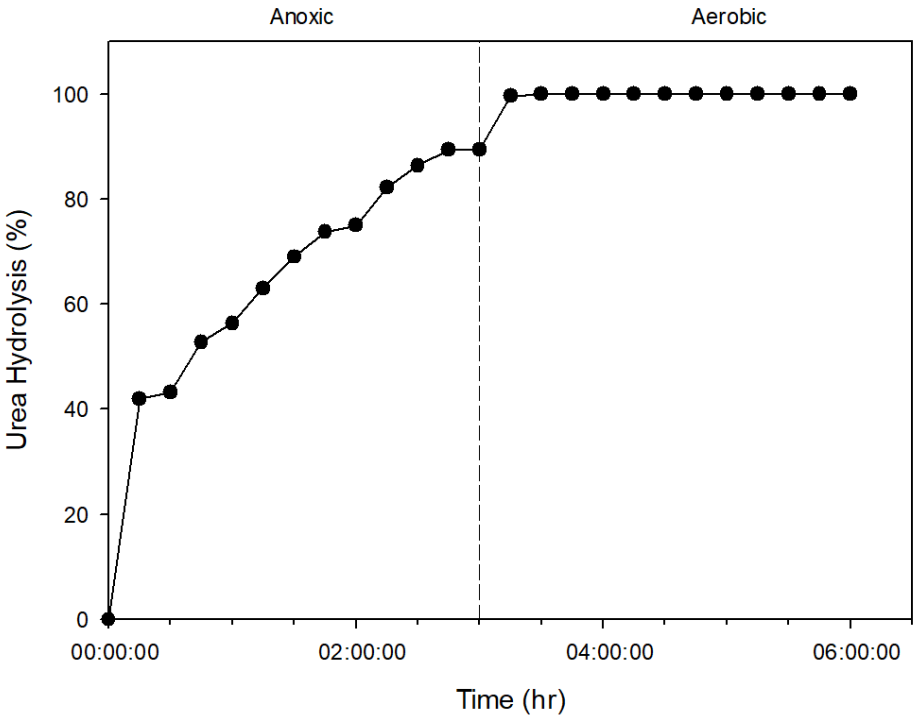

Figure 4.23. Urea removal variation in a cycle with 4 mg/L Ni feeding

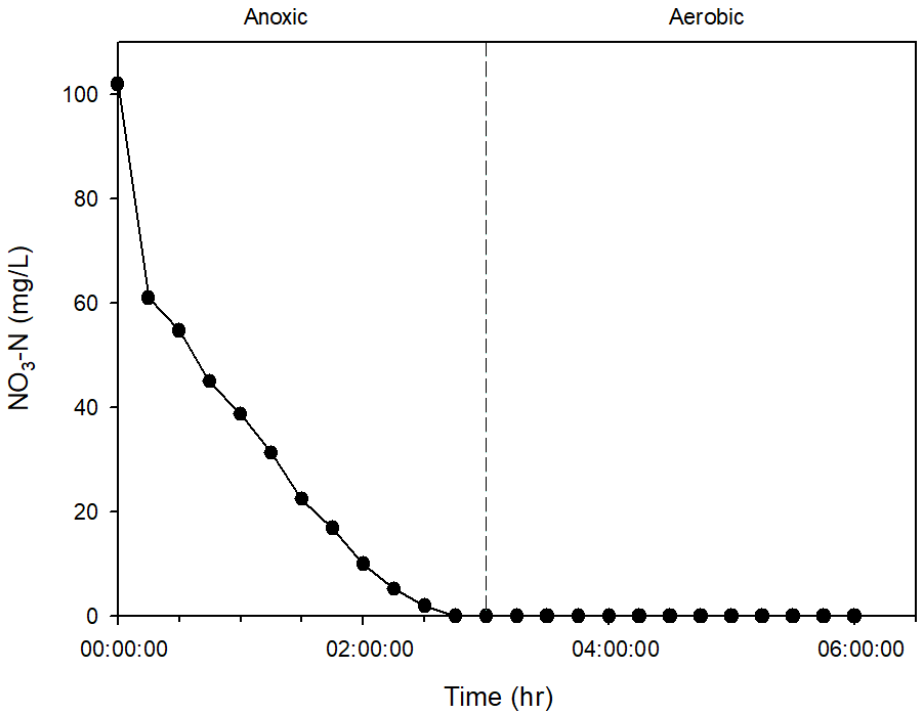

Figure 4.24. NO_3-N concentration variation in one cycle with Ni feeding

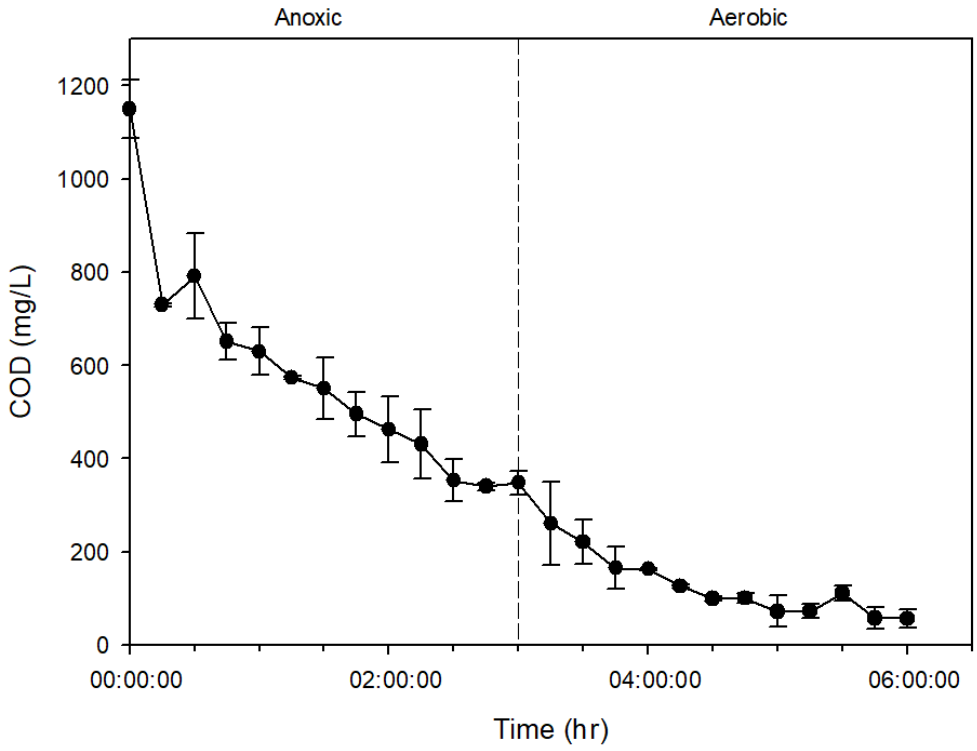

Figure 4.25. COD concentration variation in one cycle with Ni feeding

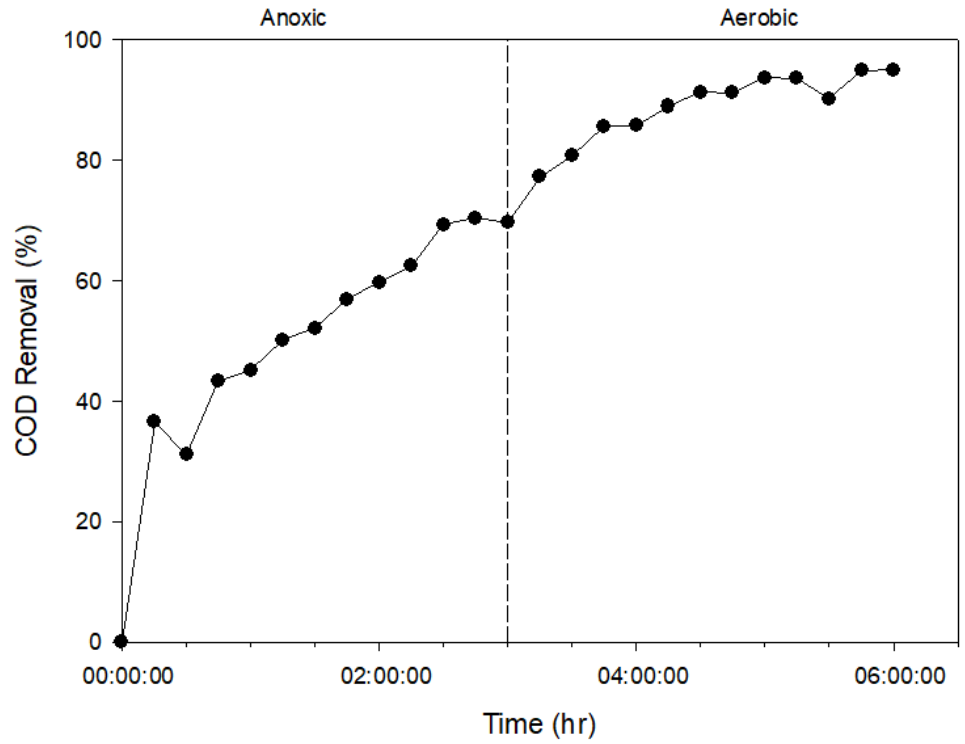

Figure 4.26. COD removal variation in one cycle with Ni feeding

4.2. Selective Nickel Recovery from Bioleachate Solution via Biomineralization

4.2.1. COD Concentration Change

COD analyzes were performed on the samples to examine bacterial activation during the biomineralization experiment. It was observed that after 6 hours, the amount of COD was completely consumed at all metal concentrations. At the end of the first 3 hours, 70.1%, 83.3%, 66.6% and 41.2% of the organic substrate was oxidized in reactors prepared with 1:20, 1:10, 1:5 ,1:2.5 bioleachate dilutions, respectively. It was found that as the metal concentration increased, the microbial activity slowed down. However, the amount of COD oxidation in 1:10 dilution increased slightly. The COD change in the samples during the biomineralization process was given in Figure 4.27.

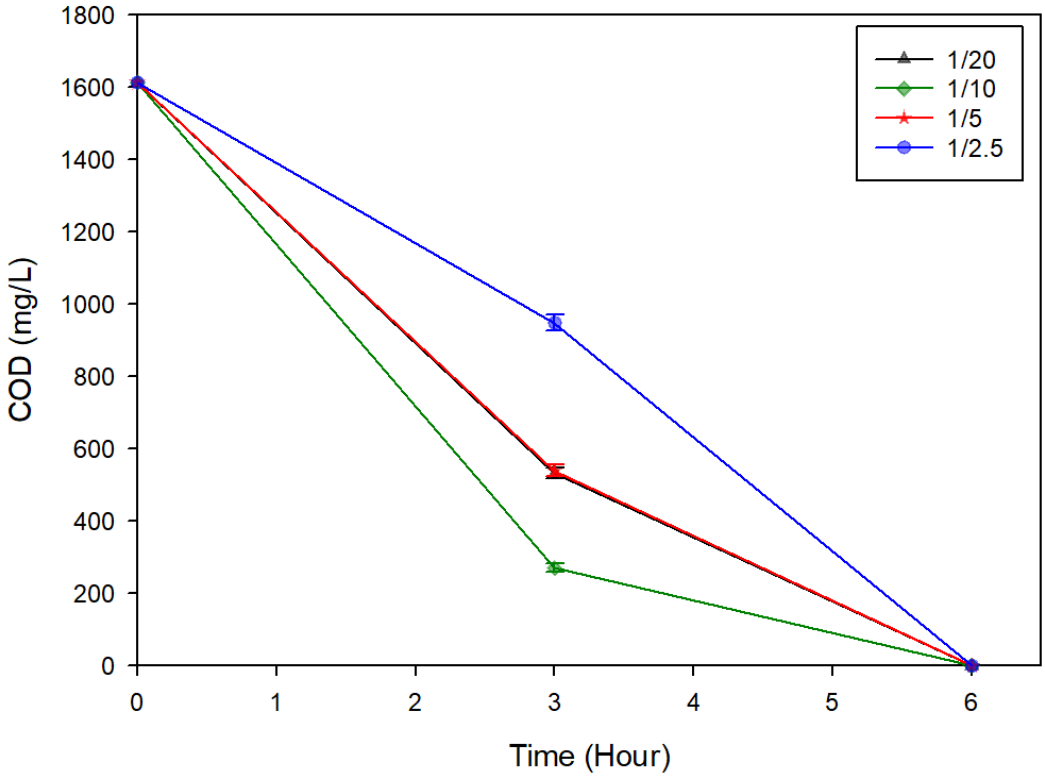

Figure 4.27. COD changes during biomineralization

4.2.2. NO_3 Concentration Change

Since the biomineralization process is mostly carried out under anoxic conditions, NO_3-N reduction would greatly affect the biomineralization efficiency. In this context, NO_3-N analyzes were carried out on the samples and the data obtained were given in Figure 4.28. At the end of the 6th hour, it was observed that all NO_3-N was consumed in all reactors.

At the end of the first 3 hours, 76.4±3.7%, 85.4±3.5%, 71.4±6.1% and 53.4±3.2% of NO_3-N was consumed in reactors containing 20, 10, 5 ,2.5 times diluted bioleachate solution, respectively. Similar to COD consumption, the nitrate reduction activity increased slightly in 10 times diluted bioleachate solution, then the NO_3-N reduction efficiency decreased when metal concentrations increased.

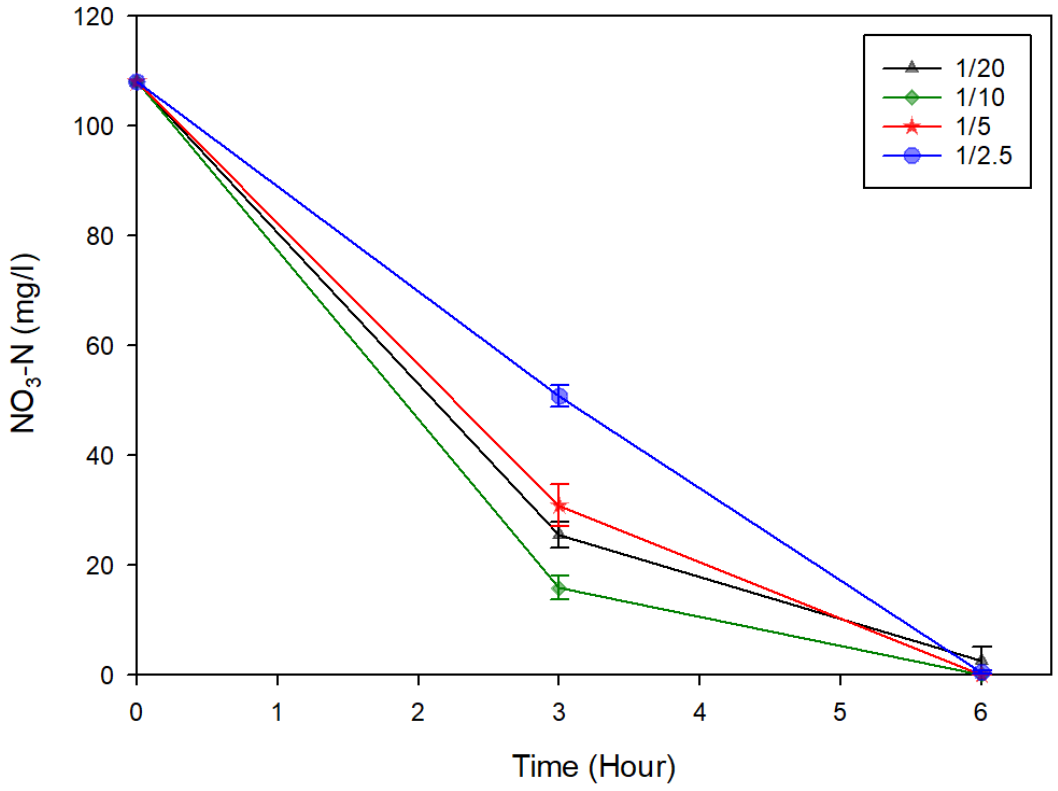

Figure 4.28. NO_3-N concentration change during biomineralization

4.2.3. NH_4-N Concentration Change

One of the most important factors affecting carbonate formation is urea hydrolysis. The change in the amount of total ammonium nitrogen (TAN) formed in the reactors as a result of urea hydrolysis was analyzed and given in the Figure 4.29. With the TAN values obtained in the analysis, the approximate urea hydrolysis efficiencies were calculated. The values of change in urea hydrolysis throughout the process were given in the Table 4.4. There is no significant differences between urea hydrolysis efficiency of diluted bioleachate solutions ($p>0.05$).

Table 4.4. Urea removal during biomineralization

Reactor Metal Concentration	3rd Hour Urea hydrolysis (%)	Standard Deviation	6th Hour Urea hydrolysis (%)	Standard Deviation
1/20	35	11,4	44	7,6
1/10	31	3,5	42	6
1/5	31	4,6	45	3
1/2.5	21	3	38	3,5

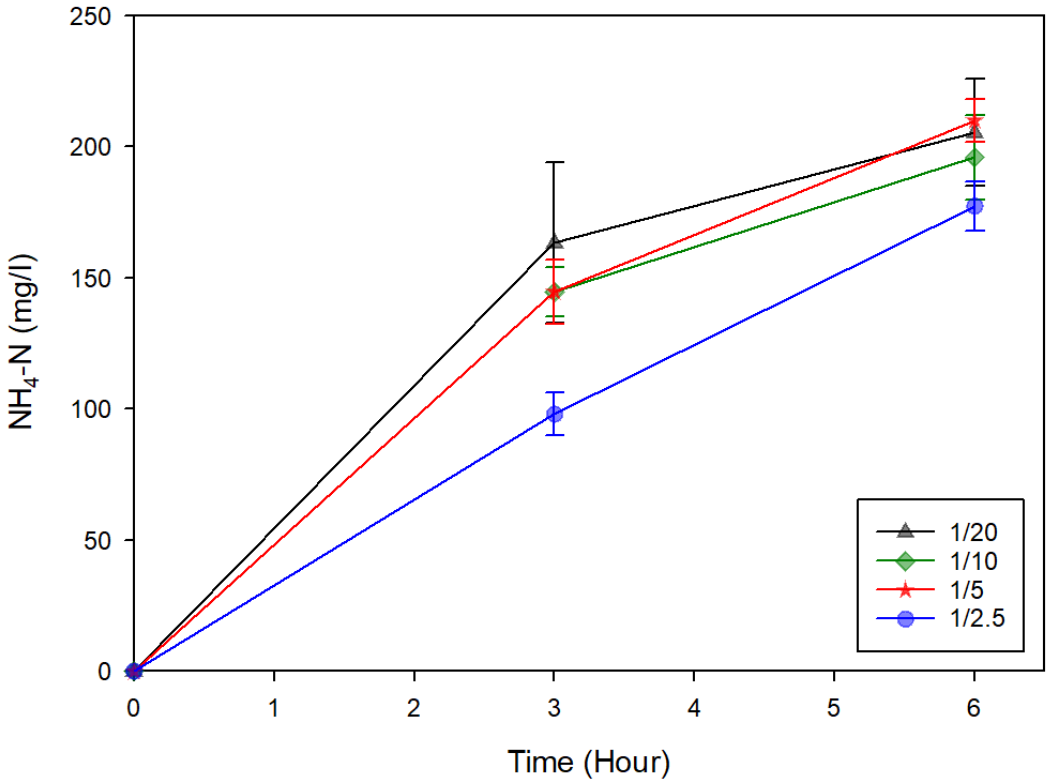

Figure 4.29. NH_4-N concentration change during biomineralization

4.2.4. Total Carbonate Determination

In order to demonstrate that dissolved metals precipitate as metal carbonates in the biomineralization process, the carbonate amounts formed at the end of the process in all reactors were measured and the results are given in Figure 4.30. As can be seen, there was no significant difference amount of CO_3^{2-} formed in the reactors that were prepared by different dilution of bioleachate solution ($p<0.05$). It was found logical that the amount of CO_3^{2-} formed was approximately the same (60-65 mg) due to the urea, COD and nitrate added to all reactors were completely depleted at the end of the 6th hour.

During the biomineralization process with carbonate, carbonates bind divalent metal ions with higher affinity than trivalent ions. Since carbonate analysis can only be done at the end of the 6th hour, the amount of carbonate in the 3rd hour cannot be known. It is thought that the carbonates formed at the beginning of the experiment primarily precipitated divalent metal ions (Ni, Cu, Zn, Pb). However, after a certain period of time, it is observed that trivalent ions also begin to precipitate due to the reduction of divalent metal ions in the aqueous medium. In this context, the fact that the amount of carbonate formed in the reactors at the end of the process is approximately the same, but the amount of precipitated metal is different can be explained by the affinity between carbonate and divalent metal ions.

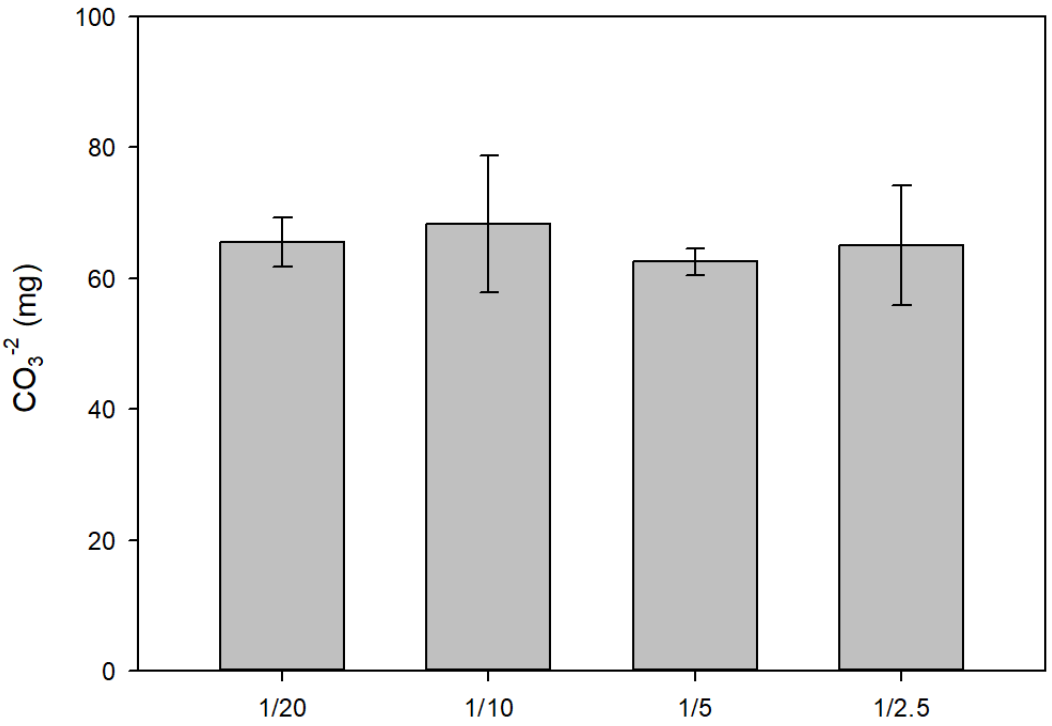

Figure 4.30. Amount of CO_3^{-2} production in 20, 10, 5 and 2.5 times diluted bioleachate solution end of biomineralization process (No carbonate formation was detected in any of the abiotic reactors)

4.2.5. Metal Concentrations Change

Samples were analyzed to determine how much dissolved metal was left in the reactors at the 3rd and 6th hours aiming to evaluate the biomineralization of metals. Biomineralization efficiencies were given in Table 4.5.

It was found that Ni, Cu, Zn metals were completely precipitated at the end of the first 3 hours in all dilutions. At the end of the 3rd hour, 0%, 41.8±10%, 67.9±5.5%, and 81.5±2.5% of Pb precipitated in 1:20, 1:10, 1:5, and 1:2.5 dilutions, respectively. In addition, Al precipitated at a rate of 9.6±12.6% in only 1:2.5 dilution at the end of the 3rd hour.

At the end of the 6th hour, 15.7±4.8% and 46.5±20.2% of Al precipitated in 1:5 and 1:2.5 dilutions, respectively. On the other hand, 50.3±2.4%, 70.3±1.4% and 84.1±2.0% of Pb precipitated in 1:10, 1:5 and 1:2.5 dilutions respectively. According to the results, as the process time increases, precipitation of other metals increase as shown in the Figure 4.31 and therefore, selective metal recovery cannot be performed efficiently. In this context, the reaction time of the selective metal recovery process should be under 3 hours. In addition, how much metals precipitated abiotically at different dilutions is given in the Figure 4.32.

Table 4.5. Biomineralization percentage of metals (%)

Dilutions	Metals	Initial Conc. (ppb)	Abiotic Precipitation		Bioprecipitation	
			3 hr (%)	6 hr (%)	3 hr (%)	6 hr (%)
1:20	Al	510.7	0	100	0	0
	Ni	273.2	42.1	48.5	100	100
	Cu	631.8	84.7	88.0	100	100
	Zn	57.9	100	100	100	100
	Pb	77.7	0	9.1	0	0
1:10	Al	853.4	0	78.5	0	0
	Ni	520.6	9.5	9.8	100	100
	Cu	1361.5	32.1	43.1	100	100
	Zn	115.9	100	100	100	100
	Pb	238.2	0	49.0	41.8±10	50.3±2.4
1:5	Al	1458.5	0	40.2	0	15.7±4.8
	Ni	1176.6	1.2	8.3	100	100
	Cu	2917	3.1	16.5	100	100
	Zn	231.8	20.3	20.3	100	100
	Pb	460.3	0	11.9	67.9±5.5	70.3±1.4
1:2.5	Al	3231.8	0	69.5	9.6±12.6	46.5±20.2
	Ni	2536.8	0	5.2	100	100
	Cu	6189.8	0	7.2	100	100
	Zn	463.5	0	0	100	100
	Pb	925.9	0	0	81.5±2.5	84.1±2.0

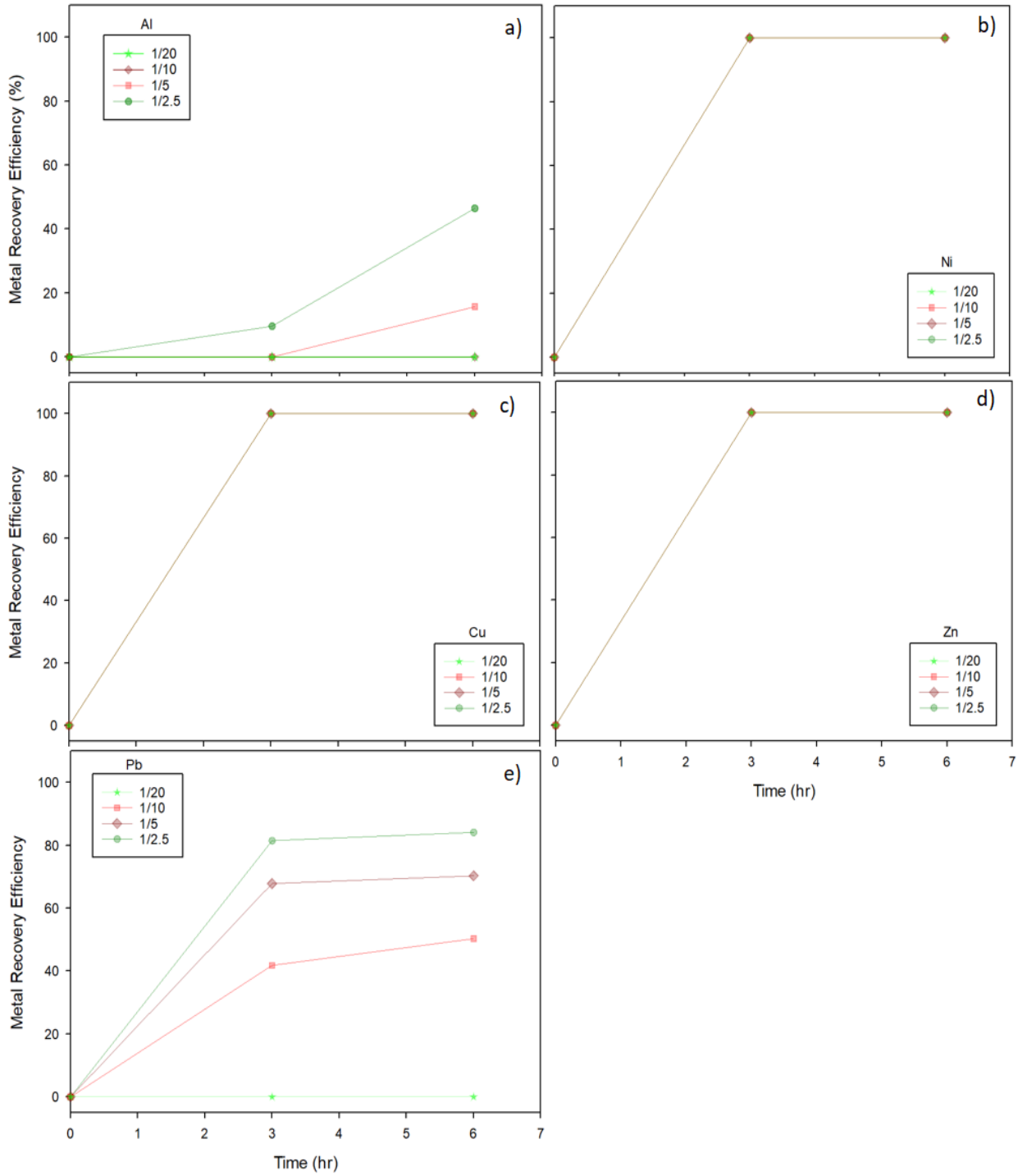

Figure 4.31. Removal efficiencies of metals in different diluted synthetic leachate solution; a) Al recovery efficiency, b) Ni recovery efficiency, c) Cu recovery efficiency, d) Zn recovery efficiency, e) Pb recovery efficiency

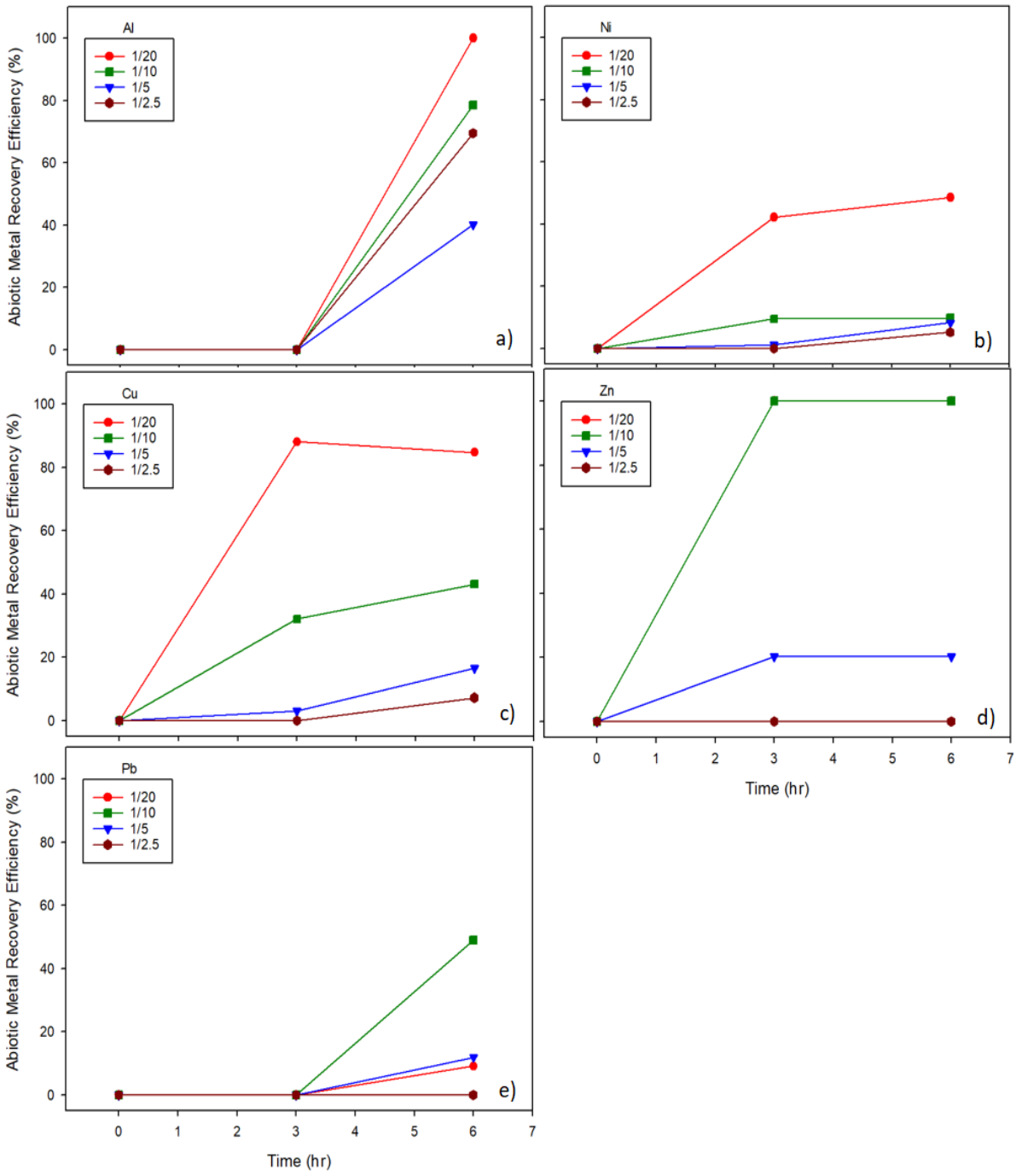

Figure 4.32. Abiotic metal precipitation in different diluted synthetic leachate solution; a) Al abiotic recovery efficiency, b) Ni abiotic recovery efficiency, c) Cu abiotic recovery efficiency, d) Zn abiotic recovery efficiency, e) Pb abiotic recovery efficiency

Metals are precipitated not only by the biomineralization process, but also abiotically by chemical interactions. As can be seen in Table 4.3., abiotic precipitation at low metal concentrations decrease as the concentrations increase. While determining dissolved metal concentrations by ICP-MS, it is estimated that organic substances form complexes

with metals and reduce dissolved metal values in samples with very low metal concentrations. As can be seen in Figure 4.33., no precipitation was observed in abiotic reactors. As can be seen in Figure 4.34., visibly residues are formed in biomineralization bottles via precipitation.

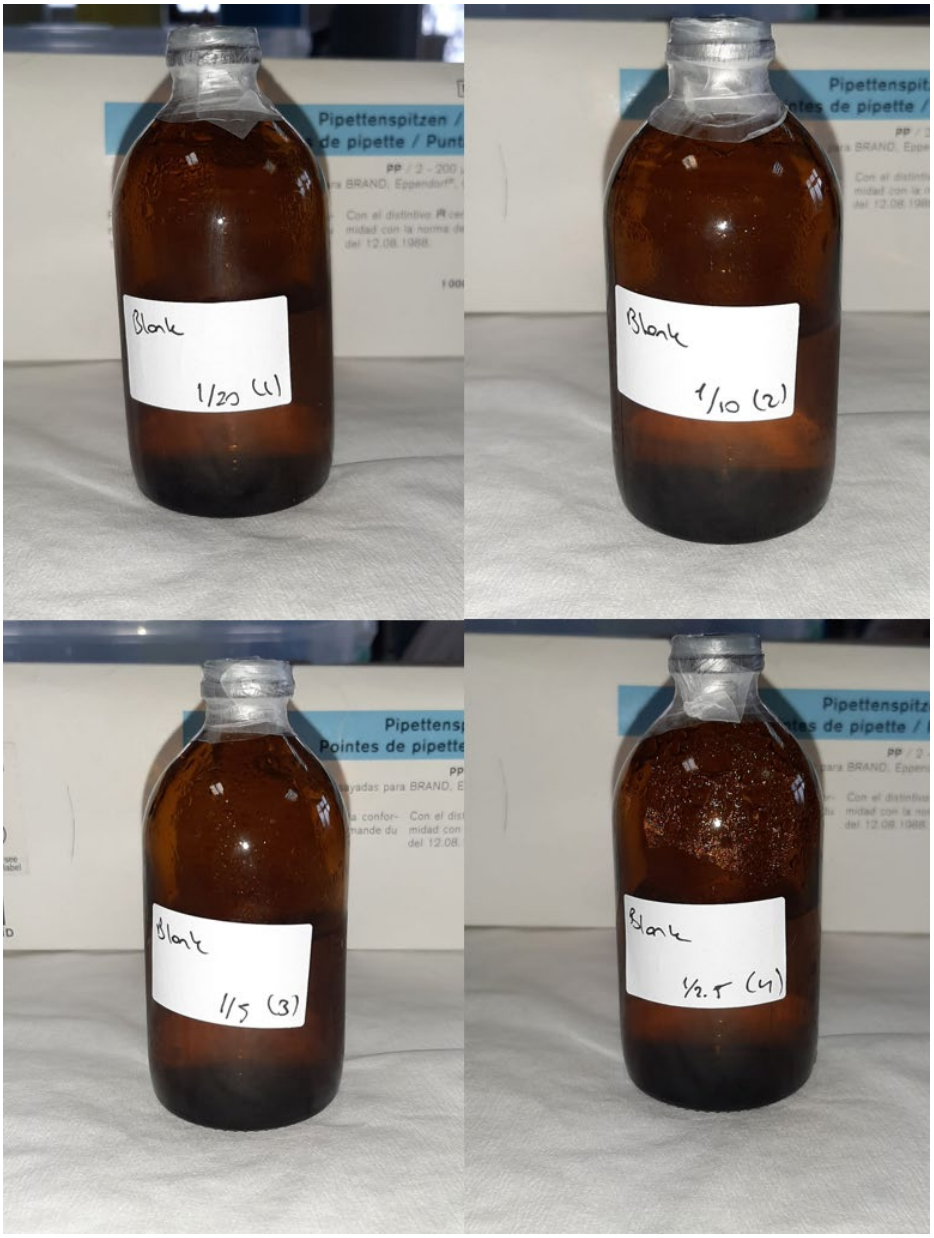

Figure 4.33. Images of blank batch bottles at the end of 6th hour

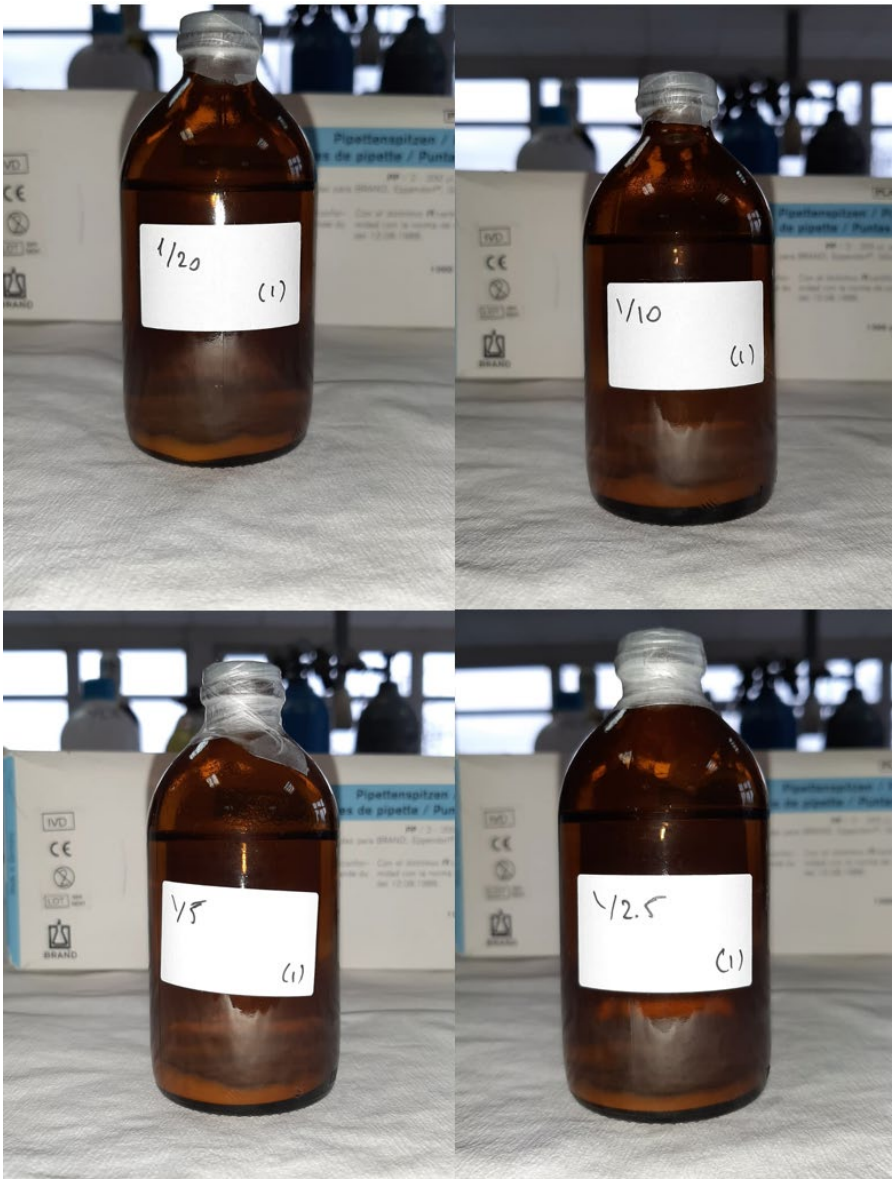

Figure 4.34. Images of biomineralization batch bottles at the end of 6th hour

In bioprecipitation, carbonate formed as a result of microbial activities, and further precipitated with metals that are attracted to the negative cell surface as previously described for MICP mechanism. In this case, instead of Ca^{2+}, negative charge of the bacteria attracted the dissolved metal ions. Upon formation of CO_3^{2-} metals precipitated by forming $NiCO_3$, $CuCO_3$, $ZnCO_3$, $PbCO_3$ and $Al_2(CO_3)_3$ compounds. The reason why $Al_2(CO_3)_3$ with the lowest solubility is the least precipitated metal at the end of the process is due to the higher affinity between carbonate and divalent metal ions. The solubility constants (Ksp at 25 °C) of the resulting compounds are as follows;

$NiCO_3 = 6.6\times10^{-9}$ [277]
$CuCO_3 = 1.4\times10^{-10}$ [277]

$ZnCO_3 = 1.4\times10^{-11}$ [277]
$PbCO_3 = 7.4\times10^{-14}$ [277]
$Al_2(CO_3)_3 = 7.2x10^{-25}$ [278]

The data obtained are not sufficient to explain the effect of Ni acclimation period on selective biomineralization. Ni, Cu, Zn and Pb divalent ions precipitated after 3 hours in all dilutions due to the long process time and low metal concentrations used for the experiment. In order to better understand the effect of Ni acclimation on selective biomineralization, the same tests should be performed with non-nickel acclimated granules.

At the beginning of the process, the purity by mass of dissolved Ni in all dilutions was adjusted to be approximately 18.1±0.9 %. According to the data at the 3rd hour, the purity rates of precipitated Ni in 1:20, 1:10, 1:5, 1:2.5 dilutions were found as 28.4%, 24.8%, 25.4%, 19.4%, respectively. In this context, it can be said that the biomineralization process performed with low metal concentrations increases the purity of Ni. In addition, as a result of more detailed research on the process, it seems possible to recover Ni at higher purity rates.

The residue obtained as a result of the biomineralization process is mostly composed of Cu, Ni and Zn. Since these metals are present with carbonate, solid metal oxides are obtained by removing carbon dioxide from the compounds and the final product can be made suitable for industrial use. The CO_2 they contain can be removed by introducing the residue containing metal carbonates to a highly acidic or alkaline environment. The metal oxides obtained can be used in brass alloys containing copper-nickel-zinc.

5. CONCLUSION

In the thesis study, selective metal recovery was aimed by means of aerobic granules from the synthetic polymetallic bioleachate solution obtained as a result of the bioleaching process of WPCBs. First of all, mature biogranules were obtained in SBR, then metal recovery experiments were carried out by bioprecipitation process.

When the reactor stability was achieved during the granulation period, biogranules with an average diameter of 0.4-0.6 mm (%61) were obtained. Despite the increase in microbial performance during nickel acclimation, deterioration in granule structure and reduction in granule size were observed. Average granule size decreased to a range of 0.2-0.3 mm.

A highly stable reactor configuration was formed prior to nickel acclimation. The highest VSS/TSS value was obtained as 88.7% on the 111th day of the reactor operation, and the highest SVI_{30}/SVI_5 value was obtained with 90.7% on the 134th day. In a single cycle, average COD consumption, NO_3-N reduction and urea hydrolysis performances of the biogranules were recorded as 98.2%, 100% and 82.6%, respectively. Specific activities of the biogranules were recorded as 0.181, 0.020 and 0.044 g substrate/ g VSS-h.

It was revealed that microbial urea hydrolysis is not a strictly aerobic process and can also be performed by nitrate reducing microorganisms. Nitrate reducing microorganisms hydrolysed 55.1% of the fed urea during the anoxic period.

It was observed that the microbial activities in the reactor increased when low concentration of nickel was fed into the reactor. The highest microbial activity was obtained during 2 mg/L Ni feeding. In this period, urea hydrolysis efficiency in a single cycle was 100%, organic carbon oxidation efficiency was 91.3% and NO_3-N reduction efficiency was 100%. Specific activities were recorded as 0,091, 0.251, 0.036.

In the biomineralization process, selective nickel recovery studies were carried out in bioleachate solutions diluted in 4 different ratios. In addition to metal precipitation efficiencies, the microbial activities of the granules during the process were also investigated. In general, the highest microbial activity was obtained in 1:10 dilution of the bioleachate solution. In addition, the purity (w%) of the recovered solid nickel

achieved in 3 hours from the 1:10 dilution was 24.82%. Considering the microbial activity performance and the purity of the recovered nickel, 1:10 dilution appeared to be more suitable than other dilutions for future selective nickel recovery studies. It was also determined that shorter durations should be investigated to determine if there is a sequence in precipitation of the metal carbonates.

Finally, as a result of the thesis study, nickel recovery to high purity rates could not be obtained. One of the main reasons for this is the long process duration. During the process, the amount of carbonate formed as a result of microbial activities increased and caused the precipitation of most of the metals at ppb level in the reactors.

Taking all things into the consideration, bioleaching and biomineralization appeared to be useful techniques for the recovery of precious and base metals in e-waste and WPCBs that are increasing day by day in the world. The use of biomineralization mechanism for selective metal recovery from polymetallic leachate solution obtained after bioleaching should be further investigated in detail in order to overcome the purity issues presented in this thesis study. It is predicted that especially in future studies, shortening the biomineralization process time and evaluating different acclimation options for selective metal recovery will increase the process efficiency.

6. REFERENCES

[1] R. Ahirwar, A.K. Tripathi, Environmental Nanotechnology, Monitoring & Management, 15 (**2021**) 100409.

[2] European Union, Directive 2002/96/EC of The European Parliament and of The Council of 27 January 2003 on Waste Electrical and Electronic Equipment (WEEE), **2003**.

[3] I.M.S.K. Ilankoon, Y. Ghorbani, M.N. Chong, G. Herath, T. Moyo, J. Petersen, Waste Management, 82 (**2018**), 258-275.

[4] E. Ekdahl, State Water Resources Control Board Division of Water Quality GAMA Program, WHO Regional Office for Europe Groundwater Information Sheet, Copenhagen, **2000**.

[5] K. Huang, J. Guo, Z. Xu, Journal of Hazardous Materials, 164 (**2009**) 399-408.

[6] J. Guo, J. Guo, Z. Xu, Journal of Hazardous Materials, 168 (**2009**) 567-590.

[7] M. Colledani, Demanufacturing Exercises Year 2020-21, ANDREADD.IT, **2021**.

[8] R. Qiu, M. Lin, J. Ruan, Y. Fu, J. Hu, M. Deng, Y. Tang, R. Qiu, Journal of Cleaner Production, 244 (**2020**) 118690.

[9] L. Pietrelli, I. Francolini, A. Piozzi, M. Vocciante, Chemical Engineering Transactions, 70 (**2018**) 271-276

[10] J. Ruan, J. Zheng, L. Dong, Z. Xu, Journal of Cleaner Production, 142 (**2017**) 2021-2027.

[11] J. Li, H. Duan, K. Yu, L. Liu, S. Wang, Resources, Conservation and Recycling, 54 (**2010**) 810-815.

[12] Y. Xu, J. Li, L. Liu, Procedia Environmental Sciences, 31 (**2016**) 162-170

[13] H. Wang, M. Hirahara, M. Goto, T. Hirose, The Journal of Supercritical Fluids, 29 (**2004**) 251-256.

[14] A. Priya, S. Hait, Process Safety and Environmental Protection, 143 (**2020**) 262-272.

[15] A. Ozkan, AKU Journal of Science and Engineering, 18 (**2018**) 529-537.

[16] J.A. Brierley, C.L. Brierley, Hydrometallurgy, 59 (**2001**) 233-239.

[17] M. Baniasadi, F. Vakilchap, N. Bahaloo-Horeh, S.M. Mousavi, S. Farnaud, Journal of

Industrial and Engineering Chemistry, 76 (**2019**) 75-90.

[18] H. Tao, L. Dongwei, Biotechnology Reports, 4 (**2014**) 107-119.

[19] T.J. Xu, T. Ramanathan, Y.P. Ting, Biotechnology Reports, 3 (**2014**) 8-14.

[20] J.S. Kadukova, R. Marcincakova, A. Luptakova, M. Vojtko, M. Fujda, P. Pristas, Scientific Reports, 10 (**2020**) 14594.

[21] K.A. Natarajan, Biotechnology of Metals, Elsevier, Chapter 1, **2018**.

[22] A.G. Guezennec, K. Bru, J. Jacob, P. d'Hugues, Minerals Engineering, 75 (**2015**) 45-53.

[23] H.R. Watling, D.M. Collinson, J. Li, L.A. Mutch, F.A. Perrot, S.M. Rea, F. Reith, E.L.J. Watkin, Minerals Engineering, 56 (**2014**) 35-44.

[24] J.A. Garzon, A. Hubau, C. Joulian, A.G. Guezzennec, Frontiers in Microbiology, 12 (**2021**) 669738.

[25] R. Qiu, M. Lin, B. Qin, Z. Xu, J. Ruan, Journal of Cleaner Production, 279 (**2021**) 123738.

[26] C.G. Bryan, E.L. Watkin, T.J. McCredden, Z.R. Wong, S.T.L. Harrison, A.H. Kaksonen, Hydrometallurgy, 152 (**2015**) 33-43.

[27] A. Işıldar, Biological versus chemical leaching of electronic waste for copper and gold recovery, PhD Thesis, UNESCO-IHE Institute for Water Education, Delft, The Netherlands, **2016**.

[28] D. Kumari, X. Y. Qian, X. Pan, V. Achal, Q. Li, G. M. Gadd, Advances in Applied Microbiology, 94 (**2016**) 79-108.

[29] Y.Ç. Erşan, Overlooked Strategies in Exploitation of Microorganisms in the Field of Building Materials, **2018**.

[30] T. Sugio, K. Matsumoto, M. Takai, S. Wakasa, T. Sogawa, K. Kamimura, Process Metallurgy, 9 (**1999**) 789-797.

[31] P.R. Yaashikaa, B. Priyanka, P.S. Kumar, S. Karishma, S. Jeevanantham, S. Indraganti, Chemosphere, 287 (**2022**) 132230.

[32] A.A.L.D. Silva, M.A.R.D. Carvalho, S.A.L.D. Souza, P.M.T. Dias, R.S. Filho, C.S.D.M. Saramago, C.A.M. Bento, Brazilian Journal of Microbiology, 43 (**2012**) 1620-163.

[33] H. Tan, C. Wang, G. Zeng, Y. Luo, H. Li, H. Xu, Journal of Hazardous Materials, 386 (**2020**) 121628.

[34] H. Brandl, R. Bosshard, M. Wegmann, Process Metallurgy, 9 (**1999**) 569-576.

[35] K. Milferstedt, J. Hamelin, C. Park, J. Jung, Y. Hwang, S.K. Cho, K.W. Jung, D.H. Kim, International Journal of Hydrogen Energy, 42 (**2017**) 27801-27811.

[36] C.Y. Lin, M.L. Lin, Journal of Environmental Science & Health Part A, 32 (**1997**) 1933-1944.

[37] D. Bourguignon, European Parliamentary Research Service, Understanding Waste Streams Treatment of Specific Waste, European Parliament Briefing, **2015**.

[38] European Union, Directive 2008/98/EC of The European Parliament and of The Council of 19 November 2008 on Waste and Repealing Certain Directives, **2008**.

[39] D.S. Khetriwal, P. Kraeuchi, M. Schwaninger, Environmental Impact Assessment Review, 25 (**2005**) 492-504.

[40] R. Widmer, H.O. Krapf, D.S. Khetriwal, M. Schnellman, H. Böni, Environmental Impact Assessment Review, 25 (**2005**) 436-458.

[41] V. Forti, C.P. Balde, R. Kuehr, G. Bel, The Global E-waste Monitor 2020: Quantities, Flows and the Circular Economy Potential, United Nations University, **2020**.

[42] C.P. Balde, V. Forti, V. Gray, R. Kuehr, P. Stegmann, The Global E-waste Monitor 2017: Quantities, Flows and Resources, United Nations University, **2017**.

[43] J. Lepawsky, Geoforum, 43 (**2012**) 1194-1206.

[44] A. Kumar, M. Holuszko, D.C.R. Espinosa, Resources, Conservation and Recycling, 122 (**2017**) 32-42.

[45] M. Sagnak, Y. Berberoglu, İ. Memis, O. Yazgan, Waste Management, 127 (**2021**) 37-47.

[46] H.S. Kilic, U. Cebeci, M.B. Ayhan, Resources, Conversation and Recycling, 95 (**2015**) 120-132.

[47] R.Ü. Sayman, O. Akpulat, Regulatory Impact Assessment of EU Waste Electrical and Electronic Equipment (WEEE) Directive, REC Turkey Final Report, **2011**.

[48] Republic of Turkey Ministry of Environment and Urbanization, 2019 Hazardous Waste Statistics Bulletin, Ankara, **2019**.

[49] F. Magali, F. Wang, J. Huisman, R. Kuehr, Study on Collection Rates of Waste Electrical and Electronic Equipment (WEEE), European Commission, **2014**.

[50] R.Ü. Sayman, O. Akpulat, Regulation on Control of Waste Electrical and Electronic Equipment Municipal Implementation Guide, REC Turkey, **2016**.

[51] J. Molto, S. Egea, J.A. Conesa, R. Font, Waste Management, 31 (**2011**) 2546-2552.

[52] P. Kiddee, R. Naidu, M.H. Wong, Waste Management, 33 (**2013**) 1237-1250

[53] A. Kaifie, T. Schettgen, J. Bertram, K. Löhndorf, S. Waldschmidt, M.K. Felten, T. Kraus, J.N. Fobil, T. Küpper, Science of The Total Environment, 723 (**2020**) 138073.

[54] L. Rocchetti, A. Amato, F. Beolchini, Journal of Clenaer Production, 178 (**2018**) 814-832

[55] S.K. Fan, C. Fan, J.H. Yang, K.F.R. Liu, Journal of Cleaner Production, 39 (**2013**) 209-219.

[56] Ö.A. Kocatüfek, Investigation of The Melting Conditions for The Recovery of Precious Metal from Printed Circuit Boards, Master Thesis, Istanbul Technical University Institute of Science, Istanbul, **2012**.

[57] Y.J. Park, D.J. Fray, Journal of Hazardous Materials, 164 (**2009**) 1152-1158.

[58] P.T. Williams, Waste and Biomass Valorization, 1 (**2010**) 107-120.

[59] E. Tanısalı, M. Özer, F. Burat, Mineral Processing and Extractive Metallurgy Review, 42 (**2021**) Issue 1.

[60] M. Kaya, Waste Management, 57 (**2016**) 64-90.

[61] B. Ghosh, M.K. Chosh, P. Parhi, P.S. Mukherjee, B.K. Mishra, Journal of Cleaner Production, 94 (**2015**) 5-19.

[62] H. Duan, K. Hou, J. Li, X. Zhu, Journal of Environmental Management, 92 (**2011**) 392-399.

[63] J. Wang, J. Guo, Z. Xu, Waste Management, 53 (**2016**) 218-224.

[64] J. Li, P. Shrivastava, Z. Gao, H.C. Zhang, IEEE Transactions on Electronics Packaging Manufacturing, 27 (**2004**) 1.

[65] M. Luda, Integrated Waste Management, 2 (**2011**) 285-298.

[66] S. Salhofer, M. Tesar, Journal of Hazardous Materials, 186 (**2011**) 1481-1488.

[67] S. Zhang, E. Forssberg, Powder Technology, 105 (**1999**) 295-301.

[68] J. Li, H. Duan, K. Yu, L. Liu, S. Wang, Resources, Conservation and Recycling, 54

(**2010**) 810-815.

[69] S. Ilyas, M.A. Anwar, S.B. Niazi, M.A. Ghauri, Hydrometallurgy, 88 (**2007**) 180-188.

[70] N.N. Adhapure, P.K. Dhakephalkar, A.P. Dhakephalkar, V.R. Tembhurkar, A.V. Rajgure, A.M. Deshmukh, MethodX, 1 (**2014**) 181-186.

[71] S. Mir, N. Dhawan, Resources, Conservation and Recycling, 178 (**2022**) 106027.

[72] S. Janyasuthiwong, R. Ugas, E. R. Rene, C. Alessandra, G. Esposito, P.N. Lens, Journal of Chemical Technology and Biotechnology, 91 (**2016**) 2038-2046.

[73] Z. Huang, J. Zhu, X. Wu, R. Qiu, Z. Xu, J. Ruan, Journal of Cleaner Production, 312 (**2021**) 127755.

[74] F. Hamerski, A. Krummenauer, A.M. Bernardes, H.M. Veit, Journal of Environmental Chemical Engineering, 7 (**2019**) 102896.

[75] J. Yang, H. Wang, G. Zhang, X. Bai, X. Zhao, Y. He, Resources, Conservation and Recycling, 146 (**2019**) 264-269.

[76] J. Li, Y. Jiang, Z. Xu, Journal of Cleaner Production, 141 (**2017**) 1316-1323

[77] Y. Higashiyama, K. Asano, Particulate Science and Technology, 16-1 (**1998**) 77-90.

[78] B. Ruj, V. Pandey, P. Jash, V.K. Srivastava, International Journal of Science and Engineering Research, 4 (**2015**) 564-571.

[79] S.P. Regana, Rare Earth Elements Recovery from E-Wastes by Solvent Extraction and Supported Liquid Membrane Processes, PH.D. Thesis, Barcelona School of Industrial Engineering, Barcelona, **2019**.

[80] T. Havlik, D. Orac, M. Petranikova, A. Miskufova, F. Kukurufya, Z. Takacova, Journal of Hazardous Materials, 183 (**2010**) 866-873.

[81] U. Jadhav, H. Hocheng, Scientific Reports, 5 (**2015**) 14574.

[82] A. Kumari, M.K. Jha, J.C. Lee, R.P. Singh, Journal of Cleaner Production, 112 (**2016**) 4826-4834.

[83] C.J. Oh, S.O. Lee, H.S. Yang, T.J. Ha, M.J. Kim, Journal of the Air & Waste Management Association, 53 (**2003**) 897-902.

[84] F.R. Xiu, Y. Qi, F.S. Zhang, Waste Management, 53 (**2013**) 1251-1257.

[85] T.I. Mudder, M.M. Botz, The European Journal of Mineral Processing and Environmental

Protection, 4 (**2004**) 62-74.

[86] R. Dorin, R. Woods, Journal of Applied Electrochemistry, 21 (**1991**) 419-424.

[87] R. Montero, A. Guevara, E.D.L. Torre, Journal of Earth Science and Engineering, 2 (**2012**) 3513-3519.

[88] H. Li, J. Eksteen, E. Oraby, Resources, Conservation and Recycling, 139 (**2018**) 122-139.

[89] B. Xu, W. Kong, Q. Li, Y. Yang, T. Jiang, X. Liu, Metals, 7 (**2017**) 222.

[90] Y. Zhang, S. Liu, H. Xie, X. Zeng, J. Li, Procedia Environmental Science, 16 (**2012**) 560-568.

[91] J. Cui, L. Zhang, Journal of Hazardous Materials, 158 (**2008**) 228-256.

[92] L. Zhang, Z. Xu, Journal of Cleaner Production, 127 (**2016**) 19-36.

[93] M. Gurung, B.B. Adhikari, H. Kawakita, K. Ohto, K. Inoue, S. Alam, Hydrometallurgy, 133 (**2013**) 84-93.

[94] A. Akcil, C. Erust, C.S. Gahan, M. Ozgun, M. Sahin, A. Tuncuk, Waste Management, 45 (**2015**) 258-271.

[95] S. Zheng, Y.Y. Wang, L.Y. Chai, Minerals Engineering, 19 (**2006**) 1301-1306.

[96] A.H. Kaksonen, N.J. Boxall, Y. Gumulya, H.N. Khaleque, C. Morris, T. Bohu, K.Y. Cheng, K.M. Usher, A.M. Lakaniemi, Hydrometallurgy, 180 (**2018**) 7-25.

[97] A.H. Kaksonen, X. Deng, T. Bohu, L. Zea, H.N. Khaleque, Y. Gumulya, N.J. Boxall, C. Morris, K.Y. Cheng, Hydrometallurgy, 195 (**2020**) 105376.

[98] A. Işıldar, J.V.D. Vossenberg, E.R. Rene, E.D.V. Hullebusch, P.N.L. Lens, Waste Management, 57 (**2016**) 149-157.

[99] E. Karwowska, D.A. Morzuch, M. Lebkowska, A. Tabernacka, M. Wojtkowska, A. Telepko, A. Konarzewska, Journal of Hazardous Materials, 264 (**2014**) 203-210.

[100] G. Natarajan, Y.P. Ting, Bioresource Technology, 152 (**2014**) 80-85.

[101] A.D. Bas, H. Deveci, E.Y. Yazici, Hydrometallurgy, 138 (**2013**) 65-70.

[102] R. Jujun, X. Zhu, Y. Qian, J. Hu, Waste Management, 34 (**2014**) 901-907.

[103] J.E.M. Arias, R.A. Delira, A. Alarcon, M.R.M. Lopez, O.G. Barradas, J.S.C. Sanchez, R.F. Cerrato, M.J. Fernandez, Brazilian Journal of Technology, 46 (**2015**) 707-713.

[104] T.D. Chi, J.C. Lee, B.D. Pandey, K. Yoo, J. Jeong, Mineral Engineering, 11 (**2011**) 1219-1222.

[105] J. Li, J. Wen, Y. Guo, N. An, C. Liang, Z. Ge, Hydrometallurgy, 194 (**2020**) 105260.

[106] I.N. Rizki, Y. Tanaka, N. Okibe, Waste Management, 84 (**2019**) 158-165.

[107] D. Mishra, D.J. Kim, J.G. Ahn, Y.H. Rhee, Metals and Materials International, 11 (**2005**) 249-256.

[108] U. Farooq, J.A. Kozinski, M.A. Khan, M. Athar, Bioresource Technology, 101 (**2010**) 5043-5053.

[109] K. Vijayaraghavan, Y.S. Yun, Biotechnology Advances, 26 (**2008**) 266-291.

[110] B. Volesky, Z.R. Holan, Biotechnology Progress, 11 (**1995**) 235-250.

[111] Y.L. Han, J.H. Wu, C.L. Cheng, D. Nagarajan, C.R. Lee, Y.H. Li, Y.C. Lo, J.S. Chang, Bioresource Technology, 239 (**2017**) 160-170.

[112] T. Ogi, T. Makino, F. Iskandar, E. Tanabe, K. Okuyama, Bioresource Technology, 218 (**2016**) 140-145.

[113] N. Saxena, International Journal of Latest Trends in Engineering and Technology, 6 (**2015**) 255-259.

[114] G.J. Olson, J.A. Brierley, C.L. Brierly, Applied Microbiology and Biotechnology, 63 (**2003**) 249-257.

[115] J. Valdes, I. Pedroso, R. Quatrini, R.J. Dodson, H. Tettelin, R. Blake, J.A. Eisen, D.S. Holmes, BMC Genomics, 9 (**2008**) 597.

[116] G.S. Rao, L.R. Berger, Archives of Microbiology, 79 (**1971**) 338-344.

[117] S. Ilyas, R. Chi, J.C. Lee, Mineral Processing and Extractive Metallurgy Review, 34 (**2013**) 185-194.

[118] T.D. Chi, J.C. Lee, B.D. Pandey, K. Yoo, J. Jeong, Minerals Engineering, 24 (**2011**) 1219-1222.

[119] G. Natarajan, Y.P. Ting, Bioresource Technology, 152 (**2014**) 80-85.

[120] T. Rohwerder, T. Gehrke, K. Kinzler, W. Sand, Applied Microbiology and Biotechnology, 63 (**2003**) 239-248.

[121] H. Tao, L. Dongwei, Biotechnology Reports, 4 (**2014**) 107-119.

[122] Y. Jia, Q. Tan, H. Sun, Y. Zhang, H. Gao, R. Ruan, Green Energy & Environment, 4 (**2019**) 29-37.

[123] H. Srichandan, R.K. Mohapatra, P.K. Parhi, S. Mishra, Hydrometallurgy, 189 (**2019**) 105122.

[124] I. Asghari, S.M. Mousavi, F. Amiri, S. Tavassoli, Journal of Industrial and Engineering Chemistry, 19 (**2013**) 1069-1081.

[125] R. Liu, J. Li, Z. Ge, Procedia Environmental Sciences, 31 (**2016**) 947-953.

[126] A. Işıldar, E.D.V. Hullebusch, M. Lenz, G.D. Laing, A. Marra, A. Cesaro, S. Panda, A. Akcil, M.A. Kucuker, K. Kuchta, Journal of Hazardous Materials, 362 (**2019**) 467-481.

[127] S. Chen, Y. Yang, C. Liu, F. Dong, B. Liu, Chemosphere, 141 (**2015**) 162-168.

[128] R. Jain, A. Pathak, T.R. Sreekrishnan, M.G. Dastidar, Journal of Environmental Science, 22 (**2010**) 230-236.

[129] H.I. Gomes, V. Funari, W.M. Mayes, M. Rogerson, T.J. Prior, Journal of Environmental Management, 222 (**2018**) 30-36.

[130] H. Srichandan, A. Pathak, S. Singh, K. Blight, D.J. Kim, S.W. Lee, Hydrometallurgy, 150 (**2014**) 130-143.

[131] Y. Qu, B. Lian, B. Mo, C. Liu, Hydrometallurgy, 136 (**2013**) 71-77.

[132] O. Velgosova, J. Kadukova, R. Marcincakova, P. Palfy, J. Trpcevska, Waste Management, 33 (**2013**) 456-461.

[133] Y. Xin, X. Guo, S. Chen, J. Wang, F. Wu, B. Xin, Journal of Cleaner Production, 116 (**2016**) 249-258.

[134] W. Gu, J. Bai, B. Dong, X. Zhuang, J. Zhao, C. Zhang, J. Wang, K. Shih, Hydrometallurgy, 171 (**2017**) 172-178.

[135] H.R. Watling, Hydrometallurgy, 84 (**2006**) 81-108.

[136] F. Jalali, J. Fakhari, A. Zolfaghari, Hydrometallurgy. 185 (**2019**) 194-203.

[137] C.G. Bryan, E.L. Watkin, T.J. McCredden, Z.R. Wong, S.T.L. Harrison, A.H. Kaksonen, Hydrometallurgy, 152 (**2015**) 33-43.

[138] X.I. Fan, S.Q. Lv, J.I. Xia, Z.Y. Nie, D.R. Zhang, X. Pan, L.Z. Liu, W.Wen, L. Zheng, Y.D. Zhao, Chemical Engineering Journal, 370 (**2019**) 1407-1424.

[139] D. Pradhan, D. Mishra, D.J. Kim, J.G. Ahn, G.R. Chaudhury, S.W. Lee, Journal of Hazardous Materials, 175 (**2010**) 267-273.

[140] K. Zhao, G.H. Gu, G. Qui, X. Wang, Bioscience Journal, 33 (**2017**) 721-729.

[141] H. Srichandan, S. Singh, A. Pathak, D.J. Kim, S.W. Lee, G. Heyes, Journal of Environmental Science and Health - Part A, 49 (**2014**) 807-818.

[142] A. Heydarian, S.M. Mousavi, F. Vakilchap, M. Baniasadi, Journal of Power Sources, 378 (**2018**) 19-30.

[143] X.L. Fan, S.Q. Lv, J.I., Xia, Z.Y. Nie, D.R. Zhang, X. Pan, L.Z. Liu, W. Wen, L. Zheng, Y.D. Zhao, Chemical Engineering Journal, 370 (**2019**) 1407-1424.

[144] Y.V. Nancharaiah, S.V. Mohan, P.N.L. Lens, Bioresource Technology, 195 (**2015**) 102-114.

[145] E. Sahinkaya, D. Uçar, A.H. Kaksonen, Bioprecipitation of metals and metalloids, Vol. 8., Springer, 199–231, **2017**.

[146] A. Hussain, A. Hasan, A. Javid, J.I. Qazi, 3 Biotech, 6 (**2016**) 119.

[147] D. Park, Y.S. Yun, J.M. Park, Biotechnology and Bioprocess Engineering, 15 (**2010**) 86-102.

[148] R.K. Thauer, E. Stackebrandt, W.A. Hamilton, Sulphate-Reducing Bacteria, Cambridge University Press, Chapter 1, **2009**.

[149] M. Sethurajan, P.N.L. Lens, E.R. Rene, J.V.D. Vossenberg, D. Huguenot, H.A. Horn, L.H.A. Figueiredo, E.D.V. Hullebusch, Journal of Chemical Technology and Biotechnology, 92 (**2017**) 512-521.

[150] J. Cao, G. Zhang, Z. Mao, Z. Fang, C. Yang, Minerals Engineering, 22 (**2009**) 289-295.

[151] N.K. Dhami, M.S. Reddy, A. Mukherjee, Journal of Microbiology and Biotechnology, 23 (**2013**) 707-714.

[152] Y.Ç. Erşan, N.D. Belie, N. Boon, Biochemical Engineering Journal, 101 (**2015**) 108-118

[153] H. Chung, S.H. Kim, K. Nam, Science of The Total Environment, 740 (**2020**), 140194.

[154] K. Plee, M. Pacton, D. Ariztegui, Geomicrobiology Journal, 27 (**2010**) 391-399.

[155] O. Braissant, A.W. Decho, C. Dupraz, C. Glunk, K.M. Przekop, P.T. Visscher, Geobiology, 5 (**2007**) 401-411.

[156] W.S. Reeburgh, Chemical Reviews, 107 (**2007**) 486-513.

[157] T. Zhu, M. Dittrich, Frontiers in Bioengineering and Biotechnology,4:4 (**2016**).

[158] Y.Ç. Erşan, Ecological Wisdom Inspired Restoration Engineering, (**2019**) 19-45.

[159] G. Tang, G. Wang, Y. An, H. Zhang, International Biodeterioration & Biodegradation, 145 (**2019**) 104767.

[160] C.H. Kang, Y.J. Kwon, J.S. So, Ecological Engineering, 89 (**2016**) 64-69.

[161] B. Krajewska, Journal of Advanced Research, 13 (**2018**) 59-67.

[162] A.E.T. Aravena, C.D. Nass, L. Azocar, R.M. Herrera, M. Rivas, D. Jeison, Crystals, 8 (**2018**) 438.

[163] Q. Li, L. Csetenyi, G.M. Gadd, Environmental Science and Technology, 48 (**2014**) 14409-14416.

[164] Y.Ç. Erşan, H. Verbruggen, I.D. Graeve, W. Verstraete, N.D. Belie, N. Boon, Cement and Concrete Research, 83 (**2016**) 19-30.

[165] N. Jalilvand, A. Akhgar, H.A. Alikhani, H.A. Rahmani, F. Rejali, Journal of Soil Science and Plant Nutrition, 20 (**2020**) 206-219.

[166] J.P. Maity, G.S. Chen, Y.H. Huang, A.C. Sun, C.Y. Chen, Geomicrobiology Journal, 36 (**2019**) 612-623.

[167] S. Jain, C. Fang, V. Achal, Bioengineered, 12 (**2021**) 7529-7551.

[168] Y.Ç. Erşan, N. Boon, N.D. Belie, Granules with Activated Compact Denitrifying Core (ACDC) for Self-Healing Concrete with Corrosion Protection Functionality, PRO 123: Final Conference of RILEM TC 253-MCI: Microorganisms-Cementitious Materials Interactions, Toulouse, **2018**, 475-484.

[169] D. Gao, L. Liu, H. Liang, W.M. Wu, Critical Reviews in Biotechnology, 31 (**2011**) 137-152.

[170] M. Alves, A.J. Cavaleiro, E.C. Ferreira, A.L. Amaral, M. Mota, M. da Motta, H. Vivier, M.N. Pons, Water Science & Technology, 41 (**2000**) 207-214.

[171] L.D.A. Purba, H.T. Ibiyeye, A. Yuzir S.E. Mohamad, K. Iwamoto, A. Zamyadi, N. Abdullah, Environmental Technology & Innovation, 20 (**2020**) 101045.

[172] B.M. Wilen, R. Liebana, F. Persson, O. Modin, M. Hermansson, Applied Microbiology

and Biotechnology, 102 (**2018**) 5005-5020.

[173] S.J. Lim, T.H. Kim, Biomass and Bioenergy, 60 (**2014**) 189-202.

[174] A.R. Masegosa, B.M. Palazon, A.G. Martinez, M. Fenice, S. Gorrasi, J.G. Lopez, Water, 13 (**2021**) 1792.

[175] D.P. Cassidy, E. Belia, Water Research, 39 (**2005**) 4817-4823.

[176] M.K. Kreuk, N. Kishida, S. Tsuneda, M.C.M. van Loosdrecht, Water Research, 44 (**2010**) 5929-5938.

[177] M.A. Fulazzaky, M. Nuid, A. Aris, K. Muda, Process Safety and Environment Protection, 107 (**2017**) 259-268.

[178] E. Cetin, E. Karakas, E. Dulekgurgen, S. Ovez, M. Kolukirik, G. Yilmaz, Water Research, 131 (**2018**) 74-89.

[179] Y. Liu, J.H. Tay, Water Research, 36 (**2002**) 1653-1665.

[180] S.J. Sarma, J.H. Tay, A. Chu, Trends in Biotechnology, 35 (**2017**) 66-78.

[181] S.L.D.S. Rollemberg, A.R.M. Barros, P.I.M. Firmino, A.B.D. Santos, Bioresource Technology, 270 (**2018**) 678-688.

[182] M.K.H. Winkler, R. Kleerebezem, L.M.M. de Bruin, P.J.T. Verheijen, B. Abbas, J. Habermacher, M.C.M. van Loosdrecht, Environmental Biotechnology, 97 (**2013**) 7447-7458.

[183] J.H. Tay, Q.S. Liu, Y. Liu, Journal of Applied Microbiology, 91 (**2001**) 168-175.

[184] J.J. Beun, A. Hendriks, M.C.M. van Loosdrecht, E. Morgenroth, P.A. Wilderer, J.J. Heijnen, Water Research, 33 (**1999**) 2283-2290.

[185] N. Schwarzenbeck, R. Erley, P.A. Wilderer, Water Science & Technology, 49 (**2004**) 41-46.

[186] Y.Ç. Erşan, E. Gruyaert, G. Louis, C. Lors, N.D. Belie, N. Boon, Frontiers in Microbiology, 6 (**2015**) 1228.

[187] S.S. Adav, M.Y. Chen, D.J. Lee, N.Q. Ren, Chemosphere, 67 (**2007**) 1566-1572.

[188] D.J. Lee, Y.Y. Chen, K.Y. Show, C.G. Whiteley, J.H. Tay, Biotechnology Advances, 28 (**2010**) 919-934.

[189] J. Garrity, J.G. Gardner, W. Hawse, C. Wolberger, J.C.E. Semerena, Journal of Biological

Chemistry, 282 (**2007**) 30239-30245.

[190] S.F. Yang, J.H. Tay, Y. Liu, Journal of Environmental Engineering, 131 (**2005**) 86-92.

[191] Y.Q. Liu, B.Y.P. Moy, J.H. Tay, Enzyme and Microbial Technology, 42 (**2007**) 23-28.

[192] J. Luo, T. Hao, L. Wei, H.R. Mackey, Z. Lin, G.H. Chen, Water Research, 62 (**2014**) 127-135.

[193] I. Kocaturk, T.H. Erguder, Ecological Engineering, 90 (**2016**) 12-24.

[194] S.S. Adav, D.J. Lee, J.Y. Lai, Bioresource Technology, 100 (**2009**) 3465-3470.

[195] B.Y.P. Moy, J.H. Tay, S.K. Toh, Y. Liu, S.T.L. Tay, Letters in Applied Microbiology, 34 (**2002**) 407-412.

[196] Q.S. Liu, J.H. Tay, Y. Liu, Environmental Technology, 24 (**2003**) 1235-1242.

[197] B. Long, C.Z. Yang, W.H. Pu, J.K. Yang, F.B. Liu, L. Zhang, J. Zhang, K. Cheng, Bioresource Technology, 182 (**2015**) 314-322.

[198] Y.N. Peyong, Y. Zhou, A.Z. Abdullah, V. Vadivelu, Biochemical Engineering, 67 (**2012**) 52-59.

[199] Y. Shi, Y. Liu, Chemosphere, 262 (**2021**) 128033.

[200] J.A. Xavier, L.B. Guimaraes, B.S. Magnus, W.R. Leite, V.J.P. Vilar, R.H.R.D. Costa, Journal of Water Process Engineering, 40 (**2021**) 101917.

[201] Y. Chen, W. Jiang, D.T. Liang, J.H. Tay, Applied Microbiology and Biotechnology, 76 (**2007**) 1199-1208.

[202] J.H. Tay, S.F. Yang, Y. Liu, Applied Microbiology and Biotechnology, 59 (**2002**) 332-337.

[203] S.S. Adav, D.J. Lee, K.Y. Show, J.H. Tay, Biotechnology Advances, 26 (**2008**) 411-423.

[204] L. Qin, J.H. Tay, Y. Liu, Process Biochemistry, 39 (**2004**) 579-584.

[205] B.K. Bindhu, G. Madhu, Indian Journal of Chemical Technology, 22 (**2015**) 241-247.

[206] Y.Q. Liu, X. Zhang, R. Zhang, W.T. Liu, J.H. Tay, Applied Microbiology and Biotechnology, 100 (**2016**) 469-477.

[207] X. Zhang, J.H. Tay, W.J. Jiang, Fresenius Environmental Bulletin, 22 (**2013**).

[208] Y.Q. Liu, X. Zhang, R. Zhang, W.T. Liu, J.H. Tay, Applied Microbiology and

Biotechnology, 100 (**2016**) 469-477.

[209] Y.Q. Liu, J.H. Tay, Enzyme and Microbial Technology, 41 (**2007**) 516-522.

[210] N. Li, X. Wang, N. Ren, K. Zhang, H. Kang, Chemical and Biochemical Engineering Quarterly, 22 (**2008**) 453-458.

[211] M.K.H. Winkler, J.P. Bassin, R. Kleerebezem, L.M.M. de Bruin, T.P.H. van den Brand, M.C.M. van Loosdrecht, Water Research, 45 (**2011**) 3291-3299.

[212] M. Figueroa, A.V. del Rio, J.L. Campos, R. Mendez, A.M. Corral, Bioprocess and Biosystems Engineering, 38 (**2015**) 841-851.

[213] Y. Liu, Q.S. Liu, Biotechnology Advances, 24 (**2006**) 115-127.

[214] J.P. Bassin, D.C. Tavares, R.C. Borges, M. Dezotti, Journal of Environmental Management, 230 (**2019**) 168-182.

[215] M. Jungles, J.L. Campos, R.H.R. Costa, Brazilian Journal of Chemical Engineering, 31 (**2014**) 27-33.

[216] J.J. Beun, M.C.M. van Loosdrecht, J.J. Heijnen, Water Science & Technology, 41 (**2000**) 41-48.

[217] Y.M. Lin, Y. Liu, J.H. Tay, Applied Microbiology and Biotechnology, 62 (**2003**) 430-435.

[218] Y. Liu, J.H. Tay, Biotechnology Advances, 22 (**2004**) 533-563.

[219] Z.H. Li, T. Kuba, T. Kusuda, Enzyme and Microbial Technology, 38 (**2006**) 670-674.

[220] F. Wang, F.I. Yang, X.W. Zhang, Y.H. Liu, H.M. Zhang, J. Zhou, World Journal of Microbiology and Biotechnology, 21 (**2005**) 1379-1384.

[221] J. Dong, Z. Zhang, Z. Yu, X. Dai, X. Xu, P.J.J. Alvarez, L. Zhu, Chemical Engineering Journal, 330 (**2017**) 596-604.

[222] A. Pal, A.K. Paul, Journal of Polimers, (**2013**) 692374.

[223] G.P. Sheng, H.Q. Yu, X.Y. Li, Biotechnology Advances, 28 (**2010**) 882-894.

[224] Y. Liu, J.H. Tay, Biotechnology Advances, 22 (**2004**) 533-563.

[225] P. Rusanowska, A.C. Kwiatkowska, P. Swiatczak, I.W. Baryla, Bioresource Technology, 272 (**2019**) 188-193.

[226] Y. Shi, Y. Liu, Chemosphere, 262 (**2021**) 128033.

[227] S.F. Corsino, M. Capodici, F.D. Pippo, V. Tandoi, M. Torregrossa, Water Research, 148 (**2019**) 425-437.

[228] Y. Wang, J. Wang, Z. Liu, X. Huang, F. Fang, J. Guo, P. Yan, Science of The Total Environment, 795 (**2021**) 148682.

[229] J. Xia, L. Ye, H. Ren, X.X. Zhang, Applied Microbiology and Biotechnology, 102 (**2018**) 3967-3979.

[230] Z.W. Wang, Y. Liu, J.H. Tay, Applied Microbiology and Biotechnology, 69 (**2005**) 469-473.

[231] M. Sajjad, K.S. Kim, Process Biochemistry, 50 (**2015**) 966-972.

[232] L. Liu, D.W. Gao, M. Zhang, Y. Fu, Journal of Hazardous Materials, 181 (**2010**) 382-387.

[233] H.L. Jiang, J.H. Tay, Y. Liu, S.T.L. Tay, Biotechnology Letters, 25 (**2003**) 95-99.

[234] X.M. Li, Q.Q. Liu, Q. Yang, L. Guo, G.M. Zeng, J.M. Hu, W. Zheng, Bioresource Technology, 100 (**2009**) 64-67.

[235] J.H. Tay, Q.S. Liu, Y. Liu, Environmental Technology, 23 (**2002**) 931-936.

[236] R. Lepisto, J. Rintala, Water Research, 33 (**1999**) 3162-3170.

[237] M.K.D. Kreuk, M. Pronk, M.C.M.V. Loosdrecht, Water Research, 39 (**2005**) 4476-4484.

[238] M.H.A. Halim, A.N. Anuar, S. Chelliapan, N.A. Wahab, H.F. Basri, Z. Ujang, M.M. Bob, Journal Teknologi (Science and Engineering), 81 (**2019**) 57-66.

[239] H. Vashi, O.T. Iorhemen, J.H. Tay, Environmental Technology & Innovation, 9 (**2018**) 265-274.

[240] Y.Y. Chen, D.J. Lee, Journal of Taiwan Institute of Chemical Engineers, 52 (**2015**) 118-119.

[241] Y.Ç. Erşan, I. Kocaturk, T.H. Erduger, Effect of Seed Sludge Type on Aerobic Granulation and Treatment Efficiency of Granules, International Conference on Environmental Science and Technology, Houston, Texas, USA, **2012**.

[242] M. Verawaty, M. Pijuan, Z. Yuan, P.L. Bond, Water Research, 46 (**2012**) 761-771.

[243] A.M. Maszenan, Y. Liu, W.J. Ng, Biotechnology Advances, 29 (**2011**) 111-123.

[244] K.H. Ahn, S.W. Hong, Desalination and Water Treatment, 53 (**2015**) 2388-2402.

[245] Y. Liu, S.F. Yang, H. Xu, K.H. Woon, Y.M. Lin, J.H. Tay, 38 (**2003**) 997-1001.

[246] H. Xu, Y. Liu, J.H. Tay, Bioresource Technology, 97 (**2006**) 359-363.

[247] N. Li, D. Wei, S. Wang, L. Hu, W. Xu, B. Du, Q. Wei, Journal of Colloid and Interface Science, 490 (**2017**) 754-761.

[248] Q. Feng, Y. Yu, C. Guo, X. Chen, J. Cao, W. Yang, RSC Advances, 7 (**2017**) 11608.

[249] H. Xu, J.H. Tay, S.K. Foo, S.F. Yang, Y. Liu, Water Science & Technology, 50 (**2004**) 155-160.

[250] M. Sonmez, Y.Ç. Erşan, Cement and Concrete Composites, 126 (**2022**) 104344.

[251] Y.Ç. Erşan, T.H. Erduger, Bioresource Technology, 148 (**2013**) 149-156.

[252] W. Zhou, T. Imai, M. Ukita, M. Sekine, T. Higuchi, Process Biochemistry, 41 (**2006**) 36-43.

[253] S. Wang, S. Teng and M. Fan, Environmental Management, Interaction between Heavy Metals and Aerobic Granular Sludge, Chapter 9, **2010**.

[254] D. Wang, G. Tang, Z. Yang, X. Li, G. Chai, T. Liu, X. Cao, B. Pan, J. Li, G. Sheng, X. Zheng, Z. Ren, Journal of Hazardous Materials, 373 (**2019**) 152-159.

[255] Z. Yu, H. Han, P. Feng, S. Zhao, T. Zhou, T. Zhou, A. Kakade, S. Kulshrestha, S. Majeed, X. Li, Bioresource Technology, 297 (**2020**) 122416.

[256] L. Huang, Q. Wang, L. Jiang, P. Zhou, X. Quan, B.E. Logan, Environmental Science and Technology, 49 (**2015**) 9914-9924.

[257] Y.Q. Liu, B. Moy, Y.H. Kong, J.H. Tay, Enzyme and Microbial Technology, 46 (**2010**) 520-525.

[258] APHA, AWWA and WEF, Standard Methods for the Examination of Water and Wastewater 3rd Edition, Washington DC, **2005**.

[259] B. Kardogan, K. Şekercioğlu, Y.Ç. Erşan, Sustainability, 13 (**2021**) 8990.

[260] J.H.F. Pereboom Water Science and Technology, 36 (**1997**) 141-148.

[261] J. Czarnota, A. Maslon, Journal of Ecological Engineering, 20 (**2019**) 202-210.

[262] B.Y.P. Moy, J.H. Tay, S.K. Toh, Y. Liu, S.T.L. Tay, Letters in Applied Microbiology, 34

(**2002**) 407-412.

[263] A.R.M. Barros, S.L.D.S. Rollemberg, C.D.A.D. Carvalho, I.H.H. Moura, P.I.M. Firmino, A.B.D. Santos, Journal of Environmental Management, 255 (**2020**) 109850.

[264] T.T. Ren, L. Liu, G.P. Sheng, X.W. Liu, H.Q. Yu, M.C. Zhang, J.R. Zhu, Water Research, 42 (**2008**) 3343-3352.

[265] F. Sadrzadeh, Effect of Decreasing Settling Time on Settleability Properties of Biomass in An Anaerobic /Aerobic Sequencing Batch Reactor System, M.Sc. Thesis, Istanbul Technical University, Graduate School of Science, Engineering and Technology, Istanbul, **2013**.

[266] X.Y. Juan, J.J. Yuan, Z. Ping, W. Lan, G. Abbas, J. Zhang, W. Ru, H.Z. Fei, Biodegradation, 29 (**2018**) 339-347.

[267] Y. Chen, Z. Zhu, W. Yu, C. Zhang, Instituto Mexicano de Tecnologia del Agua, 10 (**2019**) 156-181.

[268] M. Figueroa, A.M. Corral, J.L. Campos, R.R. Mendez, Water Science and Technology, 58 (**2008**) 479-485.

[269] T.R. Devlin, M.S. Kowalski, A.D. Biase, J.A. Oleszkiewicz, Environmental Technology, 41 (**2018**) 1455-1463.

[270] R. Du, S. Cao, H. Zhang, Y. Peng, Journal of Hazardous Materials, 384 (**2020**) 121273.

[271] A.J. Mugwar, Bioprecipitation of Heavy Metals and Radionuclides with Calcium Carbonate in Aqueous Solutions and Particulate Media, Ph.D. Thesis, Cardiff University, Geoenvironmental Research Centre Cardiff School of Engineering, Cardiff, **2015**.

[272] F. Baltar, A.G. Rodriguez, M. Meyer, I. Skudelny, S. Sander, B. Thomson, S. Nodder, R. Middag, S.E. Morales, Frontiers in Microbiology, 9 (**2018**) 3190.

[273] D. Martin, K. Dodds, B.T. Ngwenya, I.B. Butler, S.C. Elphick, Environmental Science and Technology, 46 (**2012**) 8351-8355.

[274] A. Joss, D. Salzgeber, J. Eugster, R. König, K. Rottermann, S. Burger, P. Fabijan, S. Leumann, J. Mohn, H. Siegrist, Environmental Science and Technology, 43 (**2009**) 5301-5306.

[275] Z. Bi, M. Takekawa, G. Park, S. Soda, J. Zhou, S. Qiao, M. Ike, Chemical Engineering Journal, 280 (**2015**) 606-613.

[276] A.C. Kwiatkowska, K. Bernat, M. Zielinska, I.W. Baryla, Bioprocess and Biosystems Engineering, 37 (**2014**) 1305-1313.

[277] Anonymous, Solubility Product Constants near 25 °C, https://www.chm.uri.edu/weuler/chm112/refmater/KspTable.html (Date Accessed: **3 January 2022**).

[278] Dr. Fus, Chemistry 1220, https://studylib.net/doc/8127141/chemistry-1220 (Date Accessed: **3 January 2022**).

ANNEX

ANNEX 1 – Calibration and Absorbance Curves

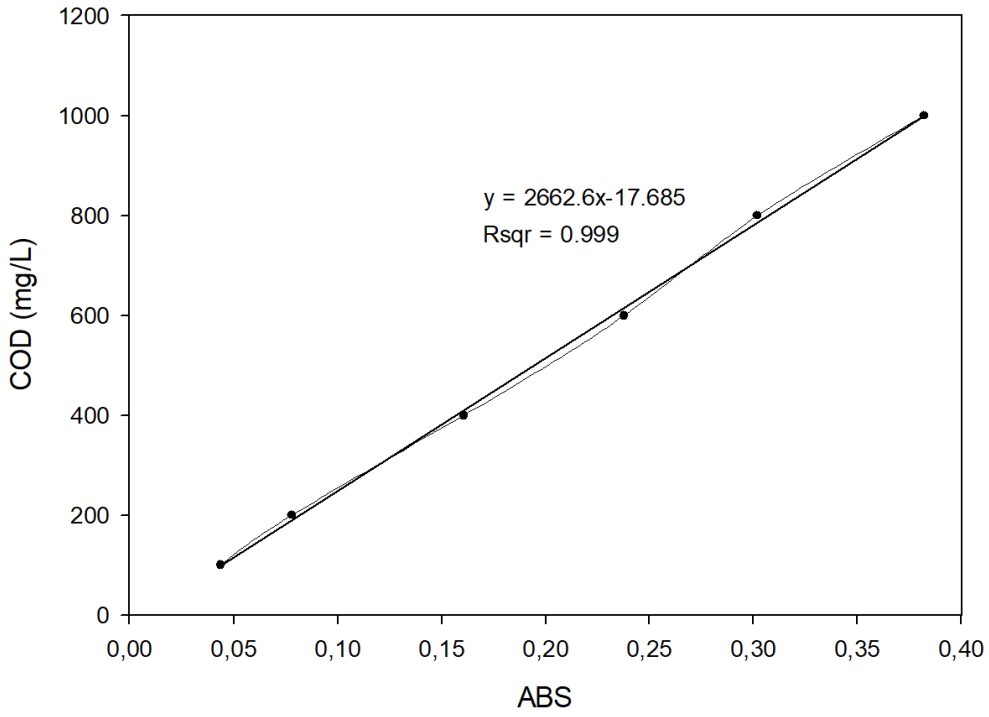

Figure Annex-1.1: Calibration curve for COD kit range of 100-1000 mg/L

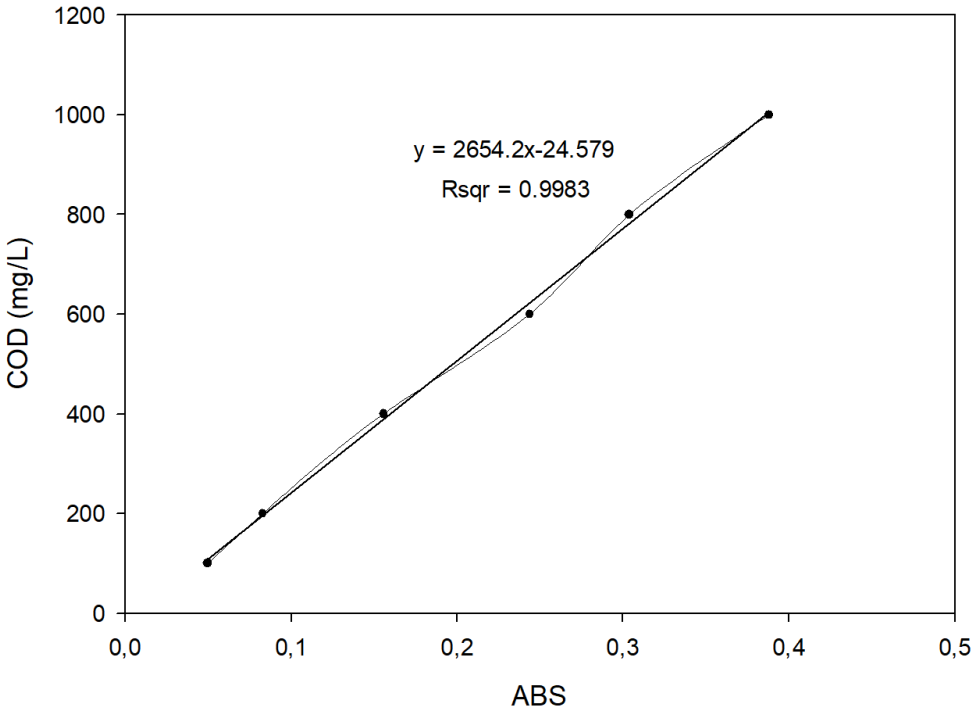

Figure Annex-1.2: Calibration curve for COD kit range of 100-1000 mg/L

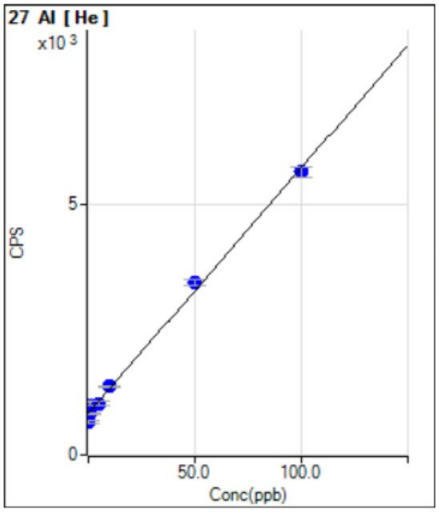

	Rjct	Conc.	Calc Conc.	CPS	Ratio	Det.	RSD
1		0.000	-3.508	659.35		P	12.4
2		0.500	3.367	996.03		P	9.0
3		1.000	0.032	832.69		P	4.3
4		5.000	4.089	1031.37		P	7.2
5		10.000	10.992	1369.40		P	2.0
6		50.000	53.173	3435.02		P	3.3
7		100.000	98.355	5647.59		P	3.5

y = 48.969983 * x + 831.135877
R = 0.9979
DL = 4.999
BEC = 16.97

Weight: <None>
Min Conc: 0

Figure Annex-1.3: Calibration curve of Al for ICP-MS analysis

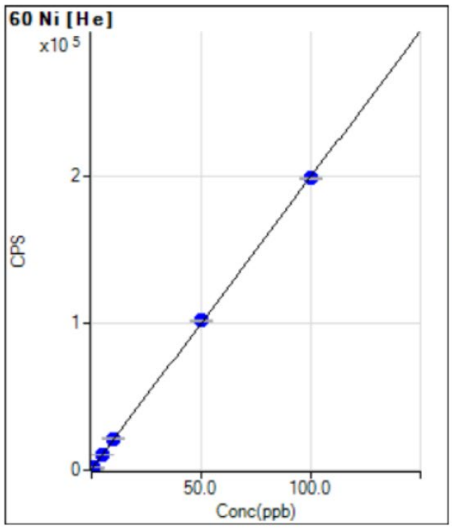

	Rjct	Conc.	Calc Conc.	CPS	Ratio	Det.	RSD
1		0.000	-0.243	200.00		P	11.8
2		0.500	0.304	1289.38		P	1.6
3		1.000	0.707	2091.80		P	1.2
4		5.000	4.949	10541.85		P	1.1
5		10.000	10.435	21467.70		P	2.5
6		50.000	50.769	101809.09		P	1.0
7		100.000	99.579	199032.89		P	0.8

y = 1991.889724 * x + 683.295846
R = 0.9999
DL = 0.03542
BEC = 0.343

Weight: <None>
Min Conc: 0

Figure Annex-1.4: Calibration curve of Ni for ICP-MS analysis

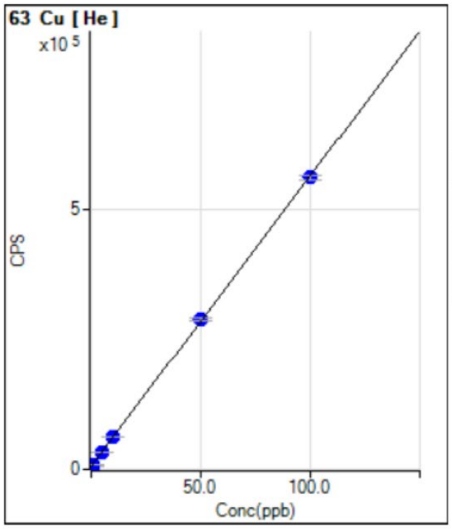

	Rjct	Conc.	Calc Conc.	CPS	Ratio	Det.	RSD
1		0.000	-0.120	5047.59		P	6.1
2		0.500	0.274	7248.48		P	5.2
3		1.000	0.660	9412.86		P	0.9
4		5.000	5.019	33817.04		P	1.1
5		10.000	10.278	63259.23		P	2.4
6		50.000	50.826	290263.36		P	1.7
7		100.000	99.563	563118.57		P	1.3

y = 5598.482563 * x + 5717.112842
R = 0.9999
DL = 0.1658
BEC = 1.021

Weight: <None>
Min Conc: 0

Figure Annex-1.5: Calibration curve of Cu for ICP-MS analysis

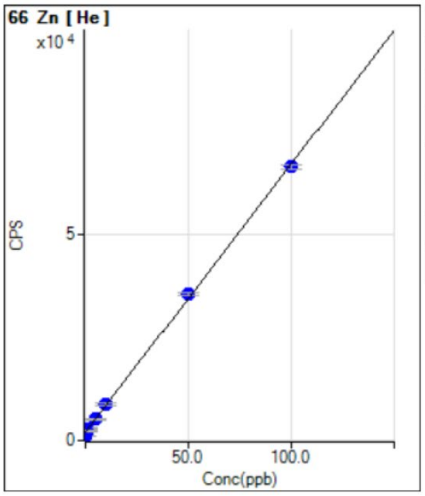

	Rjct	Conc.	Calc Conc.	CPS	Ratio	Det.	RSD
1		0.000	-1.448	1050.08		P	4.4
2		0.500	1.453	2943.71		P	6.5
3		1.000	0.319	2203.56		P	8.6
4		5.000	4.799	5127.62		P	5.5
5		10.000	10.531	8869.27		P	5.9
6		50.000	51.776	35791.10		P	2.2
7		100.000	99.071	66661.69		P	1.8

y = 652.726717 * x + 1995.432126
R = 0.9995
DL = 0.2107
BEC = 3.057

Weight: <None>
Min Conc: 0

Figure Annex-1.6: Calibration curve of Zn for ICP-MS analysis

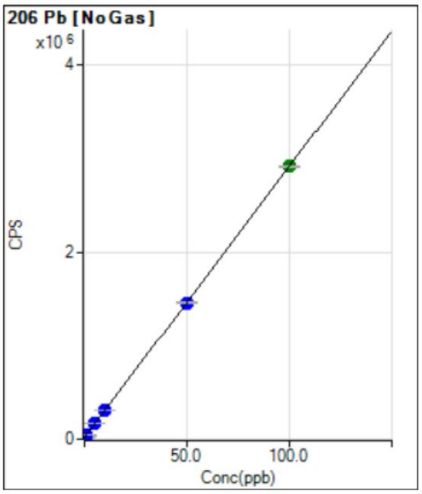

	Rjct	Conc.	Calc Conc.	CPS	Ratio	Det.	RSD
1		0.000	-0.251	8762.97		P	6.4
2		0.500	0.599	33380.01		P	1.4
3		1.000	0.988	44621.60		P	1.4
4		5.000	5.104	163850.15		P	0.7
5		10.000	10.194	311272.68		P	0.9
6		50.000	49.780	1457747.22		P	0.5
7		100.000	100.085	2914694.75		A	0.3

y = 28962.109962 * x + 16019.725432
R = 1.0000
DL = 0.0583
BEC = 0.5531

Weight: <None>
Min Conc: 0

Figure Annex-1.7: Calibration curve of Pb for ICP-MS analysis